CHAPTER 2. 3-CONFIGURATIONS.

2.0 OVERVIEW

This is the longest of our chapters, reflecting not only the long history of the topic of 3-configurations to which the overwhelming majority of the early works was devoted, but also the much more recent discovery of the deficiencies in the original works of a century or more ago, and their correction. We also present the recent developments that center on the study of configurations with a high degree of symmetry.

Section 2.1 investigates the existence of combinatorial, topological, and geometric configurations (n_3) for various values of n.

In Sections 2.2 and 2.3 this is made more detailed by describing the efforts to determine the numbers of distinct configurations (n_3) for specific values of n. These investigations started in the first period of the study of configurations more than a century ago, but have been resumed and advanced only in the recent past.

Section 2.4 is devoted to the attempts to construct all combinatorial configurations (n_3) recursively. This goal seemed to have been achieved by V. Martinetti some 125 years ago — but a few years ago his result was shown to be incomplete. The corrected result was obtained in the doctoral thesis of M. Boben!

Sections 2.5 and 2.6 present the result of the 1894 doctoral thesis of E. Steinitz. This is a remarkable work, even though it has a significant blemish in its geometric part. It is interesting that the last part of this work has remained undeciphered ever since Steinitz wrote it — nobody claims to understand what he is claiming! However, it is clear that at least some parts of the claim are not true.

The next three sections represent recent developments. These are investigations of 3-configurations with remarkably large cyclic or dihedral symmetry groups.

Section 2.10 deals with some unexpected aspects of duality and polarity of these configurations.

Finally, Section 2.11 makes explicit a few of the most intriguing problems about 3-configurations.

2.1 EXISTENCE OF 3- CONFIGURATIONS

Among the questions attacked and solved in the early years of the study of configurations is the one we formulated as question (A) in Section 1.1. We can now formulate it more specifically as follows:

Determine all values of n *such that there exists a combinatorial, or a topological, or a geometric configuration* (n_3).

The complete answer to this problem is given by:

Theorem 2.1.1. Combinatorial configurations (n_3) exist if and only if $n \geq 7$.

Theorem 2.1.2. Topological configurations (n_3) exist if and only if $n \geq 9$.

Theorem 2.1.3. Geometric configurations (n_3) exist if and only if $n \geq 9$.

To prove Theorem 2.1.1 we note that the inequalities of Section 1.3 imply, for $k = 3$, that $n \geq 7$. Hence we only have to show that for each $n \geq 7$ there exist a combinatorial configuration (n_3). Of the various ways of fulfilling this task, probably simplest is the listing of a configuration table for a *cyclic* (n_3), as illustrated in Table 2.1.1. We shall encounter this configuration repeatedly, and we reserve the symbol $\mathscr{C}_3(n)$ for it. Besides, the existence of topological and geometric configurations (n_3) for $n \geq 9$ implies the existence of the corresponding combinatorial ones.

1	2	3	4	….	n–3	n–2	n–1	n
2	3	4	5	…..	n–2	n–1	n	1
4	5	6	7	…..	n	1	2	3

Table 2.1.1. A configuration table for the cyclic combinatorial configuration $\mathscr{C}_3(n)$ for $n \geq 7$. It also shows that for $n \leq 6$ this would not be a configuration, since some pairs of points would belong to two different lines.

This completes the proof of Theorem 2.1.1.

In the exercises at the end of the section we shall enlarge upon the configurations $\mathscr{C}_3(n)$, and other cyclic configurations.

The configuration $\mathscr{C}_3(7)$ is known as the **Fano configuration**; it was described by Gino Fano in 1891 [F1, p. 111] in connection with his axiomatic studies of projective geometries. In fact, it was found earlier (in 1888) by Schönflies [S2], who dismissed it by saying that "a configuration 7_3 with all points distinct does not exist", as well as by Schroeter [S6], also in 1888. Schönflies' assertion makes a limited sort of sense when one realizes that he was thinking of geometric configurations — albeit in the complex projective plane! Schroeter was the first to stress the distinction between combinatorial and geometric configurations, and between geometric configurations in the real plane as distinct from the ones in the complex projective plane.

The configuration $\mathscr{C}_3(8)$ is known as the Möbius-Kantor configuration. In the prehistory of configurations it was described by Möbius in 1828 [M20], who proved that it cannot be realized geometrically in the real Euclidean plane. The configuration was later described by Kantor in 1881 [K3], although not as a combinatorial configuration but as a configuration *geometric in the complex plane*. Reye noted in 1882 [R2] that $\mathscr{C}_3(8)$ does not exist as a geometric configuration in the real plane. In the same paper [K3] the three configurations (9_3) are described by Kantor for the first time, as geometric configurations in the real plane.

To prove Theorems 2.1.2 and 2.1.3 it is sufficient to show that *geometric* configurations (n_3) exist for each $n \geq 9$, and that *topological* configurations (n_3) do not exist for $n = 7, 8$.

To establish the latter, we shall first prove a lemma.

Lemma 2.1.1. Let C be a family of pseudolines in the real projective plane, such that no point is incident with all members of C. Then there is a point that is contained in precisely two of the pseudolines in C.

Such a point is customarily called an *ordinary point* of the family C.

Proof of the lemma. If all intersection points of pseudolines in C are ordinary, there is nothing to prove. Otherwise, there exist "triangles" (that is, regions of the plane) bounded by three pseudolines and such that, at one of the vertices of this "triangle", one of the pseudolines L incident with that vertex V enters the interior of the "triangle". Indeed, start with any non-ordinary point of C, and three arbitrarily chosen pseudolines through V. Then any pseudoline L* not through V will determine a triangle with the required properties. See Figure 2.1.1. Call such a triangle a *good* triangle. Among the (possibly many) good triangles of C find the (or one) that has a minimal area. Then the pseudoline L that enters the triangle at V must meet L* at some point P on the boundary of the "triangle". Now P has to be an ordinary point of C, since any pseudoline through P different from L and L* would belong to a "good" triangle with smaller area.

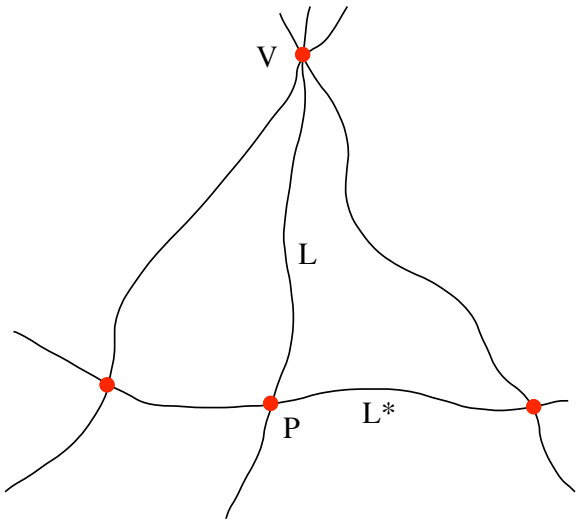

Figure 2.1.1. Any vertex incident with three or more pseudolines of a family C as in Lemma 2.1.1 can serve as one of the vertices of a "good" triangle.

Resuming now the proof of the non-realizability by pseudolines of any combinatorial configuration (7_3), we note that if a realization were possible, then the seven points of such a configuration would account for 21 pairwise incidences of points and pseudolines. On the other hand, seven pseudolines can have at most 7(7–1)/2 = 21 pairwise

intersections, that is, at most 21 pairwise incidences with points of the configuration. Thus all intersection points of the pseudolines would be at points of the configuration, hence triple points, and there would be no ordinary points – contradicting Lemma 2.1.1. It follows that there is no realization of combinatorial configurations (7_3) by pseudolines. This completes the proof of this part of our assertion.

Concerning the case of topological configurations (8_3), let us assume we have a realization C of such a configuration by pseudolines. We begin by selecting one of them, say L. It is met by six other pseudolines in the three vertices of C that are on L. Hence there is one pseudoline L* of C that meets L in an ordinary point, which is not a vertex of C. Choosing the line-at-infinity to pass through that point, we can represent L, L* and the vertices of C incident with them as shown in Figure 2.1.2.

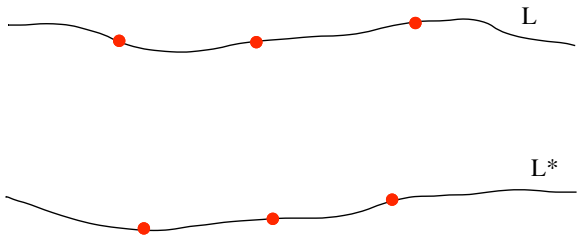

Figure 2.1.2. Two of the pseudolines and the six vertices discussed in the proof.

The remaining six pseudolines must all pass through the three vertices on L and through the three vertices of L*, as well as through the two remaining vertices of C. Let V be one of these two vertices; without loss of generality we can assume that it is in the "strip" between L and L*; then, since at the point of intersection the pseudolines must cross each other, the three pseudolines pass through V as schematically shown in Figure 2.1.3.

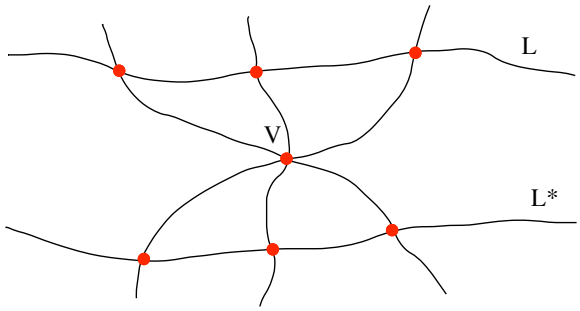

Figure 2.1.3. The arrangement of the pseudolines incident with the vertex V.

Now the last three pseudolines, that are incident with the last vertex of C, must be connected either by the scheme represented in Figure 2.1.4 by the dotted connections, or by the dashed ones. Since in either case two of them meet in a point (that therefore must be the last vertex) that is inaccessible to the third, it follows that the realization of (8_3) by pseudolines is impossible.

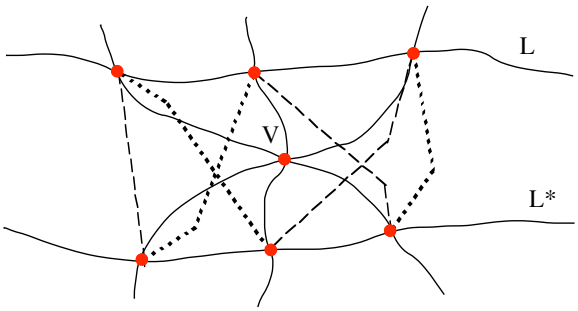

Figure 2.1.4. The three dotted connections or the three dashed ones are schematic representations of the relative positions of the three pseudolines that should be incident with the last vertex of C.

The proof of the weaker result that *geometric* configurations (7_3) and (8_3) do not exist is much older and simpler. For example, Schroeter [S6] argues that, in the notation used in Table 2.2.2, if a geometric realization of the configuration (7_3) were possible, the points 2, 3, 4, 5 would generate a complete quadrangle (in the sense of projective geometry), with diagonal points 1, 6, 7. But these points are collinear in (7_3) while diagonal points of a complete triangle cannot be collinear unless the starting points are collinear; hence there is no geometric configuration. A different proof of the impossibility of geometric realization of the (7_3) configuration appears in Bokowski-Sturmfels [B25, p. 39]; it relies on the method of "final polynomials". Essentially the same proof is used by Levi [L3, p. 95]. It shows that (7_3) can be "realized" only in projective planes with characteristic 2. Sidorov's statement in [S15] that (7_3) is realizable in the complex plane is plain wrong.

The method of "final polynomials" is used by Bokowski–Sturmfels [B25 p. 35] to show that (8_3) cannot be geometrically realized in the *real* plane, although it can be realized in the *complex* plane. That result itself belongs to the "prehistory" of configurations; it appears (in somewhat different formulation) in Moebius [M20, p. 445], as described by Schroeter [S6, p. 239]. An explicit calculation of feasible coordinates of points of a realization of (8_3) by Moebius [M20] as well as by Levi [L3, p. 99], shows that such coordinatization is possible only using complex numbers.

The only publication I am aware of in which the non-existence of *topological* configurations (7_3) and (8_3) has been considered (and proved) is Levi's book [L3, pp. 95, 100]. However, his proofs are quite laborious, and part of the argumentation in case of (8_3) is left to the reader to complete. Instead of our Lemma 2.1.1 Levi relies on a lemma (Satz 21, [L3, p. 85]) that we may formulate as follows: No topological configuration (n_k) with $k \geq 3$ contains as vertices all points determined by its pseudolines. This is clearly a weaker version of the Lemma 2.1.1. On the other hand, Kelly and Rottenberg prove in [K7] the stronger result that every family of n pseudolines, not all incident with one point, must determine at least $3n/7$ ordinary points. That result is a generalization of the well-known result of Kelly and Moser [K6] for families of straight lines. This topic has had an interesting history, and is still subject of widespread interest. It is not possible to enlarge upon it here; the interested reader should consult [B28], where Section 7.2 presents details and gives a large number of references.

In order to complete the proof of Theorem 2.1.3 (hence also of Theorem 2.1.2) we shall describe the construction of a suitable geometric configuration (n_3).

We shall show that for $n \geq 9$, the cyclic combinatorial $\mathscr{C}_3(n)$ configuration of Table 2.1.1 can be realized as a geometric configuration of points and lines (see Figure 2.1.5). We begin by placing the first triplet on the x-axis in a coordinate system, with point 2 at the origin and point 4 at $x = 2$; we shall specify the location of the point 1 shortly. We draw a line through 2 with positive slope, and place on it 3 near to 2, so

that the line $3,4$ has negative slope small in absolute value, and place 5 on the same line sufficiently far to the right so that $4,5$ has positive slope. On line $3,4$ we locate 6 so that its x–coordinate is larger than the x–coordinate of 5, then on $4,5$ we locate 7 so that its x–coordinate is larger than that of 6, and so on up to and including the line through $n–5$ and $n–4$ on which we locate $n–2$ so that its x–coordinate is larger than that of $n–3$. Clearly, all these steps can be carried out. Now, the choice of location for vertex 1 determines the only possible position of vertex $n–1$ (since it is on the already determined lines $1,n–2$ and $n–4,n–3$), as well as the position of vertex n (which must be on the by now determined lines 2, $n–1$ and $n–3,n–2$). The only remaining question is whether the last triplet $1,3,n$ is collinear — and this depends on the choice of 1 (see Figure 2.1.5). It is easy to check that if 1 is chosen to be on the x–axis between points 2 and 4 and near to 2 (see part (a) of Figure 2.1.5), then the halfplane determined by the line $1,n$ and containing the positive x-axis contains the point 3 in its interior. On the other hand, if 1 is chosen between 2 and 4 but near to 4 (see part (b)), then 3 in not in the interior of that halfplane determined by $1,n$ that contains the positive x–axis. Due to the continuity of all construction steps, it follows that there must exist a position of vertex 1 for which the line $1,n$ passes through the point 3 — thus yielding the desired geometric realization of the combinatorial configuration in question. ¨

It should be noted that the construction fails unless $n – 5 > 3$; this provides an explanation why this construction requires $n \geq 9$.

This proof is quite analogous to the first published proof by Schroeter [S6]. The main difference is that in the last part, instead of the continuity argument used in our proof, Schroeter gives a purely geometric proof which utilizes properties of sets of points on cubic curves. On this topic he published a book in the same year [S7]. The advantage of Schroeter's proof over ours is that it shows that the cyclic configuration of Table 2.1.1 can be geometrically realized, for every $n > 9$, by a *linear construction* – that is, with just a straightedge. This implies that all these configurations can also be geometrically realized in the rational plane. In their combinatorial guise these configurations were studied, more or less simultaneously, by Schoenflies [S2] and Martinetti [M2].

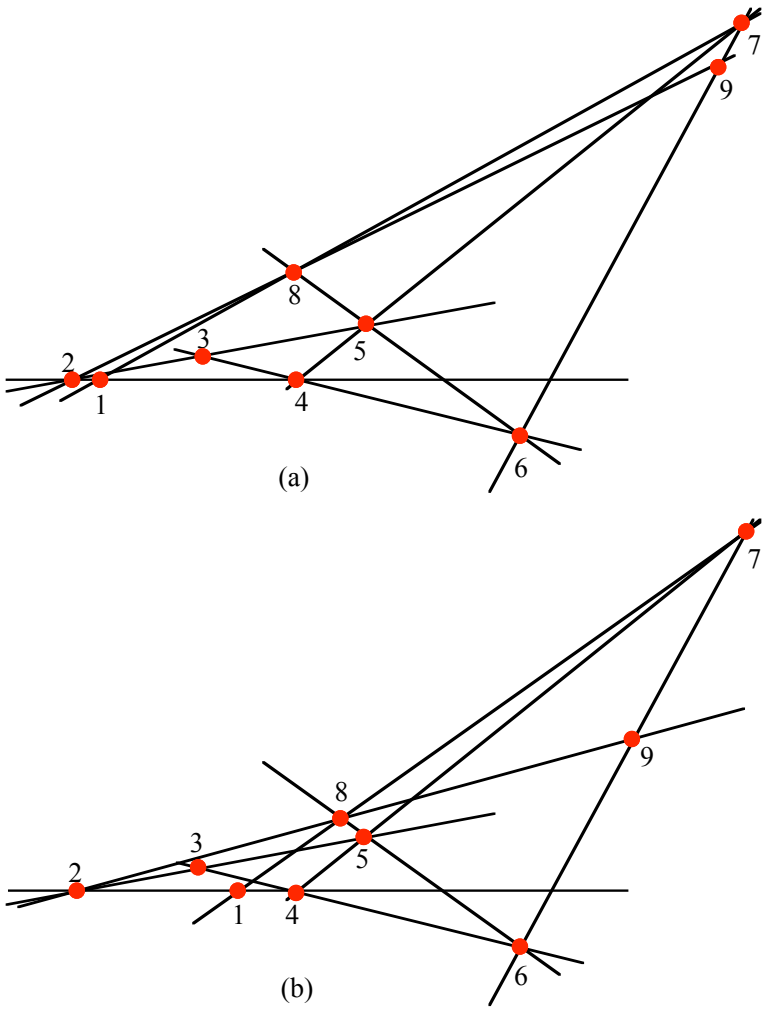

Figure 2.1.5. An illustration (for n = 9) of the construction of a geometric realization of the cyclic combinatorial configuration $\mathscr{C}_3(n)$ from Table 2.1.1.

* * * * * *

A few remarks seem appropriate at this time.

Early papers on configurations often considered configurations in the complex plane. Obviously, all geometric configurations as considered here (that is, in the real Euclidean plane) can also be considered as being in the complex plane. The interesting point is that in the complex plane Theorems 2.1.2 and 2.1.3 require modification: There exists a geometric configuration (n_3) in the complex plane if and only if $n \geq 8$. The fact that a *configuration* (8_3) exists in the complex plane was first announced by Kantor [K3], although in "prehistoric" formulation it goes back at least to Moebius [M20, p. 445].

Like many other writers on configurations in the last quarter of the nineteenth century, Kantor [K3] did not make explicit what kind of configurations (n_3) he is investigating. This is particularly amusing in connection with the configuration (8_3), which he describes as two quadrangles, each inscribed to and circumscribed about the other. Only later does he make an off-hand remark that at most four of the eight vertices of the configurations are real !!!

The cyclic configuration $\mathscr{C}_3(7)$ is the only configuration (7_3); this will be proved explicitly in Section 2.2. The configuration (7_3) does not appear in the paper by Kantor [K3] in which he considers configurations (n_3) for $n \leq 9$. Although he relies on some combinatorial arguments, the combinatorial configuration (7_3) was probably invisible to him since it cannot be realized in the complex plane; it seems that he was considering only configurations that have realizations in the complex plane, although he is not explicit about that. On the other hand, (7_3) appears in many other publications and guises – – for example, as a Steiner triple system on 7 elements, as the projective plane of order 2, and several others.

Levi [L3] established Theorem 2.1.1 by considering generalizations of the cyclic configuration $\mathscr{C}_3(n)$ in Table 2.1.1. The same idea appeared earlier, most explicitly in Schönflies [S2]. A generalization of this is the *cyclic configuration* $\mathscr{C}_3(n,m)$, which consists of triples $\{j, j+1, j+m\}$, for $1 \leq j \leq n$, all entries taken mod n. Such configurations were studied (with slightly different notation) by Levi [L3, p. 91]. Levi proved that $\mathscr{C}_3(n,m)$ is a combinatorial configuration whenever $3 \leq m < n/2$. He does not discuss their geometric realizability, and mentions no earlier works on any cyclic configurations.

There are familiar diagrams intended to illustrate the Fano (7_3) and Möbius-Kantor (8_3) configurations, shown in Figure 2.1.6. They are not topological configurations, since they involve one "line" that is a circle. If one of the incidences is not insisted

upon, then this line can be "opened up" and a geometric realization of the resulting sub-figuration is obtained.

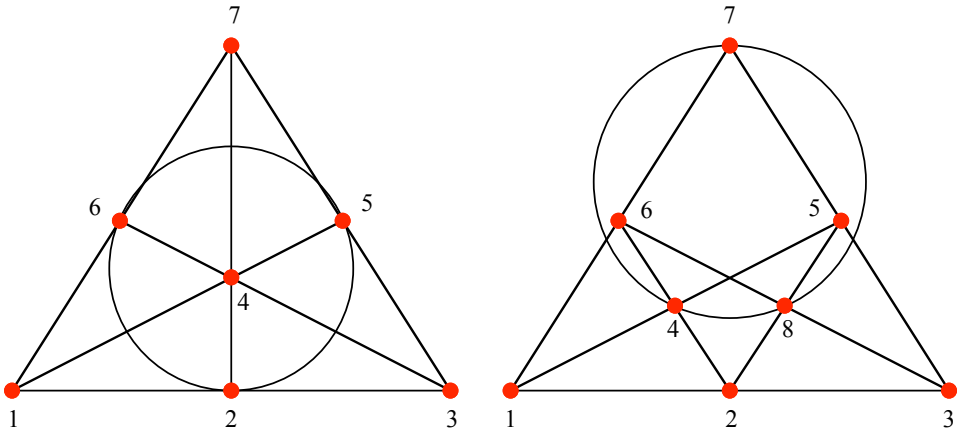

Figure 2.1.6. Diagrams often used to illustrate the combinatorial Fano (7_3) and Moebius-Kantor (8_3) configurations. The labeling shown is the "greedy" one: it uses a new mark only if unavoidable.

	L_1	L_2	L_3	L_4	L_5	L_6	L_7
Q_1	X		X				X
Q_2		X				X	X
Q_3	X				X	X	
Q_4				X	X		X
Q_5			X	X		X	
Q_6		X	X		X		
Q_7	X	X		X			

Figure 2.1.7. A Levi incidence matrix for the Fano (7_3) configuration, which shows that it is cyclic and selfdual.

Exercises and problems.

1. Find the isomorphism between the labeling of the points of the configurations (7_3) and (8_3) in Figure 2.1.6 and the cyclic configuration $\mathscr{C}_3(7)$ and $\mathscr{C}_3(8)$.

2. Use the illustration of the Moebius-Kantor (8_3) configuration given in Figure 2.1.6 to find a Levi incidence matrix for it. Can you use it to show that the configuration is selfdual?

3. A *general cyclic configuration* $\mathscr{C}_3(n,a,b)$ consists of triples {j, a+j, b+j}, for given a, b with $0 < a < b < n$ and for $1 \leq j \leq n$, all entries taken mod n. The configuration $\mathscr{C}_3(n)$ in Table 2.1.1 is, in this notation, $\mathscr{C}_3(n,1,3)$. Determine for which n, a, b is $\mathscr{C}_3(n,a,b)$ a combinatorial configuration. As a first step, investigate configurations $\mathscr{C}_3(n,1,m)$. (This was done as early as 1895, by G. Brunel in [B30].)

4. Is $\mathscr{C}_3(n,1,4)$ geometrically realizable for some n? Generalize.

2.2 ENUMERATION OF 3-CONFIGURATIONS (Part 1)

We turn now to the presentation of the results known about the number of non-isomorphic configurations (n_3) of the three kinds, for each value of n — as far as these numbers are known. As we shall see, this is not very far. Moreover, we have to discuss some other questions concerning these enumerations.

For the purposes of this section, we shall denote by $\#_c(n)$, $\#_t(n)$ and $\#_g(n)$ the number of non-isomorphic combinatorial, topological or geometric configurations (n_3), respectively. We begin with:

Theorem 2.2.1. The complete list of known numbers $\#_c(n)$, $\#_t(n)$ and $\#_g(n)$ is given in Table 2.2.1.

We start by presenting the proofs of the enumerations for $n \leq 8$. Following this we shall first discuss the case n = 9, then the rather unexpected situation for n = 10, and finally the cases of $n \geq 11$. Some general considerations will be explained next, with exercises and problems to follow.

From Section 2.1 we already know that all three numbers are 0 for $n \leq 6$. Now we first show that each of the (combinatorial) configurations (7_3) and (8_3) is unique. This follows easily from the consideration of the formation of their configuration tables. For (7_3), starting with the three lines that contain 1 and then continuing by using the freedom of assigning labels to previously uncommitted points in the only possible way, we obtain the unique configuration table shown in Table 2.2.2. For (8_3) we first note that since each point is connected (by a line of the configuration) to six other points, it is fails to be connected to a unique point. Designating the unconnected pairs by {1,5}, {2,6}, {3,7}, and {4,8}, a similar procedure leads to the unique configuration table shown in Table 2.2.3. The uniqueness of these configurations has been known since early in the study of

configurations. The uniqueness of (8_3) seems to have been established first by Kantor [K3], while $\#_c(7) = 1$ was proved by Martinetti [M2, pages 3,4] ; for other proofs see, for example, Levi [L3, pp. 94, 98], Hilbert–Cohn Vossen [H4]).

n	$\#_c(n)$	$\#_t(n)$	$\#_g(n)$
≤ 6	0	0	0
7	1	0	0
8	1	0	0
9	3	3	3
10	10	10	9
11	31	31	31
12	229	229	229
13	2,036		
14	21,399		
15	245,342		
16	3,004,881		
17	38,904,499		
18	530,452,205		
19	7,640,941,062		

Table 2.2.1. The numbers of non-isomorphic configurations (n_3) of the three kinds, for each n. All known values are shown.

1	1	1	2	2	3	3
2	4	6	4	5	4	5
3	5	7	6	7	7	6

Table 2.2.2. A configuration table of the unique combinatorial configuration (7_3).

1	1	1	2	2	3	3	5
2	4	7	4	5	4	6	6
3	6	8	7	8	5	7	8

Table 2.2.3. A configuration table of the unique combinatorial configuration (8_3).

Similar arguments can be applied to the determination of the different combinatorial configurations (9_3). Easier to carry out is an application of the "remainder figures" method described in Section 1.4. First comes the observation that each point fails to be

connected to precisely two other points. Drawing an edge (segment) between any two unconnected points, we see that the unconnected pairs form one or more circuits. (This is the *deficiency graph* of this configuration introduced in Section 1.4.) Since a circuit has to have at least three points, there are four potential sets of circuits: A single 9-circuit, a 6-circuit and a 3-circuit, a 5-circuit and a 4-circuit, and three 3-circuits. It is obvious that different sets of circuits imply that the configurations are not isomorphic, since any isomorphism preserves connected pairs of points, hence also disconnected pairs. Similarly to the earlier cases, it is possible to show that each case corresponds to a (unique) configuration, except that the case of one 5-sided and one 4-sided circuits corresponds to no configuration. The reason for this is the following: Assume that it is possible, and consider the lines incident with the vertices of the 4-circuit. Two lines correspond to the "diagonals" of the 4-circuit, while each of the four vertices has to be on two additional lines, all distinct and different from the earlier two; this would require the existence of at least 10 lines. Hence such a possibility cannot lead to a configuration. The result, using these or other arguments, appears in Kantor [K3], Martinetti [M2], Schroeter [S6], and again in Levi [L3, p. 103], Hilbert–Cohn Vossen [H4], Gropp [G23].

Configuration tables of the three combinatorial configurations (9_3) are shown in Tables 2.2.4, 2.2.5, and 2.2.6. All three of these configurations can be geometrically realized; this was first proved by Kantor [K3], and more thoroughly analyzed by Schroeter [S6]. Representative examples of such realizations are shown in Figure 2.2.1, and the same representatives are shown in Figure 2.2.2 with the circuits formed by non-connected pairs of points.

1	1	1	2	2	2	3	3	3
4	5	6	4	5	6	4	5	6
7	8	9	8	9	7	9	7	8

Table 2.2.4. A configuration table for the configuration $(9_3)_1$.

1	1	1	2	2	2	3	3	4
3	4	5	4	5	6	5	6	7
7	6	8	8	7	9	9	8	9

Table 2.2.5. A configuration table for the configuration $(9_3)_2$.

1	1	1	2	2	2	3	3	3
4	5	8	4	5	7	4	6	7
7	6	9	6	8	9	5	9	8

Table 2.2.6. A configuration table for the configuration $(9_3)_3$.

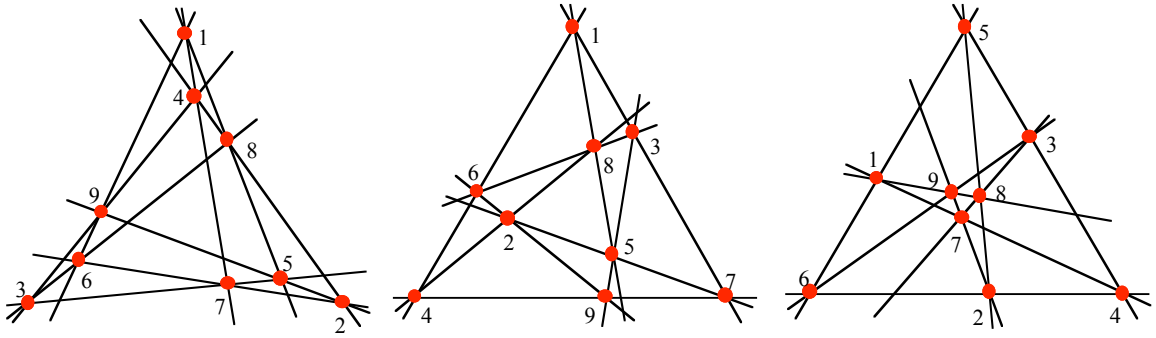

$(9_3)_1$ $(9_3)_2$ $(9_3)_3$

Figure 2.2.1. Examples of the three types of geometric configurations (9_3). The claim by Steinitz [S19, p. 489] that H. A. Schwarz [S12] found the form of the configuration $(9_3)_3$ with 3-fold rotational symmetry is not correct.

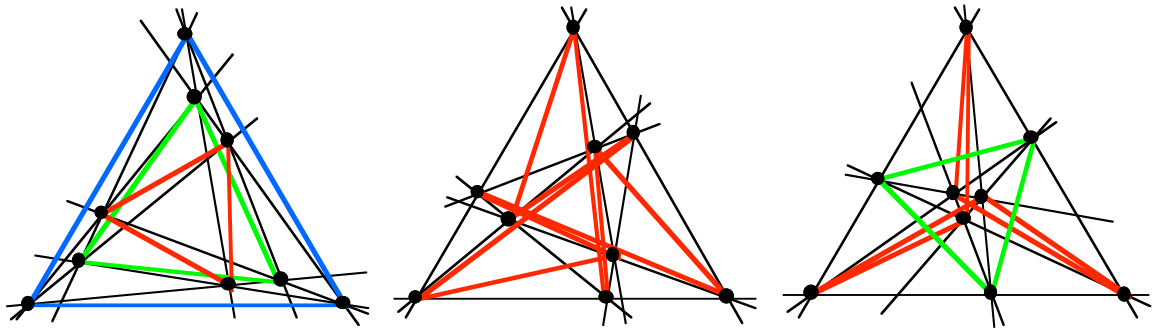

$(9_3)_1$ $(9_3)_2$ $(9_3)_3$

Figure 2.2.2. The circuits formed by the non-connected pairs in the three types of geometric configurations (9_3).

Concerning the (10_3) configurations, we start by presenting in Table 2.2.7 configuration tables for all ten combinatorial configurations. The existence of precisely ten non-isomorphic combinatorial configurations (10_3) has been established repeatedly, by more-or-less brute force enumeration; historical details and references will be given be-

low. In order to prove that these configurations are distinct, we shall use the concept of "remainder figures" which was introduced in Section 1.4: For each vertex of the combinatorial configuration (10_3) consider the three vertices that are not on any of the lines passing through the given vertex. There are three possibilities concerning these three points: Either all three are on one configuration line, or they determine two lines of the configuration, or they determine three such lines (a *trilateral* or "triangle"). We shall denote the three possibilities by I, V, Δ. No other situations are possible. Indeed, if the three points were collinear, but on a line that is not in the configuration, there would be nine configuration lines through them, and three additional lines through the original vertex – while only ten lines are available. But if the three points are not collinear, they determine a triangle. If none of the three lines determined by the points were a configuration line, the configuration would again have to have at least 12 lines. On the other hand, if just one of the lines determined by the sides of the triangle were a line of the configuration, then there would have to be present in the configuration at least 1 + 2 + 2 + 3 + 3 = 11 lines. Thus, the three cases listed earlier are the only ones possible.

The above arguments that the remainder figure in case of (10_3) must be one of I, V, Δ are taken from Schroeter [S8], together with his notation. By very exhaustive and exhausting argumentation one can show that only ten combinations of the different remainder figures (listed in Table 2.2.8) can occur in a combinatorial configuration (10_3), and that each corresponds to a unique isomorphism type of combinatorial configurations, represented by one of the ten configurations in Table 2.2.7. The detailed discussion of the possible combinatorial configurations depending on the kind and number of the remainder figures is spread over 22 pages in [S8]. It leads to the conclusion that each column in Table 2.2.8 corresponds to one and only one combinatorial configuration (10_3).

As far as geometric realizations go, in Figure 2.2.3 are shown sketches similar to the ones in the first enumeration of the (10_3) configurations by Kantor [K4]; our Figure 1.2.2 is a copy of one of the Kantor diagrams. The diagram of $(10_3)_1$ is easily checked to be an illustration of the Desargues configuration. We shall encounter $(10_3)_{10}$ in Section 2.6 as the astral configuration denoted 5#(2,2;1).

$(10_3)_1$

1	1	1	8	2	3	2	3	4	5
2	4	6	9	4	5	6	7	6	7
3	5	7	0	8	8	9	9	0	0

$(10_3)_2$

1	1	1	8	2	3	2	3	4	5
2	4	6	9	4	7	6	5	6	7
3	5	7	0	8	8	9	9	0	0

$(10_3)_3$

1	1	1	8	2	3	2	3	4	5
2	4	6	9	4	6	7	5	6	7
3	5	7	0	8	8	9	9	0	0

$(10_3)_4$

1	1	1	8	2	3	2	3	4	5
2	4	6	9	4	6	5	7	6	7
3	5	7	0	8	8	9	9	0	0

$(10_3)_5$

1	1	1	8	2	3	2	4	3	5
2	4	6	9	4	7	5	6	6	7
3	5	7	0	8	8	9	9	0	0

$(10_3)_6$

1	1	1	8	2	3	2	5	3	4
2	4	6	9	4	7	6	7	5	6
3	5	7	0	8	8	9	9	0	0

$(10_3)_7$

1	1	1	2	4	6	5	3	7	2
2	4	6	8	8	9	7	5	3	4
3	5	7	9	0	0	8	9	0	6

$(10_3)_8$

1	1	1	3	5	7	2	6	4	2
2	4	6	8	8	9	7	5	3	4
3	5	7	9	0	0	8	9	0	6

$(10_3)_9$

1	1	1	2	4	6	5	3	2	3
2	4	6	8	8	9	7	5	7	4
3	5	7	9	0	0	8	9	0	6

$(10_3)_{10}$

1	1	1	3	2	7	5	6	4	2
2	4	6	8	8	9	7	5	3	4
3	5	7	9	0	0	8	9	0	6

Table 2.2.7. The ten non-isomorphic combinatorial configurations (10_3), in the notation of Schroeter [{S2]. They were first determined by Kantor [K4], using other methods and different notation and labeling.

	$(10_3)_1$	$(10_3)_2$	$(10_3)_3$	$(10_3)_4$	$(10_3)_5$	$(10_3)_6$	$(10_3)_7$	$(10_3)_8$	$(10_3)_9$	$(10_3)_{10}$
I	10	4	2	6	1	1	0	0	0	0
V	0	6	6	0	3	9	9	3	6	0
Δ	0	0	2	4	6	0	1	7	4	10
	X	VIII	V	II	I	IX	III	VI	IV	VII
	B	G	D	C	H	F	E	J	K	A

Table 2.2.8. The number of occurrences of the different remainder figures in the ten combinatorial configurations (10_3). The last two rows give the notation by Martinetti [M2] and Kantor [K4

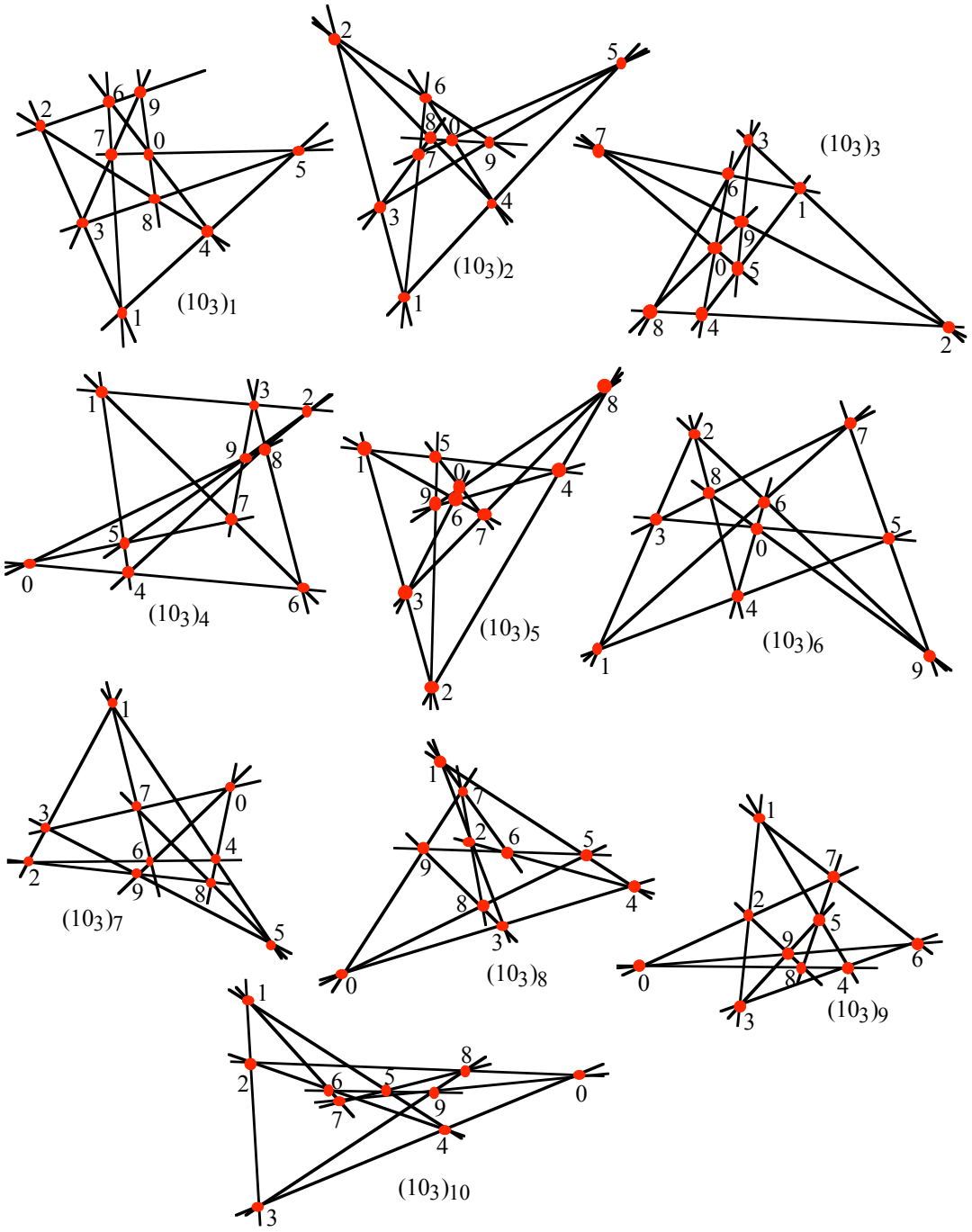

Figure 2.2.3. Sketches of configurations (10_3), analogous to the ones presented in Kantor's paper [K4].

One of the most striking features exhibited by Table 2.2.1 is the inequality $\#_t(10) = 10 > \#_g(10) = 9$. This arises because the diagram in Figure 2.2.4, which *appears* to show a (10_3) geometric configuration (which is a cleaner drawing of the configuration

$(10_3)_4$ in Figure 2.2.3), cannot in fact be realized by straight lines—although the diagram clearly indicates that a topological realization is possible.

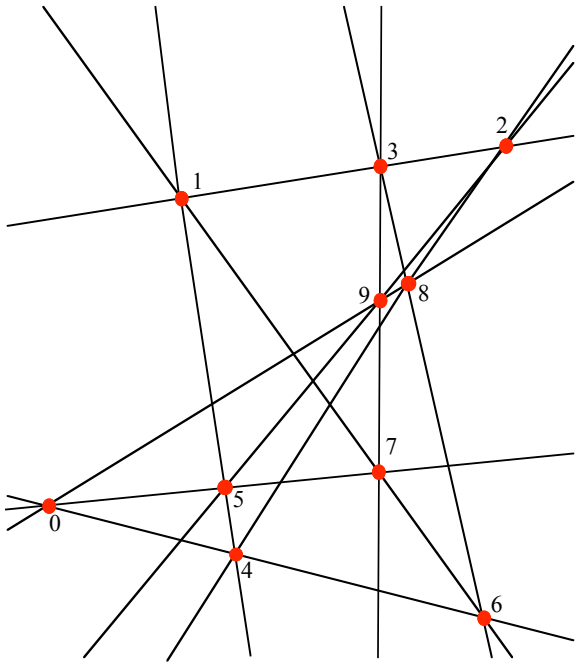

Figure 2.2.4. An apparent geometric realization of the combinatorial configuration $(10_3)_4$, which was also shown in Figure 1.2.2. However, both diagrams are misleading. This configuration is not isomorphic to any configuration of points and (straight) lines. On the other hand, the "lines" are (very mildly curved) pseudolines, hence a topological realization of this configuration is possible.

The impossibility of a geometric realization of $(10_3)_4$ can be established as follows.

The complete quadrangle 2,3,8,9 contains the three pairs of opposite sides

23-1	28-4	29-5
89-0	39-7	38-6

while the complete quadrangle 6,7,9,0 contains the three pairs of opposite sides

67-1	60-4	70-5
90-8	97-3	96-*

By a basic theorem of projective geometry, the three pairs of lines of each quadrangle intersect the line 145 in three pairs of points of an involution. But these involutions must coincide, since two of the pairs coincide: 1 and 890∩145, and 4 and 379∩145. Then the point paired with 5 in the involution must be the intersection point of the three lines 145, 368, 96*. This cannot be 6, since then 145 would contain four points; the only alternative is that 368 and 96* coincide – but then 368 would contain the fourth point 9. Hence the configuration $(10_3)_4$ cannot be realized geometrically.

This proof of the impossibility of a geometric realization of the configuration $(10_3)_4$ is due to Schroeter [S8]. The difference between topological and geometric realizability seems to have been taken as a challenge by many people, leading to a variety of proofs of geometric non-realizability, or at least mention of it; see Carver [C2], Laufer [L1], van de Craats [V1], Glynn [G2], Killgrove *et al.* [K10], Sternfeld et al. [S22], and others. Zacharias [Z5] is not aware of the earlier works and attempts to enumerate all the (10_3) configurations. There are several errors in [Z5] (as well as in the review [T1] by Togliati); corrections appear in [Z7]. Some other publications discuss just the enumeration of combinatorial (10_3) configurations; for example, we may mention Betten and Schumacher [B15].

This situation makes it even more important to make sure that the remaining nine combinatorial configurations (10_3) are geometrically realizable. Following Schroeter [S8], we present here a method of stepwise construction for each of the nine *geometric* configurations (10_3). The method leads to several important conclusions; among them are: the number of parameters needed to determine each of these configurations (that is, the number of "degrees of freedom"), the possibility of constructing each of them using only an unmarked ruler, and the possibility of realizing each in the rational plane (or, equivalently, with all vertices at points of the integer lattice). Since these are quite non-trivial results, which can be found in few of the more recent publications, Schroeter's constructions are shown in Figure 2.2.5. Naturally, each of these constructions requires justification, which is given in the paper; examples follow.

From the configuration table for $(10_3)_1$ we see that the intersections (24,35) = 8, (26, 37) = 9 and (46, 57) = 0 are collinear, hence by the Desargues' theorem the triangles 246 and 357 are in perspective from a point – which in the table is identified as 1. This justifies the construction in Figure 2.2.5. Moreover, it enables one to find out how many degrees of freedom are there in the construction (precisely 11), and that the construction is linear. By this is meant that only systems of linear equations need to be solved, and hence that it can be carried out in the rational plane (the plane in which only points with rational coordinates are considered).

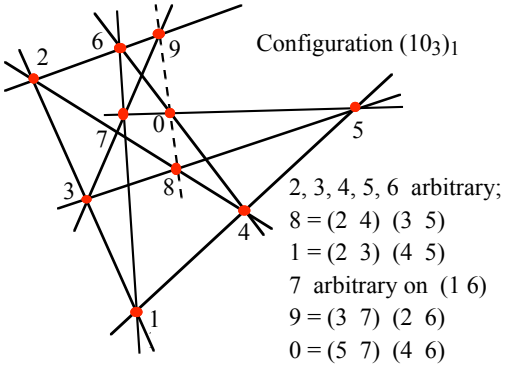

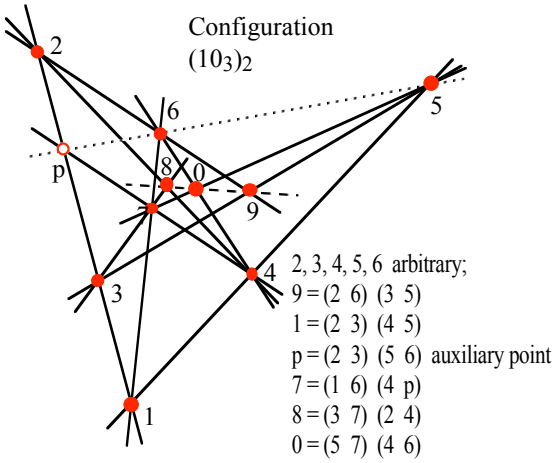

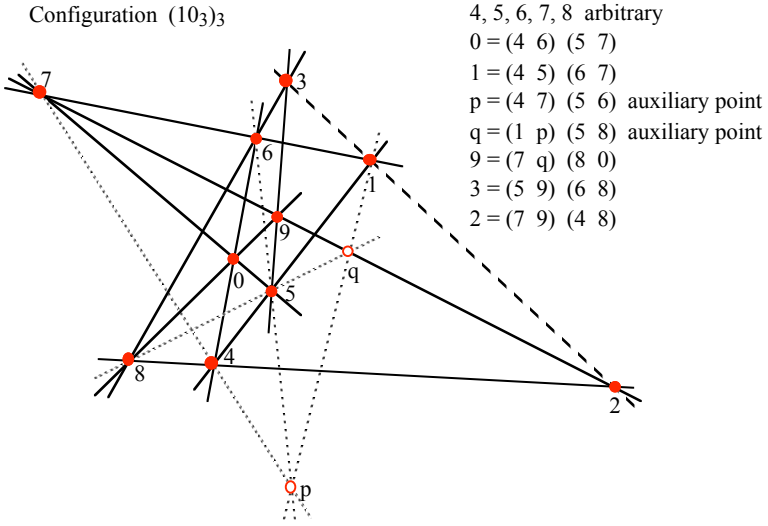

Configuration $(10_3)_5$

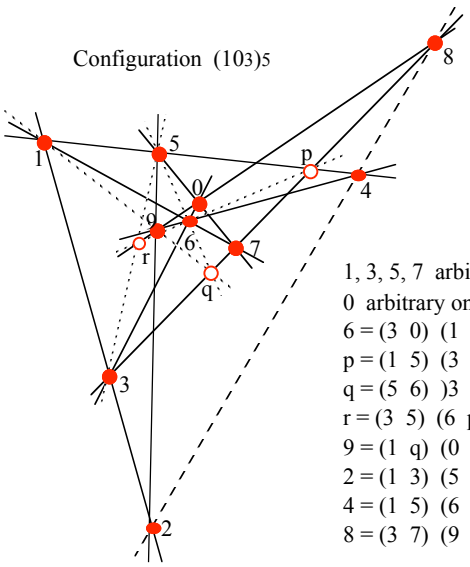

1, 3, 5, 7 arbitrary
0 arbitrary on (5 7)
6 = (3 0) (1 7)
p = (1 5) (3 7) auxiliary point
q = (5 6))3 7) auxiliary point
r = (3 5) (6 p) auxiliary point
9 = (1 q) (0 r)
2 = (1 3) (5 9)
4 = (1 5) (6 9)
8 = (3 7) (9 0)

Configuration $(10_3)_6$

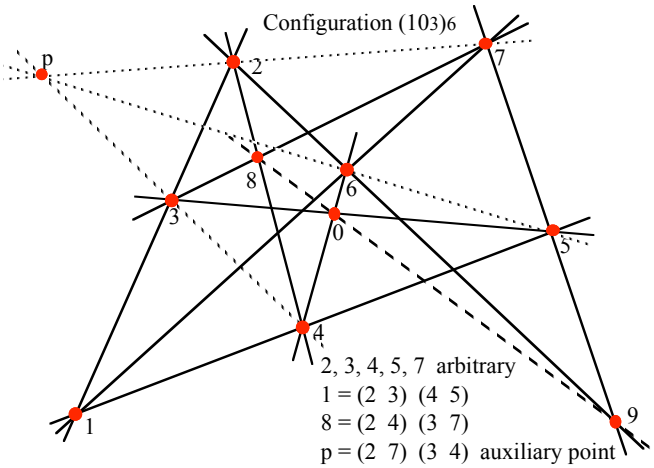

2, 3, 4, 5, 7 arbitrary
1 = (2 3) (4 5)
8 = (2 4) (3 7)
p = (2 7) (3 4) auxiliary point
6 = (1 7) (5 p)
9 = (2 6) (5 7)
0 = (4 6) (3 5)

Configuration $(10_3)_7$

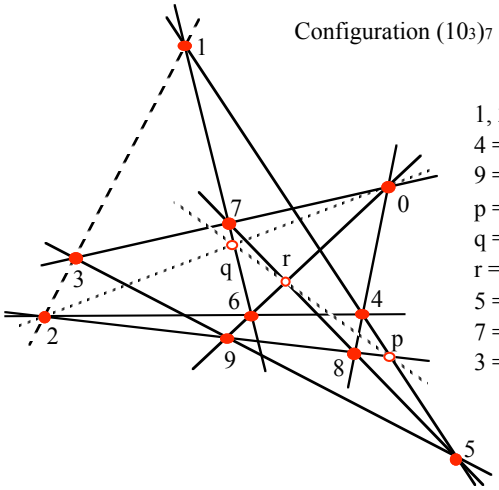

1, 2, 6, 8, 0 arbitrary
4 = (2 6) (8 0)
9 = (2 8) (6 0)
p = (1 4) (2 8) auxiliary point
q = (1 6) (2 0) auxiliary point
r = (6 0) (p q)
5 = (1 4) (8 r)
7 = (1 6) (8 r)
3 = (5 9) (7 0)

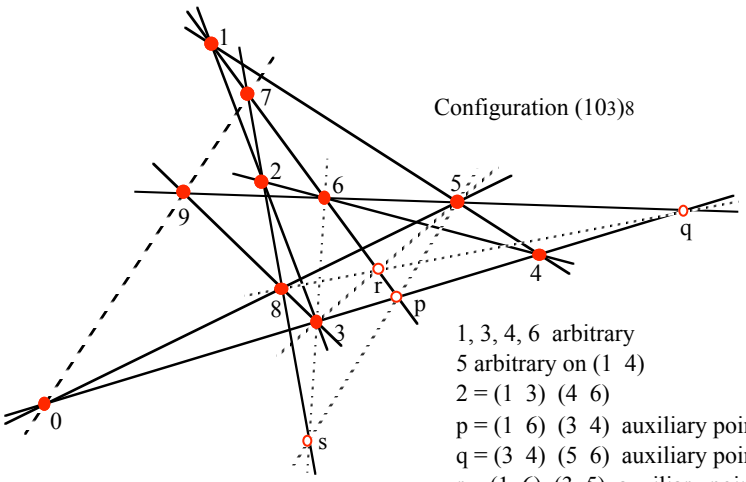

Configuration $(10_3)_8$

1, 3, 4, 6 arbitrary
5 arbitrary on (1 4)
2 = (1 3) (4 6)
p = (1 6) (3 4) auxiliary point
q = (3 4) (5 6) auxiliary point
r = (1 6) (3 5) auxiliary point
s = (3 6) (5 p) auxiliary point
8 = (2 s) (q r)
7 = (1 6) (2 8)
9 = (3 8) (5 6)
0 = (3 4) (5 8)

Configuration $(10_3)_9$

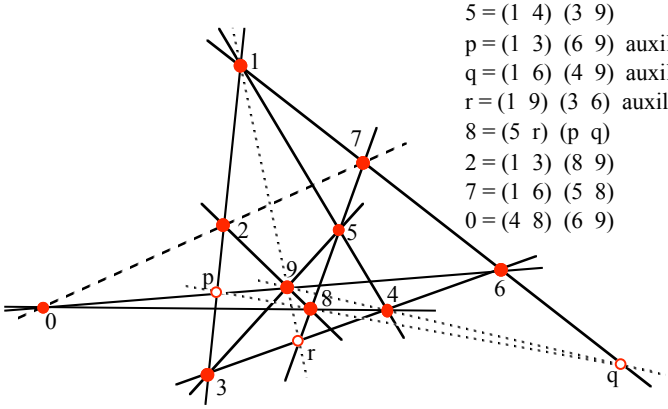

1, 3, 6, 9 arbitrary
4 arbitrary on (3 6)
5 = (1 4) (3 9)
p = (1 3) (6 9) auxiliary point
q = (1 6) (4 9) auxiliary point
r = (1 9) (3 6) auxiliary point
8 = (5 r) (p q)
2 = (1 3) (8 9)
7 = (1 6) (5 8)
0 = (4 8) (6 9)

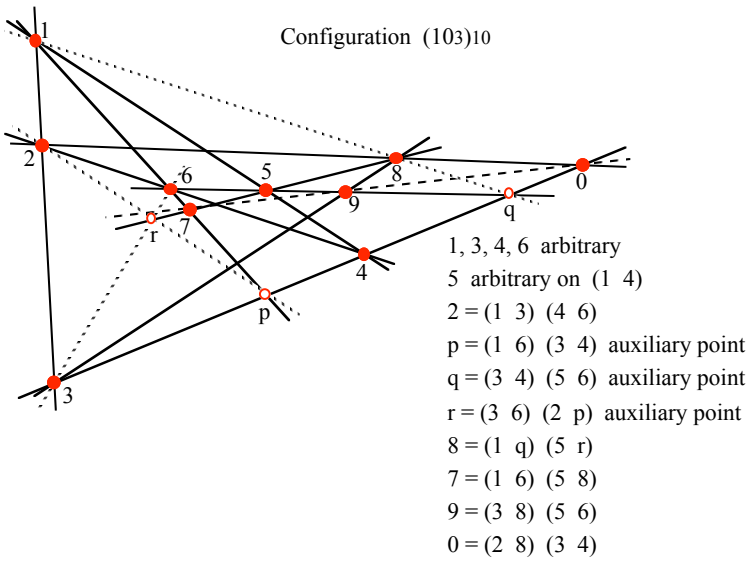

Figure 2.2.5. The construction of the nine geometric configurations (10_3) following Schroeter [S8].

For the combinatorial configuration $(10_3)_2$ we see that the triangles 246 and 357 are again perspective from point 1, but the sides of the triangles 246 and 375 (in that order!) intersect in the collinear points 8, 9 and 0, hence by Desargues they must be perspective from some point. This is a point p that is not a point of the configuration. The construction now follows. Note that in this case there are only 10 degrees of freedom.

Arguments of similar kinds can be made in the seven remaining cases. They are explained in detail in Schroeter [S8]. The steps outlined with each construction enable the determination of the degree of freedom of each configuration. The result -- after taking into account that projective transformations account for eight degrees of freedom, which are not deemed essential in the present context – is shown in Table 2.2.9.

$(10_3)_1$	$(10_3)_2$	$(10_3)_3$	$(10_3)_4$	$(10_3)_5$	$(10_3)_6$	$(10_3)_7$	$(10_3)_8$	$(10_3)_9$	$(10_3)_{10}$
3	2	2	--	1	2	2	1	1	1

Table 2.2.9. The number of degrees of freedom beyond projective transformations, for each of the geometric configurations (10_3).

Exercises and problems.

1. Since the configuration (7_3) is combinatorially unique, the configuration in Table 2.1.1 for n = 7 must be isomorphic with the configuration in Table 2.2.2. Find the mapping that transforms one into the other. The same task for Table 2.1.1 for n = 8 and Table 2.2.3.

2. Verify the entries for $(10_3)_2$, $(10_3)_4$, and $(10_3)_9$ in Table 2.2.8.

3. Justify the numbers in Table 2.2.9.

4. Explain and justify Schroeter's construction of the configurations $(10_3)_5$ and $(10_3)_6$.

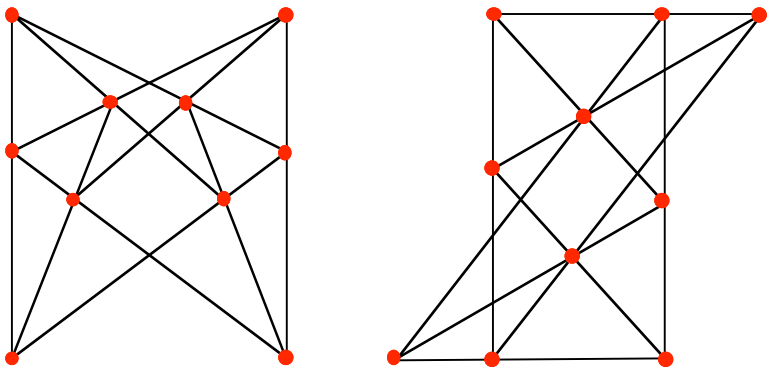

Figure 2.2.6. Two (10_3) configurations.

5. For each of the two configurations in Figure 2.2.6 decide whether it is a "fake". If not, find the coordinates of its points, and determine with which of the configurations in Figure 2.2.5 it is isomorphic.

6. Use the configurations tables of the (10_3) configurations to find the automorphism group of each.

7. Is there a topological realization of the $(10_3)_4$ configuration that has a nontrivial symmetry?

8. In Section 1.7 we demonstrated that the configuration $(10_3)_9$ has no geometric realization with nontrivial symmetry. What about the configuration $(10_3)_5$?

2.3 ENUMERATION OF 3-CONFIGURATIONS (Part 2)

Combinatorial configurations (11_3) were first enumerated by Martinetti [M2] in 1887; using the method we shall describe in the next section, he found that $\#_c(11) = 31$. The enumeration of these configurations was independently carried out by Daublebsky [D1] in 1894; he used a variant of the remainders method. Diagrams supposed to show geometric realizations of all 31 combinatorial configurations (that is $\#_g(n) = 31$) were provided by Daublebsky in an appendix to [D2] in 1895 (shown in Figure 2.3.1 below; see also Figure 2.3.2).

Daublebsky states that all these combinatorial configurations can be realized as geometric configurations (that is, with points and straight lines) given by his diagrams, but does not give any justification beyond the intimation that he followed the method of Schroeter [S8]. An independent verification of the geometric realizability of all 31 configurations (11_3) was provided only nearly a century later, by Sturmfels and White [S23], [S24] in 1988 and 1990, with a different method; we shall discuss this method a little later. Sturmfels and White also proved that each of these configurations can be realized in the rational plane, in other words, one can always draw the configurations so that the vertices are at points of the integer lattice. The value of $\#_c(11) = 31$ was independently confirmed by Gropp (see [G8]) and by Betten *et al.* [B14], among others.

* * * * * The first enumeration of the combinatorial configurations (12_3) was carried out by Daublebsky [D2] in 1895, again using the method of remainder figures. He found that only 18 different remainder figures could possibly occur in such a configuration. Through various arguments (described only in general terms) Daublebsky arrived to the conclusion that these remainder figures could be combined to yield something like 1600 configurations (12_3). Then he "… drew a schematic diagram of each configuration on a separate piece of paper …" and determined for each the "remainder system", that is, a list of the different remainder figures occurring in the configuration. Finally, configurations with the same remainder system were investigated to see whether they are isomorphic. This turned out to be the case in most—but not all—cases

(see Exercises 2.3.4 and 2.3.5). Daublebsky presented the resulting 228 combinatorial configurations by their configurations tables (in the form he gave them, these take 23 pages!!!). He also gave some other data and provided drawings for geometric realizations of a few of the configurations. In a later paper [D3], Daublebsky gave results of his investigations of the groups of automorphisms of each of the 228 combinatorial configurations (12_3). However, not all of these are correct. The first independent enumeration of the combinatorial (12_3) configurations was carried out only in 1990, by Gropp (see [G8]). It showed that Daublebsky missed one, so that there are in fact $\#_c(12) = 229$ such configurations. Gropp published the configuration table of this additional configuration in [G13] and communicated it to me; the table can also be read off from the illustrations in the more readily available [D10] and [G25]. As with configurations (11_3), the 229 combinatorial configurations (12_3) have been independently enumerated (by two different methods) in [B14]. Even so, Dolgachev [D8] in 2004 still quotes $\#_c(12) = 228$.

The only published proof that all 228 combinatorial configurations (12_3) found by Daublebsky are geometrically realizable was given only recently, by Sturmfels and White [S23], [S24]. Sturmfels and White also proved that all these (12_3) configurations are realizable in the rational plane. In a private communication, B. Sturmfels showed that the "new" combinatorial configuration found by Gropp is also geometrically realizable, even in the rational plane; a diagram is shown in Dorwart – Grünbaum [D10] in 1992.

The numbers $\#_c(n)$ of combinatorial configurations for $13 \le n \le 19$ were determined by various computer programs. For $12 \le n \le 14$ these values were first found by Gropp [G8], for $n = 15$ by Betten and Betten, [B11]; the values for $16 \le n \le 18$ in Table 2.2.1 are from Betten, Brinkmann and Pisanski [B14]. The value $\#_c(19) = 7{,}640{,}941{,}062$ was determined by these authors and published in [B19] and [G46]. However, there is no information available about the possibilities of realization of the combinatorial configurations (n_3) for $n \ge 13$ by topological or geometric configurations, beyond individual exam-

ples — these will be discussed in the following sections. This is not very surprising in

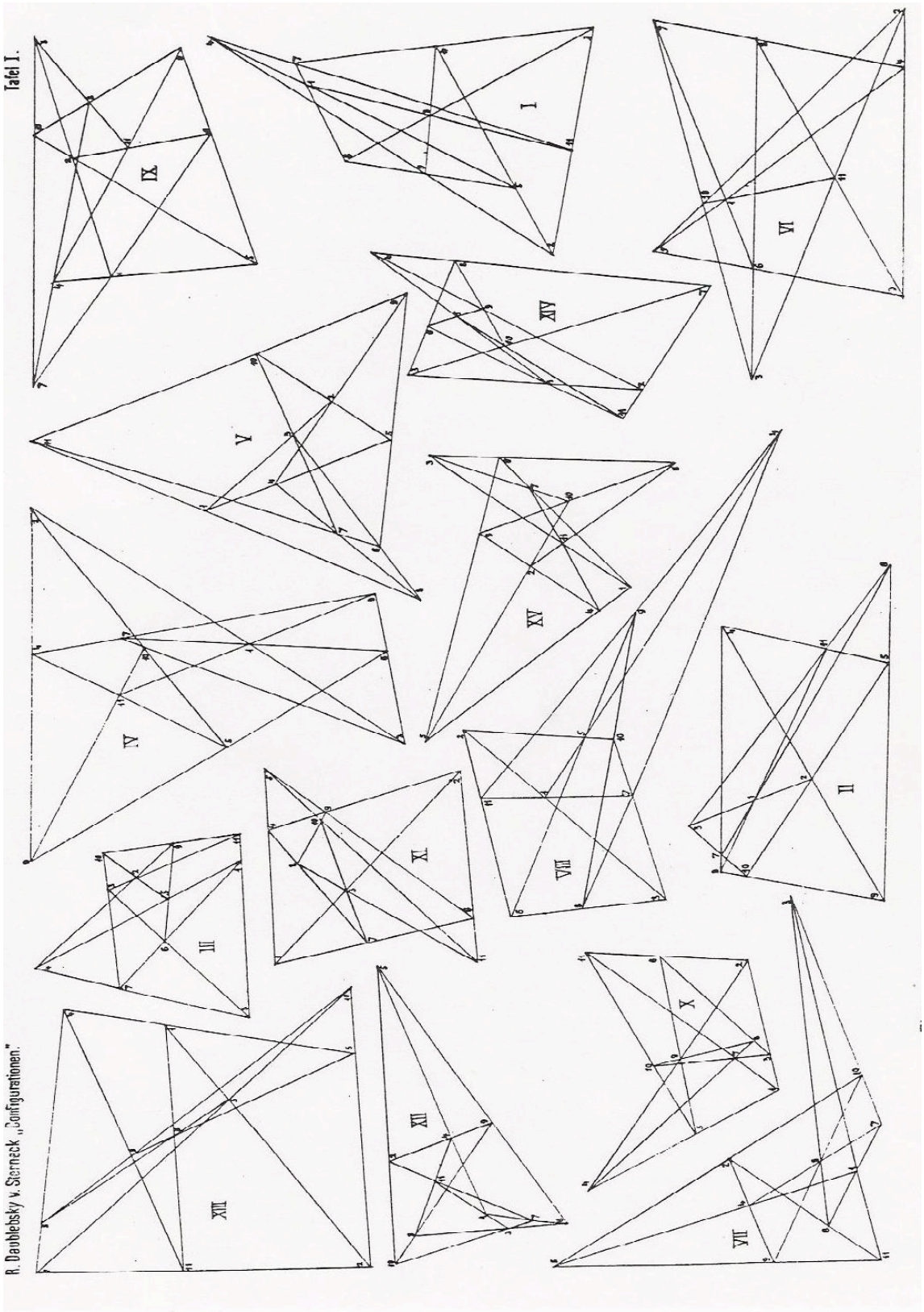

Figure 2.3.1. (first half).

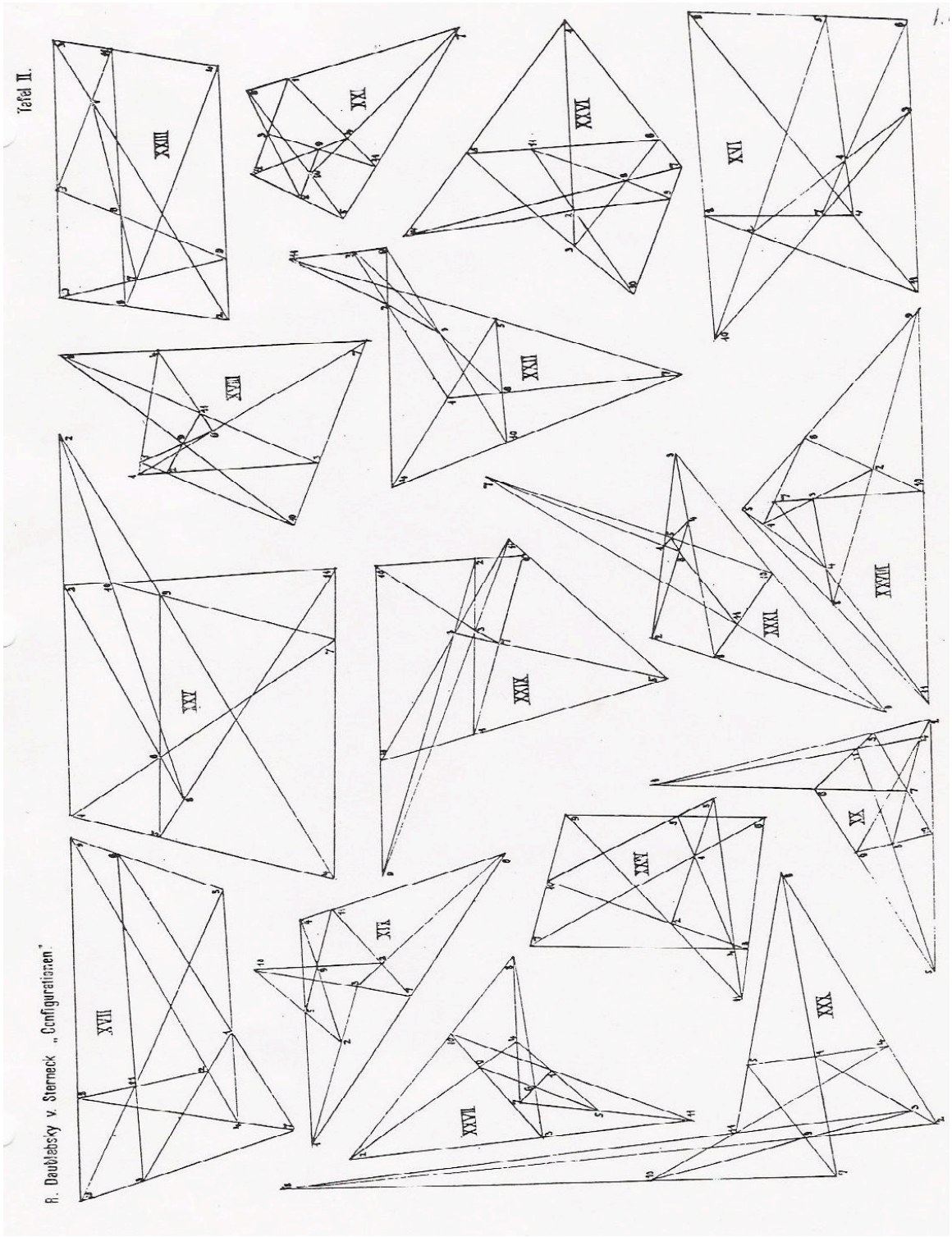

Figure 2.3.1 (second half). The diagrams of the (11_3) configurations, from Daublebsky [D2].

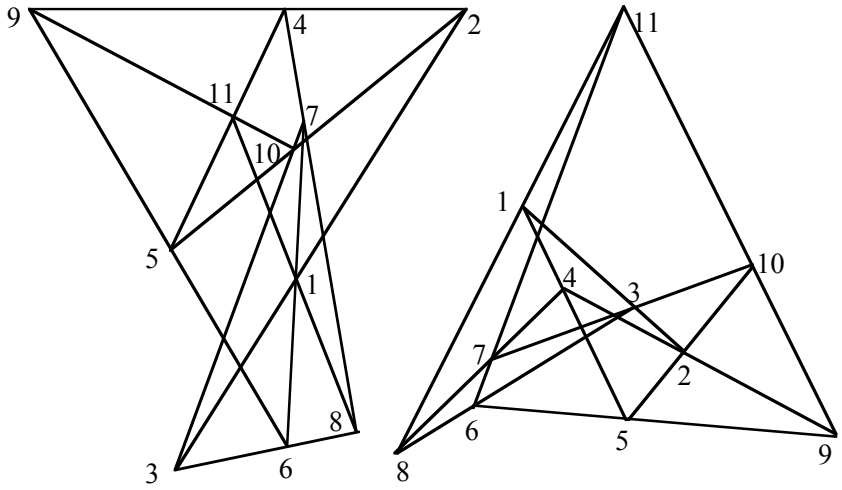

Figure 2.3.2. Diagrams of Daublebsky's configurations $(11_3)_4$ and $(11_3)_5$ redrawn for better visibility.

view of the number of combinatorial configurations. As shown in Table 2.2.1, this number is well above 2000 for n = 13, and increases by factors exceeding 10 for larger n.

This completes the discussion of the data in Table 2.2.1. The only additional information that is available is that $\#_c(n) > \#_t(n)$ for all $n \geq 14$, and that $\#_t(n) > \#_g(n)$ for all $n \geq 16$. The former happens due to the existence of **disconnected configurations** – that is, configurations that are disjoint unions of two or more configurations, between the elements of which there are no incidences.

As an example, consider the (14_3) which consists of two disjoint copies of the Fano configuration (7_3), or the (15_3) formed by disjoint copies of (7_3) and (8_3); the latter was implicitly recognized as disconnected by Betten and Betten [B11], the former is explicitly mentioned by Gropp [G7]. Since disconnected configurations arise as unions of smaller configurations, it is easy to determine the number of such configurations for all $n \leq 19$. Since the (7_3) and (8_3) set-configurations are not geometrically realizable, the smallest geometrically realizable disconnected configurations are the six arising as unions of two configurations (9_3). The same is true for topological configurations.

On the other hand, the inequality between the numbers $\#_t(n)$ and $\#_g(n)$ of topological and geometric configurations for $n \geq 16$ is a consequence of the existence of topological configurations of the kind illustrated by the scheme in Figure 2.3.3. Due to the theorem of Pappus, if this configuration scheme is rendered with straight lines instead of line segments, the points A_2, B_2, C_2, and F_3 are seen to be collinear. Hence this is a superfiguration and not a geometric configuration; clearly, this is not a problem if pseudolines are used. This example can be understood as arising by a "melding" of the Pappus configuration $(9_3)_1$ and the Fano configuration (7_3). (Note that the Fano part is missing one incidence, and this subfiguration is realizable by straight lines.) This construction can be modified in various ways. For example, instead of the Fano configuration one could use any (n_3) configuration, and instead of the Pappus configuration one could use Desargues' configuration $(10_3)_1$. This completes the proof of $\#_t(n) > \#_g(n)$ for all $n \geq 16$. It is not known whether $\#_t(n) = \#_g(n)$ for $n = 13, 14, 15$.

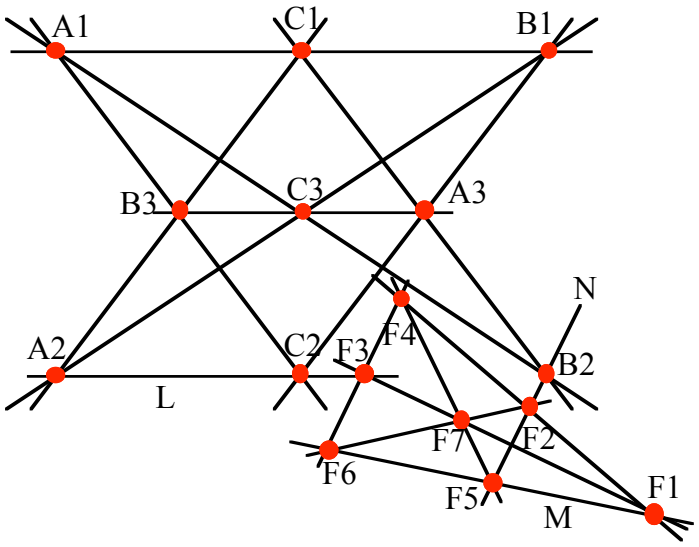

Figure 2.3.3. Pappus' theorem implies that the points A_2, B_2, C_2, and F_3 are collinear, hence this does not realize a configuration (16_3). It is obvious that using pseudolines the unwanted incidence can be avoided.

This ignorance is part of a larger open question. The single example establishing $\#_t(10) > \#_g(10)$ differs in one important respect from the examples just given with $n \geq 16$: The latter are only 2-connected, while the combinatorial and topological $(10_3)_4$ is 3-connected. The lack of any other 3-connected examples leads to

Conjecture 2.3.1. Every 3-connected topological configuration (n_3) with $n \geq 11$ is geometrically realizable.

* * * * *

The Schroeter constructions explained and illustrated above would nowadays be said to be *generic* constructions, the terminology supposing to indicate that it applies in run-of-the-mill situations. In fact, if understood literally — that all the choices can be made arbitrarily, with only the stated restrictions — the constructions may fail to lead to the *configurations* they are supposed to yield. Instead, *superfigurations* may result due to "accidental" incidences. This is illustrated in Figure 2.3.4.

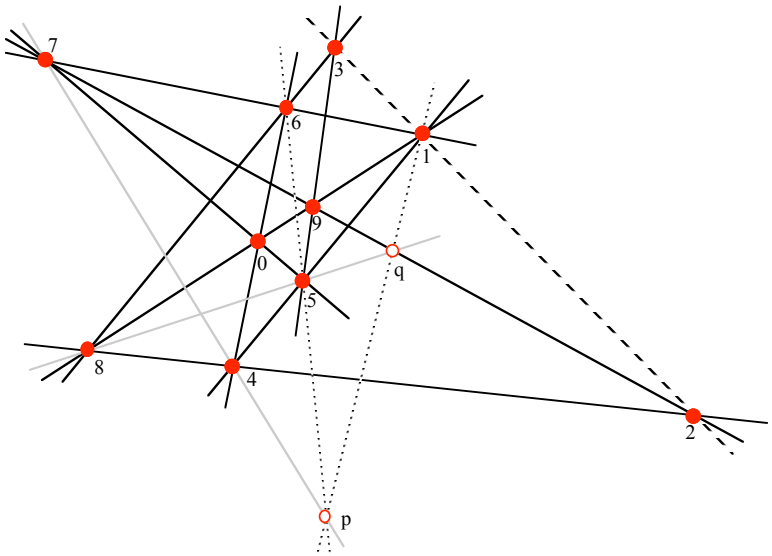

Figure 2.3.4. Failure of the Schroeder construction of the configuration $(10_3)_3$: The line 890 contains the point 1. Notation is the same as in Figure 2.2.5.

It is hard to understand that no publication on configurations during the classical period even mentioned the possibility of superfigurations arising in the construction of geometric configurations. This is astonishing since the study of accidental incidences in

the Desargues configuration was already old hat at that time. In Figure 2.3.5 we show a Desargues superfigurations, with a line on four points and a point on four lines. The exceptional point and line are shown in contrasting color. In the paper [S22] Sternfeld *et al.* study possible superfigurations of (10_3) configurations (and more general incidence systems), both combinatorial and geometric. We conjecture:

Conjecture 2.3.2. Every geometric configuration (n_3) with $n \geq 10$ admits superfigurations with at least one pair of "accidental" incidences.

It is worth mentioning that the three (9_3) configurations do not have limiting positions that are superfigurations. On the other hand, the Pappus configuration $(9_3)_1$ has representatives in which an additional point incident with three lines, or a line incident with three of the points, or both, can be found. The last alternative is illustrated in Figure 2.3.6. It is not known whether many other configurations have this property.

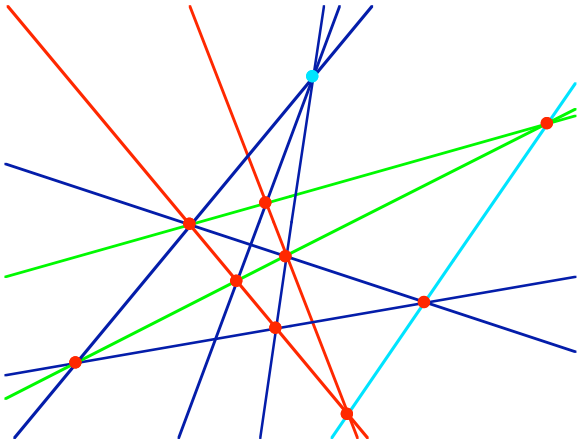

Figure 2.3.5. A superfiguration arising from the Desargues configuration $(10_3)_1$ through multiple incidences. The point and line of perspectivity are shown in teal.

1. Find the remainder systems of Daublebsky's configurations $(11_3)_4$ and $(11_3)_5$ shown in Figure 2.3.2, and use them to show that these are distinct configurations.

3. Find a superfiguration of the Desargues configuration that has three points and three lines incident with four elements of the other kind — or prove that such a configuration cannot exist.

4. Consider the two (12_3) configurations from Daublebski's paper [D2] shown in Figure 2.3.7, with their labels as given by Daublebski. Although they are tantalizingly similar, show that they are not isomorphic.

5. Determine whether the two (12_3) configurations in Figure 2.3.8 are isomorphic, and whether any is isomorphic with either of the configurations in Figure 2.3.7.

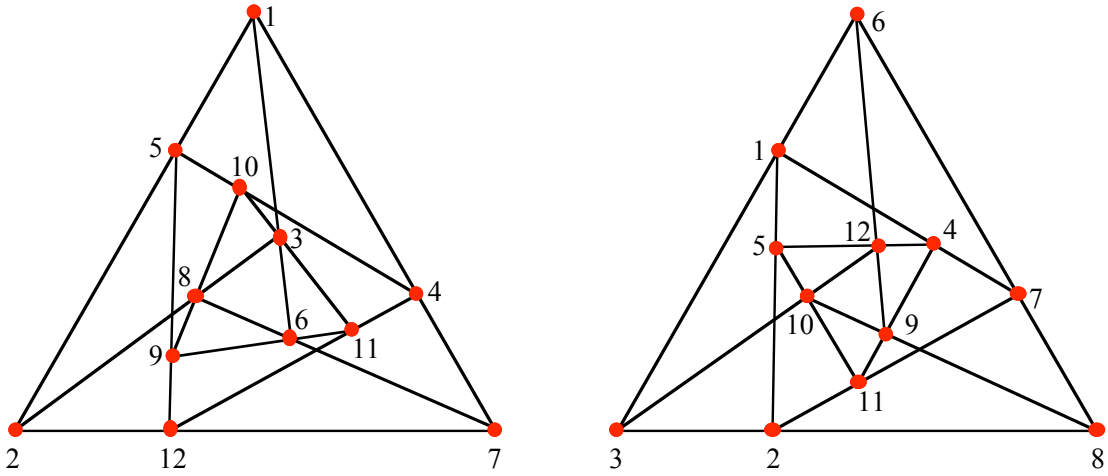

Figure 2.3.7. Two configurations (12_3) from [D2].

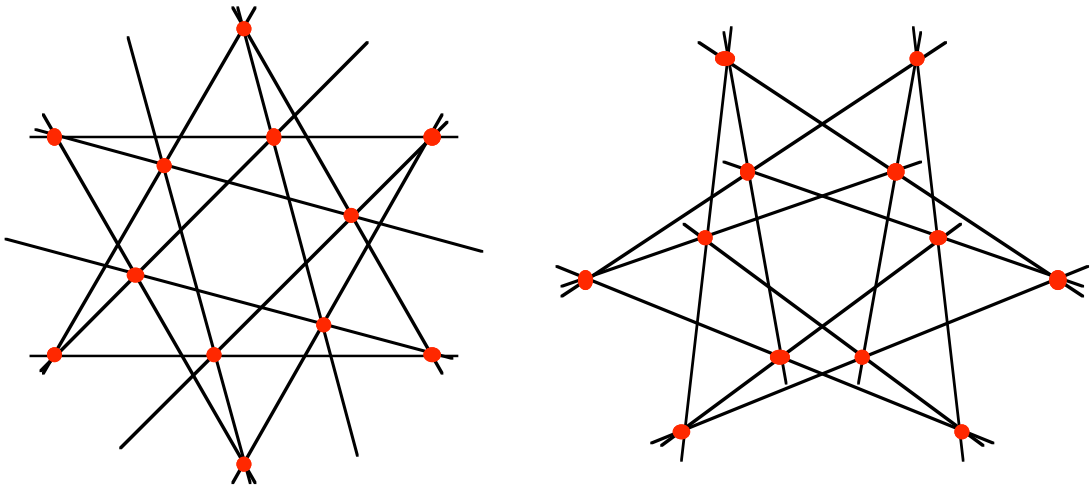

Figure 2.3.8. Two (12_3) configurations.

2.4 GENERAL CONSTRUCTIONS FOR COMBINATORIAL 3-CONFIGURATIONS

From the start of investigations of configurations, the problem of constructing all configurations (n_3) for each value of n attracted considerable attention. Many of the results on that topic have been presented in Sections 2.2 and 2.3 for specific small values of n. However, already in 1887 Martinetti [M2] described an inductive procedure that can be used to generate the (n_3) configurations if all configurations with fewer points are known. He illustrated his method by determining all configurations (n_3) with $n \leq 11$, starting from the Fano configuration (7_3). As mentioned in Section 2.3, his enumeration of the 31 configurations (11_3) was correct. However, one of his claims was unfounded: He considered the enumeration of geometric configurations (n_3) to be the same as the enumeration of the combinatorial (n_3). This claim was also stressed in the review [L54] of [M2] by E. K. Lampe. As we have seen, $\#_c(n) = \#_g(n)$ for $n = 11$ and 12, but not for $n = 10$ and certainly $\#_c(n) \neq \#_g(n)$ for all $n \geq 14$. In the remaining part of this section, we consider *only* combinatorial configurations, even though we speak of "points" and "lines".

The central idea of Martinetti's construction is the following: Assume that in a combinatorial (n_3) configuration we have two "parallel" lines (that is, lines of the configuration that have no point of the configuration in common). If [A, A', A"] and [B, B', B"] are such lines and if A and B are on no line of the configuration, then we delete the two parallel lines and introduce a new point C, together with the three lines [A, B, C], [A', A", C], [B', B", C]. This is illustrated in Figure 2.4.1. Clearly, this leads to a combinatorial configuration $((n+1)_3)$. A configuration is called **reducible** if it can be obtained from a smaller one by the process just described; otherwise it is **irreducible**. Martinetti's main result is the claim that for each n there are very few

irreducible (n_3) configurations, and he purports to give a complete description of all irreducible configurations. More precisely:

Martinetti's claim. A connected (n_3) combinatorial configuration is irreducible if and only if it is one of the following:

(i) The cyclic configuration $\mathscr{C}_3(n)$ with lines $[j, j+1, j+3]$ (mod n), for $n \geq 8$;

(ii) $n = 10m$ for some $m \geq 1$, and the configuration is the one described below and denoted $M(m)$; $M(1)$ is the Desargues configuration $(10_3)_1$.

(iii) $n = 9$, and the configuration is the Pappus configuration $(9_3)_1$.

(iv) $n = 10$, and the configuration is $(10_3)_2$ or $(10_3)_6$.

Martinetti's combinatorial configuration $M(m)$ can best be explained as consisting of m copies of the family of the ten points indicated by solid dots in Figure 2.4.2, and the ten solid lines shown there. The j^{th} copy is joined to the $(j+1)^{st}$ by identifying A'''_j , B'''_j , C'''_j with A_{j+1}, B_{j+1}, C_{j+1}, respectively; all subscripts taken (mod n).

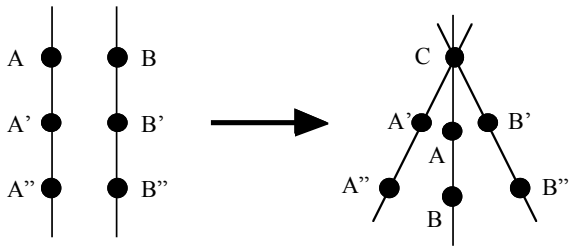

Figure 2.4.1. Martinetti's addition of a point and a line to a combinatorial configuration (n_3).

Martinetti's proof is, not surprisingly, involved and long. The result was quoted or mentioned many times over the next century; see, for example, Steinitz [S19, pp. 486-487], Steinitz-Merlin [S21, pp. 153 – 154], Gropp [G7], [G8], [G25], [G30], Carstens *et al.* [C1]. In some of these it was noticed that Martinetti should have included con-

nectedness among the requirements of his claim. Moreover, in lecture notes for my configurations courses in 1999 and 2002 I wrote:

> I have not checked the details, and I do not know it as a fact that anybody has. The statement has been accepted as true for these 115 years, and it may well be true. On the other hand, Daublebski's enumeration of the (12_3) configurations was also considered true for a comparable length of time ...

As it turned out, my suspicion has been vindicated by Boben [B16], [B17]. He showed that Martinetti's list of irreducible configurations is incomplete. The problem in Martinetti's proof arises as follows. When constructing $\mathsf{M}(m)$, we attach to each other m copies of the "module" in Figure 2.4.2 as indicated above, but stop before attaching $\mathsf{M}(m)$ to $\mathsf{M}(1)$. Martinetti formed that attachment "straight", by identifying A'''_n with A_1, and similarly for the B's and C's, thus obtaining $\mathsf{M}(m)$. However, as shown by Boben, that attachment can be done in "twisted" ways as well; two such attachments yield irreducible configurations which we may denote by $\mathsf{M}^*(m)$ and $\mathsf{M}^{**}(m)$. These are obtained by identifying A'''_n with C_1, B'''_n with B_1, and C'''_n with A_1 for the former, and A'''_n with C_1, B'''_n with A_1, and C'''_n with B_1 for the latter. A separate argument shows that the three resulting configurations are non-

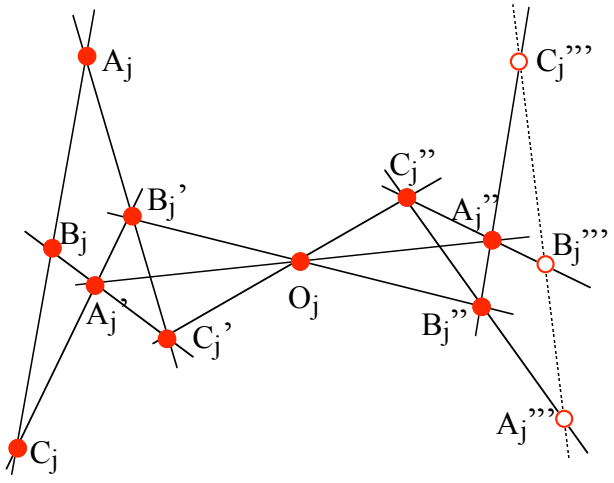

Figure 2.4.2. The "module" used in the Martinetti construction. Only the ten solid dots and the ten solid lines form one module.

isomorphic for every m. With this modification, we have the following corrected version of Martinetti's result:

Theorem 2.4.1. (Boben [B16], [B17]) A connected (n_3) combinatorial configuration is irreducible if and only if it is one of the following:

(i) The cyclic configuration $\mathscr{C}_3(n)$ with lines $[j, j+1, j+3] \pmod n$, for $n \geq 7$;

(ii) $n = 10m$ for some $m \geq 1$, and the configuration is one of $M(m)$, $M^*(m)$ or $M^{**}(m)$ described above. For $m = 1$ these are the configurations $(10_3)_1$, $(10_3)_2$ and $(10_3)_6$ (in the notation used in Section 2.2).

(iii) $n = 9$, and the configuration is the Pappus configuration $(9_3)_1$.

A remarkable aspect of the situation is that all the irreducible configurations (n_3) with $n \geq 9$ are geometrically realizable by straight lines in the Euclidean plane. For the cyclic configurations we have seen this in the proof of Theorem 2.1.3. A different construction, involving cubic curves, was given by Schroeter [S6] in 1888. For the configurations $M(m)$ the realizability is almost obvious from Figure 2.4.2, and can be proved in general.

Concerning configurations (n_3) for particular values of $n \geq 13$, there is very little specific information available in print. Gropp [G13] applied Martinetti's theorem to enumerate the combinatorial configurations with up to 14 points. He reports that there are 2036 combinatorial configurations (13_3), and 21,399 combinatorial configurations (14_3). These numbers were confirmed by [B14]; this paper reports the numbers $\#_c(n)$ of combinatorial configurations (n_3) for $n \leq 18$, see Table 2.2.1. The number $\#_c(19)$ was reported in [B19] and [G46].

One of the combinatorial configurations (14_3) consists of two disjoint copies of the (7_3) configuration, and is therefore not geometrically realizable. It is not known whether the other (13_3) and (14_3) combinatorial configurations are geomet-

rically realizable. Clearly, analogous disconnected and non-realizable configurations exist for all $n \geq 14$. However, even if considering only connected configurations, the statement in Steinitz [S19, p.490] and Steinitz-Merlin [S21, p.158] that for $n \geq 11$ all (n_3) combinatorial configurations are "probably realizable" is contradicted by the example in Figure 2.2.8 (from [D10], see also Gropp [G25]), which shows that the statement is invalid even if restricted to configurations that are "connected" and "realizable by pseudolines". (In the example in Figure 2.2.8, the left part of the figure has all but one of the incidences of the Pappus configuration, and therefore by Pappus' theorem the line L must be incident with the point P.) It is not known whether the (16_3) in Figure 2.2.8 is the smallest configuration with these properties. We shall discuss this and related question in Sections 2.5 and 2.6 dealing with a remarkable result of Steinitz.

* * * * *

Levi [L3, p. 93] mentions the possibility of obtaining a combinatorial configurations $((n+1)_3)$ from the configurations (n_3). He achieves this by manipulating Levi incidence matrices in a way that is equivalent to the Martinetti method illustrated in Figure 2.4.1. However, Levi does not mention Martinetti, or irreducible configurations — nor does he claim that all $((n+1)_3)$ configurations are obtainable in this way.

Exercises and problems 2.4.

1. Prove that all the irreducible configurations with at least nine points specified in Theorem 2.4.1 are geometrically realizable by points and straight lines.

2. Decide whether the (12_3) configurations in Figures 2.3.7 and 2.3.8 are reducible or irreducible. If any is reducible, to which irreducible one does it ultimately reduce? Is it possible for one configuration to reduce to different irreducible configurations?

3. Investigate the reducibility of the cyclic configurations $\mathscr{C}_3(n,1,4)$.

4. Give a formulation of Theorem 2.4.1 that is valid for all 3-configurations.

2.5 STEINITZ'S THEOREM – THE COMBINATORIAL PART

As we have seen in previous sections, the question whether a given combinatorial (or topological) 3-configuration can be geometrically realized is very hard. This is the reason the 1894 PhD thesis of Ernst Steinitz [S17] is remarkable in its generality: Although Steinitz fails in completely characterizing the realizability of combinatorial or topological 3-configurations, he come as close to doing so as anybody since then.

Steinitz's claim (in our terminology). Every connected combinatorial 3-configuration (n_3) has a geometric realization by points and lines as a #1-subfiguration in the Euclidean plane; moreover, the point and line of the ignored incidence can be arbitrarily chosen.

Recall from Section 1.3 that a *#1-subfiguration* of a combinatorial configuration is a family of points and (straight) lines that satisfies all the incidence requirements except possibly one that is ignored, and has no additional incidences.

In the next section we shall see that this claim is not correct. However, even the weaker result that Steinitz' arguments actually establish (see Theorem 2.6.1) is remarkable in several ways. Steinitz' proof has two parts, a combinatorial and a geometric. The combinatorial part is correct, and was much ahead of its time. However, the geometric part is defective; we discuss this in the next section. We start with the combinatorial part of Steinitz' theorem, and first recall from Section 1.3 a useful definition.

A configuration table for a combinatorial configuration is said to be **orderly** if every row of the table contains all the points (hence contains each precisely once). For example, the configuration table in Table 2.1.1 is orderly, and the configuration tables in Sections 1.3 and 2.2 are not orderly.

The following is a basic result, due to Steinitz [S17].

Theorem 2.5.1. Every combinatorial k-configuration admits an orderly configuration table.

A statement that Theorem 2.5.1 holds for $k = 3$ appears in Martinetti [M2], without any justification or hint of proof. The majority of later writers do not mention the result – much less its proof – although many seem to accept it as selfevident. On the other hand, the statement in Page and Dorwart [P1] regarding this result is incorrect, as are the consequences deduced by them from the erroneous statement. It is interesting, as stressed by Gropp [G26], that Steinitz's result is very well known in combinatorics, but under a different name and credited to other people. It is considered a part of the branch of combinatorics called *matching theory*. (For this discussion, a *matching* in a graph is a collection of disjoint edges that contain all the nodes.) In this guise Steinitz's result from 1894 was independently discovered by König [K13] in 1916; in modern terminology König's theorem can be formulated it as: *Every bipartite graph having all nodes of the same valence has a matching*. This statement is completely equivalent with Theorem 2.5.1, although neither König nor many later writers seem to have been aware of Steinitz's theorem. In still another guise, Steinitz's theorem has been generalized by the theorem of P. Hall [H1] in 1935 concerning the existence of systems of distinct representatives. For details and proofs see, for example, Roberts [R5, Chapter 12] or Brualdi [B29, Chapter 9]. None of these authors is aware of Steinitz either, although the idea of Steinitz's proof is central to the topic.

We shall start by presenting a proof of this result, and then discuss some of its corollaries. Our proof is modeled after Steinitz's presentation, but using what I hope is a better notation. For easier understanding of the proof, a worked-out example is given later in the section. Except for the names of the points and lines, the steps in the example are precisely parallel to those of the proof. In contrast to most of the proofs of the equivalent results mentioned in the preceding paragraph, Steinitz's proof is constructive; it can be used to find effectively an orderly configuration table, convenient for geometric constructions. We shall see such an application in Section 5.2.

Given a fixed combinatorial configuration (n_k), the first goal is to define a 1-to-1 correspondence between points and lines such that each point is incident with (that is, is contained in) the corresponding line. If we have such a correspondence the first step in the proof is complete. We can certainly start constructing the correspondence by a

greedy algorithm: We pick an arbitrary point and pair it with one of the lines that are incident with it; then we chose a point not on this line, and assign it to one of the lines containing it, then a point on neither of these lines, etc. Continuing with such a selection as long as possible, we find ourselves at the end in the following situation (adjusting the notation as appropriate and convenient):

The points in a subset $\mathcal{A} = \{a_1, a_2, \ldots, a_p\}$ of the set of configuration points have been assigned to the lines of the subset $\mathbf{A} = \{A_1, A_2, \ldots, A_p\}$ of the set of configuration lines, so that $a_j \in A_j$ for $j = 1, 2, \ldots, p$. We can assume that $p < n$, since otherwise we would be done with the first part of the proof. Hence there is a set $\mathcal{B} = \{b_1, b_2, \ldots, b_q\}$ of points of the configuration, and a set $\mathbf{B} = \{B_1, B_2, \ldots, B_q\}$ of lines of the configuration, such that no point in $\mathcal{B}$ is incident with any line in $\mathbf{B}$; clearly, $q = n - p$. Now we shall describe a procedure by which we shall change some of the assignments between points in $\mathcal{A}$ and lines in $\mathbf{A}$, so that it will be possible to modify and extend the assignment to include one point in $\mathcal{B}$ and one line in $\mathbf{B}$.

Let B be an arbitrarily chosen line in $\mathbf{B}$, and let $\mathcal{A}_0$ be the subset of $\mathcal{A}$ consisting of the points of B. We denote by $\mathbf{A}_0$ the set of lines in $\mathbf{A}$ that are associated with the points of $\mathcal{A}_0$. Let $\mathcal{A}_1 \subseteq \mathcal{A} \setminus \mathcal{A}_0$ be the set of points of $\mathcal{A}$ not in $\mathcal{A}_0$ that are on lines of $\mathbf{A}_0$, and let $\mathbf{A}_1$ be the set of lines associated with the points in $\mathcal{A}_1$. Next, let $\mathcal{A}_2 \subseteq \mathcal{A}\setminus(\mathcal{A}_0 \cup \mathcal{A}_1)$ be the set of points of $\mathcal{A}$ not in $\mathcal{A}_0 \cup \mathcal{A}_1$ that are on lines of $\mathbf{A}_1$, and let $\mathbf{A}_2$ be the set of lines associated with the points in $\mathcal{A}_2$. We continue with assignments of this kind till we reach an r such that $\mathcal{A}_{r+1}$ is empty. This clearly has to happen due to the finiteness of the configuration. Let now $\mathcal{A}^* = \mathcal{A}_0 \cup \mathcal{A}_1 \cup \ldots \cup \mathcal{A}_r$ and $\mathcal{A}^{**} = \mathcal{A}\setminus\mathcal{A}^*$. Note that $\mathcal{A}^*$ is the **disjoint** union of the sets $\mathcal{A}_0, \mathcal{A}_1, \ldots, \mathcal{A}_r$. Let $\mathbf{A}^*$ and $\mathbf{A}^{**}$ be the sets of lines associated with the points in $\mathcal{A}^*$ and $\mathcal{A}^{**}$, respectively.

We now pick a line $L_0 \in \mathbf{A}_0 \cup \mathbf{A}_1 \cup \ldots \cup \mathbf{A}_r$ such that L_0 is incident with at least one point b of $\mathcal{B}$, so that $b \in L_0$. (Such a line always exists, by a simple counting argument that will be given below.) Let p_0 be the point of $\mathcal{A}^*$ that corresponds to L_0; then p_0 belongs to a well-determined set $\mathcal{A}_s$ for some $s \in \{0, 1, \ldots, r\}$. Then $p_0 \in L_1$ for some $L_1 \in \mathbf{A}_{s-1}$, and let p_1 be the point of $\mathcal{A}_{s-1}$ that corresponds to L_1. Continuing

in this way we reach a line $L_S \in A_0$ and the corresponding point $p_S \in \mathcal{A}_0$. Finally, there is a line $B \in \mathbf{B}$ such that $p_S \in B$. Notice that we have the chain of incidences and correspondences

$$b \in L_0 \leftrightarrow p_0 \in L_1 \leftrightarrow p_1 \in \ldots \in L_S \leftrightarrow p_S \in B.$$

Next, we change *for the points of this chain* the assignments with which we started by making b correspond to L_0, p_0 to L_1, p_{S-1} to L_S, and p_S to B. Thus we have now a new 1-to-1 correspondence which decreased the size of the sets $\mathcal{B}$ and $\mathbf{B}$.

Repeating the procedure a finite number of times leads to an assignment of every point of the configuration to a line that is incident with it; this completes the first step of the proof, except for the demonstration of the assertion that we always can pick a line $L_0 \in \mathbf{A}^*$ which contains a point of $\mathcal{B}$. If this were not the case then all points of $\mathcal{B}$ would have to belong to $\mathbf{A}^{**}$, since they do not belong to lines in $\mathbf{B}$ either. But this is not possible, since the cardinalities of $\mathcal{A}^{**}$ and $\mathbf{A}^{**}$ are the same due to the correspondence established at the beginning, and all incidences of points in $\mathcal{A}^{**}$ are with lines in $\mathbf{A}^{**}$ and vice versa — implying that no line in $\mathbf{A}^{**}$ can be incident with any point of $\mathcal{B}$.

For the second step we rewrite the configuration table in such a way that for each line (that is, each column) the point assigned to it is in the first row. Then the first row contains all the points, each once. The other rows of the configuration table form now a configuration (n_{k-1}), for which we repeat the steps we just did for the original configuration. Continuing in this way, we clearly reach an orderly configuration table in a finite number of steps. □

It may be mentioned that when we have only two rows to deal with, a simple interchange of the order of the entries in some columns may be used instead of the more complicated procedure used in the general case.

We next illustrate the algorithm used in the proof of Theorem 2.5.1 by an example, the construction of an orderly configuration table for the combinatorial configuration (14_4) given below.

A	B	C	D	E	F	G	H	J	K	L	M	N	P.
a	a	a	a	b	b	b	c	c	c	d	d	d	e
b	f	g	h	g	h	e	h	e	f	e	f	g	f
c	k	n	p	k	m	p	k	m	n	k	q	m	g
d	m	r	q	q	n	r	r	q	p	n	r	p	h

We select the starting assignments as follows:

A	B	C	D	E	F	G	H	J	K	L	M	N	$\mathbf{A}$
a	f	g	h	b	m	e	c	q	n	d	r	p	$\mathcal{A}$

and rewrite the table as

A	B	C	D	E	F	G	H	J	K	L	M	N	P
a	f	g	h	b	m	e	c	q	n	d	r	p	e
b	a	a	a	g	b	b	h	c	c	e	d	d	f
c	k	n	p	k	h	p	k	e	f	k	f	g	g
d	m	r	q	q	n	r	r	m	p	n	q	m	h

so that the assigned points are in the first row for better visibility. We are left with

$\{k\} = \mathcal{B}$ $\{P\} = \mathbf{B}$.

We put:

$\mathcal{A}_0$ = {e, f, g, h} = set of points on P, which happens to be the only line of $\mathbf{B}$. Then

$\mathbf{A}_0$ = {G, B, C, D} = associated set of lines of $\mathbf{A}$.

$\mathcal{A}_1$ = {b, p, r, a, m, n, q} = points of $\mathcal{A} \setminus \mathcal{A}_0$ on lines of $\mathbf{A}_0$.

$\mathbf{A}_1$ = {E, N, M, A, F, K, J} = associated set of lines of $\mathbf{A}$.

$\mathcal{A}_2$ = {d, c} = points of $\mathcal{A} \setminus (\mathcal{A}_0 \cup \mathcal{A}_1)$ on lines of $\mathbf{A}_1$.

$\mathbf{A}_2$ = {L, H} = associated set of lines of $\mathbf{A}$. Finally

$\mathcal{A}_3$ = empty.

Hence we have

$\mathcal{A}^* = \mathcal{A}_0 \cup \mathcal{A}_1 \cup \mathcal{A}_2$ = {a, b, c, d, e, f, g, h, m, n, p, q, r}

$\mathcal{A}^{**} = \mathcal{A} \setminus \mathcal{A}^{*}$ in this case empty but need not be empty in general.

Now we pick a line of $\mathbf{A}_0 \cup \mathbf{A}_1 \cup \mathbf{A}_2$ that contains an element of $\mathcal{B}$. In our case there is only one such element, k, and we have a choice of lines: B, E, or L. In each case we can form a chain:

$k \in B \leftrightarrow f \in P$ or

$k \in E \leftrightarrow b \in G \leftrightarrow e \in P$ or

$k \in L \leftrightarrow d \in N \leftrightarrow p \in G \leftrightarrow e \in P$ and use it to change the assignments.

We use the last, and it leads to a rewritten table:

A	B	C	D	E	F	G	H	J	K	L	M	N	P
a	f	g	h	b	m	p	c	q	n	k	r	d	e
b	a	a	a	g	b	e	h	c	c	d	d	p	f
c	k	n	p	k	h	b	k	e	f	e	f	g	g
d	m	r	q	q	n	r	r	m	p	n	q	m	h

Now we deal in the same way with the last three rows.

A	B	C	D	E	F	G	H	J	K	L	M	N	
b	a	n	p	g	h	e	k	c	f	d	q	m	$\mathcal{A}$

Then we are left with

$\{r\} = \mathcal{B}$ $\{P\} = \mathbf{B}$

This time we put:

$\mathcal{A}_0 = \{f, g, h\}$ = set of points on a line (P) of $\mathbf{B}$.

$\mathbf{A}_0 = \{K, E, F\}$ = associated set of lines in $\mathbf{A}$.

$\mathcal{A}_1 = \{c, p, k, q, b, n\}$ = points of $\mathcal{A} \setminus \mathcal{A}_0$ on lines of $\mathbf{A}_0$.

$\mathbf{A}_1 = \{J, D, H, M, A, C\}$ = associated set of lines in $\mathbf{A}$.

$\mathcal{A}_2 = \{e, m, d, a\}$ = points of $\mathcal{A} \setminus (\mathcal{A}_0 \cup \mathcal{A}_1)$ on lines of $\mathbf{A}_1$.

$\mathbf{A}_2$ = {G, N, L, B} = corresponding set of lines in $\mathbf{A}$.
$\mathcal{A}_3$ = empty.

Then we put:

$\mathcal{A}^* = \mathcal{A}_0 \cup \mathcal{A}_1 \cup \mathcal{A}_2$ = {a, b, c, d, e, f, g, h, m, n, p, q, r}

$\mathcal{A}^{**} = \mathcal{A} \backslash \mathcal{A}^*$ = in this case empty (need not be empty in general) .

Now we pick a line of $\mathbf{A}_0 \cup \mathbf{A}_1 \cup \mathbf{A}_2$ that contains an element of $\mathcal{B}$.

In our case there is only one such element, r, and we have a choice of the lines C and G. In each case we can form a chain:

$r \in C \leftrightarrow n \in F \leftrightarrow h \in P$

$r \in G \leftrightarrow e \in J \leftrightarrow c \in K \leftrightarrow f \in P$.

We shall use the former to change the assignments.

A	B	C	D	E	F	G	H	J	K	L	M	N	P
a	f	g	h	b	m	p	c	q	n	k	r	d	e
b	a	r	p	g	n	e	k	c	f	d	q	m	h
c	k	a	a	k	b	b	h	e	c	e	d	p	f
d	m	n	q	q	h	r	r	m	p	n	f	g	g

Making interchanges in columns C, E, G, J, K, N we finally reach the orderly table

A	B	C	D	E	F	G	H	J	K	L	M	N	P
a	f	g	h	b	m	p	c	q	n	k	r	d	e
b	a	r	p	g	n	e	k	c	f	d	q	m	h
c	k	n	a	q	b	r	h	m	p	e	d	g	f
d	m	a	q	k	h	b	r	e	c	n	f	p	g

in which each point appears in every row.

* * * * *

Before proceeding with the next step in our study of Steinitz's theorem and its ramifications, we recall from Section 1.3 the concept of "multilaterals". A **multilateral**

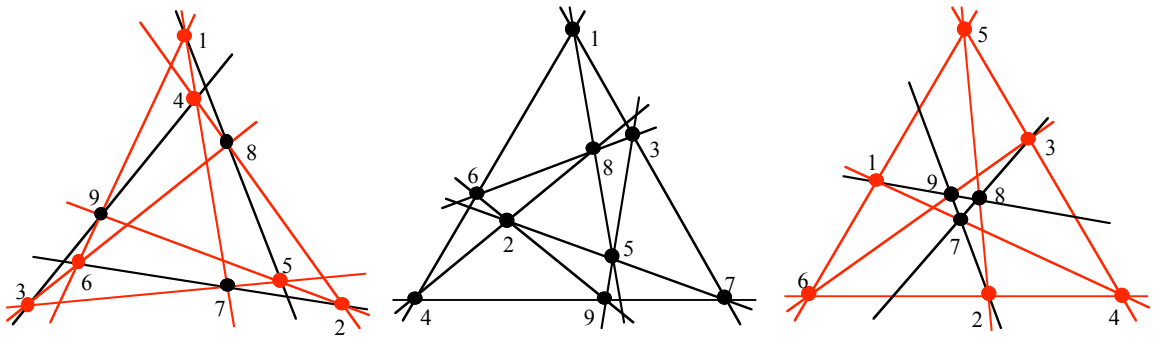

$(9_3)_1$ $(9_3)_2$ $(9_3)_3$

Figure 2.5.1. Some examples of multilaterals, in the three configurations (9_3) shown in Figure 2.2.1. The first is a 6-lateral with sequence of points 1,4,2,5,3,6 (1) in the configuration $(9_3)_1$. The second is 9-lateral, with sequence of points 1,8,3,7,5,9,4,2,6 (1); since this multilateral involves all points (and hence also all lines) it is a Hamiltonian multilateral. The last diagram shows a trilateral 7,8,9 (7), and a 6-lateral 1,6,3,5,2,4 (1). Note that another 6-lateral is 1,5,2,6,3,4 (1). The 3-lateral and either of the 6-laterals taken together form a multilateral decomposition of the configuration $(9_3)_3$.

(often inconsistently called "polygon" in the literature) is any sequence of distinct points and distinct lines of a configuration that can be written as P_0, L_0, P_1, L_1, … , P_{r-1}, L_{r-1}, P_r (= P_0), with each L_i incident with P_i and P_{i+1} (all subscripts understood mod r). Some examples of multilaterals are shown in Figure 2.5.1. If the last point is not required to coincide with the first one, we are dealing with a **multilateral** path. A family of multilaterals in a configuration, that contains all points and all lines but each just once, is called a **multilateral decomposition** of the configuration. We shall return to the topic of multilaterals later (for example, in Chapter 5).

Our next aim is to modify an orderly configuration table in a way that will preserve its orderly character but will be useful for the geometric steps. We assume that a line and one if its points are selected to be ignored in the geometric implementation, and that, as before, the configuration is connected. We also assume that we are concerned with a 3-configuration.

First, the rows are permuted so that the selected point of the selected line is in the first row. Note that since the table is orderly, this yields a correspondence (possibly dif-

ferent from the one we started with) in which each point is associated with a line that contains it. As mentioned earlier, and as is easily seen, by possibly interchanging the order of the columns (that is, lines) the orderly configuration table can be rearranged to show the multilateral decomposition in such a way that the lines of each constituent multilateral occur consecutively. In each of the multilaterals we can assume that the point in the last position in one column is in the middle position in the following column (understood modulo length of the multilateral). We rearrange the columns in such a way that the multilateral that contains the chosen line is placed last, and the selected line is chosen as the last line in the multilateral. If the multilateral is Hamiltonian, this part of the proof is completed. Otherwise, since the configuration is connected, at least one of the points of the last multilateral must be associated to (that is, be in the first row of) a line which is not in the multilateral. Choose the multilateral containing this line to be the next-to-last, and the line in question to be its last line. Then some point of this multilateral must be associated with another multilateral not used so far, and we continue in the same way. At the end we reach what we may call an **arranged** configuration table. This proves

Theorem 2.5.2. Every connected 3-configuration has an arranged configuration table.

As an illustration, we show in Table 2.5.2 an orderly configuration table of a configuration (14_3). Rearranging the columns so as to make the multilateral decomposition visible, we obtain the arranged configuration table, Table 2.5.3.

A	B	C	D	E	F	G	H	J	K	L	M	N	P
c	k	n	a	q	b	r	h	m	p	e	d	g	f
d	m	a	q	k	h	b	r	e	c	n	f	p	g
b	a	r	p	g	n	e	k	c	f	d	q	m	h

Table 2.5.2. An orderly configuration table of a connected combinatorial configuration (14_3).

A	M	P	N	K	B	J	L	C	D	E	F	H	G
b	q	h	m	f	a	c	d	r	p	g	n	k	e
c	d	f	g	p	k	m	e	n	a	q	b	h	r
d	f	g	p	c	m	e	n	a	q	k	h	r	b

Table 2.5.3. A rearranged configuration table of the (14_3) configuration of Table 2.5.2, in which the lines of each multilateral appear as consecutive columns. The point e of line G was chosen as the exceptional point, so its row is the first one. The line G is the last line of its multilateral, which is the last multilateral. Each multilateral is specified by rows 2 and 3 of the table. The table is arranged, in the sense described earlier.

We shall see in the next section how such an arranged multilateral decomposition can be used geometrically. Here we shall conclude the section by discussing certain ramifications of the results we have seen so far.

Corollary 2.5.3. Every connected k-configuration C, with $k \geq 2$, admits multilateral decompositions.

Indeed, any two rows of an orderly configuration table determine, by the above, a multilateral decomposition of C.

Corollary 2.5.3. Every connected k-configuration C, with $k \geq 2$, is 2-connected.

Proof. Assume that C is a connected k-configuration such that, without loss of generality, there is a line L for which for suitable elements R' and R" there is no R'-to-R" multilateral path that misses L. By the connectedness of C, there is a multilateral path M that uses L, that is, there are two points Q' and Q" of L that are part of this path M. In an orderly configuration table of C, permuting the rows if necessary, we may put Q' and Q" in the last rows of the block L. Let S be a multilateral decomposition of C determined by the last two rows of this orderly configuration table. Then one of the multilaterals of this decompositions uses the points Q' and Q". But since the multilateral is a circuit, there is a multilateral path (formed by the lines other than L) that connects Q' and Q". Substituting this path for the one that origi-

nally connected R' and R" eliminates the use of L. Hence the assumption that each path between R' and R" uses L is incorrect, and so C is 2-connected.

We shall discuss additional connectedness results in Section 5.1.

Exercises and problems 2.5.

1. Use the procedure applied in the proof of Theorem 2.5.1 to replace the configuration table in Table 2.5.4 by an orderly configuration table.

a	b	c	d	e	f	g	h	i	j	k	l	m	n
1	1	1	1	2	2	2	3	3	3	4	4	6	7
2	5	6	10	3	5	8	4	5	11	5	9	7	8
4	8	9	13	9	6	12	6	7	12	10	11	10	9
7	11	12	14	10	14	13	8	13	14	12	13	11	14

Table 2.5.4. A (14_4) configuration table.

2. Find orderly configuration tables for the two (12_3) configurations in Figure 2.5.2.

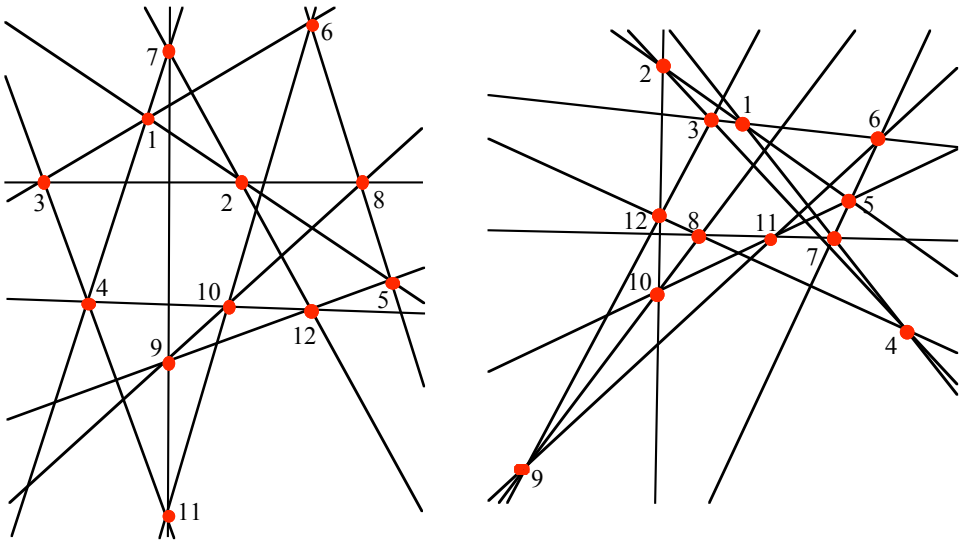

Figure 2.5.2. Two (12_3) configurations.

3. Justify the statement: *Any selection of two rows of an orderly configuration table defines a multilateral decomposition of the configuration.* List all multilateral decompositions resulting from possible choices of the rows in the orderly configuration tables found in Exercise 2.5.2 for the configurations (12_3) shown in Figure 2.5.2.

4. Justify the statement: For every k-configuration **C** and every multilateral decomposition of **C**, there is an orderly configuration table in which the multilateral decomposition can be obtained from the first two rows of the table.

5. Modify the proof of Theorem 2.5.1 to establish the following strengthening: *Every combinatorial k-configuration admits an orderly configuration table in which an arbitrarily chosen line is the last line of the table.*

2.6 STEINITZ'S THEOREM – THE GEOMETRIC PART

We turn now to a consideration of the geometric part of Steinitz's claim. We recall from Section 2.5 the claim from Steinitz' PhD thesis [S17]:

Steinitz's claim. Every connected combinatorial 3-configuration has a geometric realization by points and lines as a #1-subfiguration in the Euclidean plane; moreover, the point and line of the ignored incidence can be arbitrarily chosen.

Recall from Section 1.3 that a *#1-subfiguration* of a combinatorial configuration is a family of points and (straight) lines that satisfies all the incidence requirements except possibly one that is ignored, and has no additional incidences.

By our definition, which coincides with the definition generally used, a **geometric configuration** (n_k) is a family of n points and n (straight) lines such that each point is incident with k lines, and each line is incident with k points. The intention of this definition is that each of the points and lines is incident with **precisely** k objects of the other kind. Even though this requirement often was not explicitly stated, in many instances it was stated and it has been taken as self-understood by all nineteenth century writers on configurations.

However, the following situation does arise: We start with a combinatorial configuration and find a set of points and a set of straight lines which fulfill the incidence requirements of the combinatorial configuration. In other words, every combinatorial incidence corresponds to a geometric incidence. However, it is possible that the points and lines we found have **additional** geometric incidences, not specified in the combinatorial configuration. As mentioned in Section 1.3, in such a case we shall say that the points and lines form a **representation** (or **superfiguration**, or **weak realization** are terms also used) of the combinatorial configuration. It may happen that a different choice of points and lines will result in a geometric configuration without additional incidences; if it is necessary to stress this fact, we shall say that we have a **realization** (or, if there is need for a more specific expression, a **strong realization**). But, as is easy to see, some combinatorial configuration admits **only** superfigurations.

For example, consider the combinatorial configuration given by Table 2.6.1. A superfiguration is shown in Figure 2.6.1, in which the line H passes through the point m although they are not combinatorially incident according to Table 2.6.1. (This configuration is isomorphic to the one in Figure 2.2.6.) The reason that **every** geometric presentation of this configuration by points and lines is a *representation* (and not a *realization*) lies in the fact that the hexagon abcdef has vertices that alternate on the two lines A and B, and therefore the three points g, h, m are collinear by the Pappus theorem. More complicated examples can have several unintended geometric incidences — in fact, there is no upper bound on the possible number of such incidences. In Figure 2.6.2 we show a topological configuration (18_3) such that each of its representations in a #2-superfiguration. This possibility is also ignored in the Wikipedia article [W5] on Ernst Steinitz (as of February 4, 2008).

A more detailed analysis of this topic will be presented in [B18].

A	B	C	D	E	F	G	H	I	J	K	L	M	N	O	P
a	b	c	d	e	f	g	h	i	j	k	l	m	n	o	p
e	d	h	m	f	a	c	g	j	k	l	p	b	i	n	o
c	f	d	e	g	h	b	i	o	n	m	j	a	p	l	k

Table 2.6.1. A combinatorial configuration (16_3).

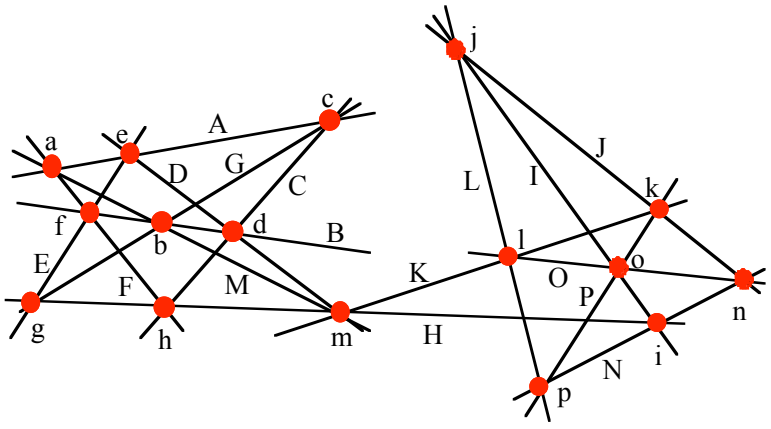

Figure 2.6.1. A *representation* of the combinatorial configuration (16_3) given by Table 2.6.1.

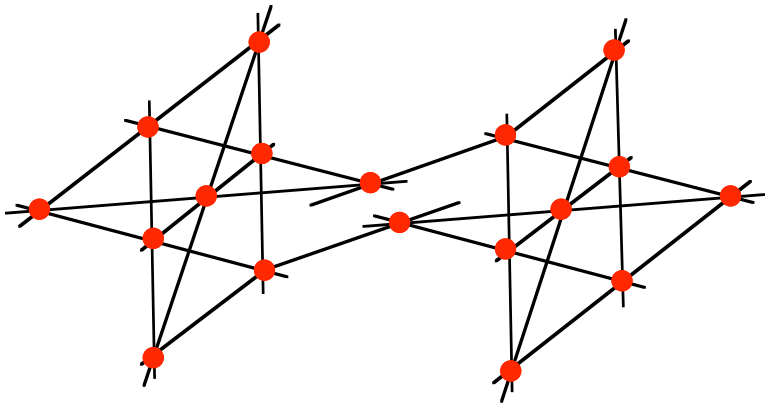

Figure 2.6.2. A topological configuration which can be realized by straight lines only as a #2-superfiguration.

The above preamble to the geometric part of Steinitz's theorem about geometric "realizations" of combinatorial 3-configurations was needed to set the stage for dealing with this rather remarkable result and its history. The following result is what Steinitz actually proved:

Theorem 2.6.1. For every connected combinatorial 3-configuration and every choice of one incident point-line pair, there is a selection of distinct points and (straight) lines which realize all the incidences except possibly the incidence of the chosen line with the chosen point.

In other words, every connected 2-configuration has a **near-representation** in the Euclidean plane, in which the point and line of the ignored incidence can be arbitrarily chosen. As shown by the example in Table 2.6.1 (and illustrated in Figure 2.6.1) there are combinatorial configurations for which no near-representation is a near-realization. (The "near" part of these terms is meant to convey that one incidence is disregarded.)

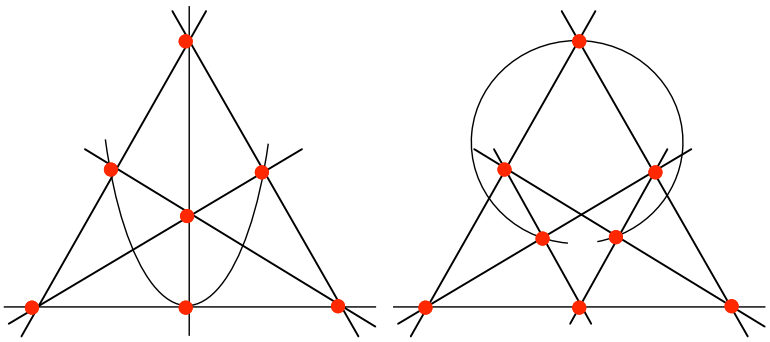

Figure 2.6.3. Frequently shown illustrations of Steinitz's theorem, by 1-subfigurations of the Fano (7_3) and Möbius-Kantor (8_3) configurations.

Note that, since the chosen line is incident with only three points (one of which is the chosen point), it is in every case possible to find a curve of degree at most two (even a circle, unless there is a straight line), incident with these three points.

There is no indication in any of the writings of Steinitz or other mathematicians during the 20th century that they were aware of the fact that Steinitz's claim as formulated by him is not valid, since it pretends to prove strong "near-realizability". The first indication (known to me) of the awareness that the theorem actually *established* by Steinitz has to be formulated in terms of weak "near-realizations" — that is, near-representations, as we did above — was in a talk by T. Pisanski [P3], at a meeting in Ein Gev (Israel) in April 2000. The fact that some combinatorial 3-configurations have only geometric representations and no geometric realization was also noticed by W. Kocay and R. Szypowski [K12] in 1999 and by Glynn [G3] in 2000; neither work mentions Steinitz.

Proof of Theorem 2.6.1. Starting from a connected combinatorial configuration (n_3) given by a configuration table, the first step is to convert the table into an orderly table. This is possible by Theorem 2.5.1. Next, the rows are permuted so that the exceptional point of the exceptional line is in the first row. Note that since the table was orderly, this yields a correspondence (possibly different from the one we started with) in which each point is associated with a line that contains it. As mentioned earlier, and as is easily seen, by possibly interchanging the order of the columns (that is, lines) the orderly configuration table can be rearranged to show the multilateral decomposition in such a way that the lines of each constituent multilateral occur consecutively. We rearrange the

columns in such a way that the multilateral that contains the chosen line is placed last, and the selected line is chosen as the last line in the multilateral. If the multilateral is Hamiltonian, this part of the proof is completed. Otherwise, since the configuration is connected, at least one of the points of this multilateral must be associated to (that is, be in the first row of) a line which is not in the multilateral. Choose the multilateral containing this line to be the next-to-last, and the line in question to be its last line. Then some point of this multilateral must be associated with another multilateral not used so far, and we continue in the same way. At the end we reach what we called an **arranged** configuration table.

As an illustration, we show in Table 2.6.2 an orderly configuration table of a configuration (14_3). Choosing as the exceptional elements the point e and the line G, and rearranging the columns so as to make the multilateral decomposition visible, we obtain Table 2.6.3.

A	B	C	D	E	F	G	H	J	K	L	M	N	P
c	k	n	a	q	b	r	h	m	p	e	d	g	f
d	m	a	q	k	h	b	r	e	c	n	f	p	g
b	a	r	p	g	n	e	k	c	f	d	q	m	h

Table 2.6.2. An orderly configuration table of a connected combinatorial configuration (14_3).

A	M	P	N	K	B	J	L	C	D	E	F	H	G
b	q	h	m	f	a	c	d	r	p	g	n	k	e
c	d	f	g	p	k	m	e	n	a	q	b	h	r
d	f	g	p	c	m	e	n	a	q	k	h	r	b

Table 2.6.3. A rearranged configuration table of the (14_3) configuration of Table 2.6.2, in which the lines of each multilateral appear as consecutive columns. The point e of line G was chosen as the exceptional point, so its row is the first one. The line G is the last line of its multilateral, which is the last multilateral. Each multilateral is specified by rows 2 and 3 of the table.

In an abbreviated form, using just the names of the vertices (second entries in the list of points in each column) and the lines to which they belong, this multilateral decomposition can be written as:

c A d M f P g N p K | k B m J e L n C a D q E | b F h H r G (1)

With line G and point e chosen as the exceptional elements, we make the final rearrangement of the columns. The multilateral containing G is placed last, and G is placed as the last line of it. The entry b of the first column in this multilateral is the first point which is associated with a line not in the multilateral. Since b is associated with the line A of the first multilateral, this multilateral is placed next-to-last, and A is placed at its last column; then M is the first line, and the corresponding first point is d. Therefore the multilateral preceding it has L as its last line (column). The rearranged multilateral decomposition (1) has now the following representation:

n C a D q E k B m J e L | d M f P g N p K c A | b F h H r G (2)

From this decomposition (2) it is obvious that each element (point or line) is incident with at most two elements that come before it, except that the last line (G in the present case) is incident with three of the preceding points. (For the other elements, the situation is indicated by the single or double underline of the symbols.) This means that elements incident with no previous element can be chosen completely arbitrarily in the plane, those incident with one previous element can be chosen freely as a point on a line or as a line through a point, while those incident with two earlier ones are determined without any freedom of choice. The last triplet may be collinear but need not be — in which case a second degree curve can be passed through it. ¨

For clarity, the final rearranged configuration table is shown in Table 2.6.4.

C	D	E	B	J	L	M	P	N	K	A	F	H	G
r	p	g	a	c	d	q	h	m	f	b	n	k	e
n	a	q	k	m	e	d	f	g	p	c	b	h	r
a	q	k	m	e	n	f	g	p	c	d	h	r	b

Table 2.6.4. The multilateral decomposition (2) in configuration table form.

The geometric subfiguration that resulted from a set of particular choices is shown in Figure 2.6.4. Figure 2.6.5 illustrates the possibility of making choices which happen to satisfy the last incidence as well, hence yield a proper geometric realization of this configuration (14_3).

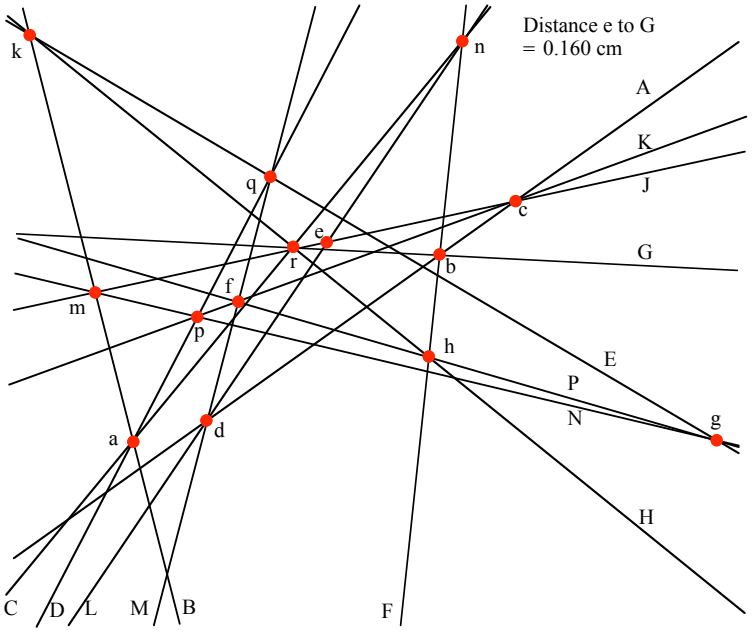

Figure 2.6.4. A "near-realization" following Table 2.4.4 of the configuration (14_3) of Table 2.6.1, in which all the incidences except the one of point e and line G are satisfied.

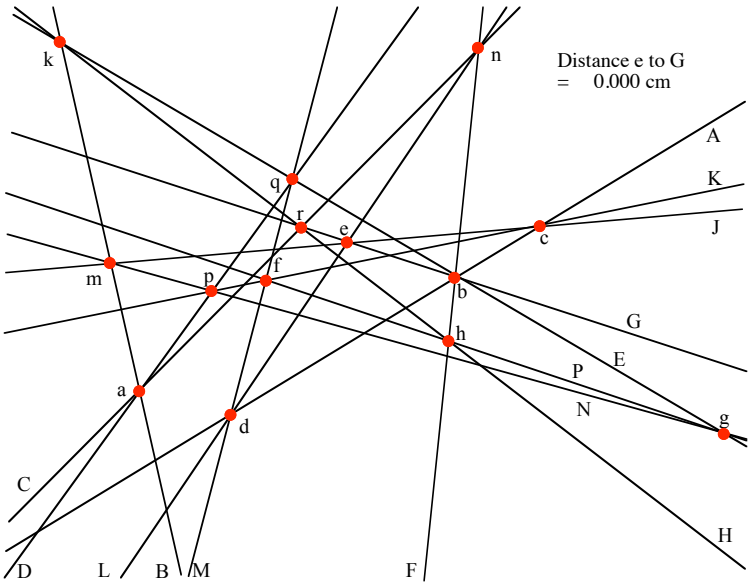

Figure 2.6.5. A *realization* of the configuration (14_3) of Table 2.6.4, in which *all* the incidences are satisfied.

As is clear from the above proof, at no point has there been made any claim that the lines and/or points we introduce have no additional incidences. It has been tacitly assumed that the construction is not undermined by (mis)using the freedom of choice to intentionally place points on already present points or lines they are not supposed to be incident with, and analogously for the selection of lines. However, as shown at the beginning of this section, there are circumstances in which unintended incidences cannot be avoided. The remarkable fact that this possibility has been ignored for a century is nearly incomprehensible.

One still remaining mystery in this context is the fact that all known instances in which unwanted incidences in geometric realizations of combinatorial 3-configurations are unavoidable deal with configurations that are connected (hence 2-connected) but not 3-connected. It is possible that the following holds:

Conjecture 2.6.1. Every 3-connected combinatorial 3-configuration admits geometric realizations by points and straight lines with no incidences except the required ones.

Steinitz's theorem 2.6.1 was proved in [S17] in 1894. In 1999 it was independently discovered by Kocay and Szypowski [K12] in a different setting, and in 2000 by Glynn [G3]. A presentation of the above material and other aspects of Steinitz's theorem appears in [G46].

* * * * *

The realization in Figure 2.6.5 was obtained by utilizing continuity: In the near-realization shown in Figure 2.6.4 the point e is above the line G, while by choosing some other appropriate positions for the points used in the construction a near-realization can be obtained in which the point e is below the line G. This is a situation that *seems* to be quite general. Steinitz made the same observation in [S17]. Steinitz devoted more than half the dissertation [S17] (24 pages) to a consideration of ways in which one could *guarantee* that the final step in the above proof can be made using a straight line instead of a curve of degree 2. While this might be another interesting result, I have not been able to follow the exposition in [S17]. (In fact, I know of nobody who

claims to have understood and verified this part of Steinitz's thesis.) The opaqueness of the exposition can best be seen from the last two sentences of Steinitz's introduction to this part of the work (see [S17, p. 22]):

> ... Without any particular assumptions about the configurations, a method will be presented below following which one can reach a linear presentation. However, for each configuration to which we want to apply this method, an additional investigation is necessary since the method becomes *illusory in certain cases*. [My translation and italics]

In mentioning [S17] in the survey [S19, p. 490], Steinitz is equally uninformative. Stating that his method is an extension of Schroeter's approach in [S6], [S8], he ends the explanation by stating:

> Schroeter's method can be generalized so that it is applicable to *most* configurations n_3. [My translation and italics]

It seems that the "method of Schroeter" is rooted in arguments due to Möbius in the early part of the nineteenth century, in particular in [M20].

However, even if the proof in [S17] is valid, and if somebody were to make the exposition understandable — this would prove only that every connected configuration has *representations*. It would not be a proof of Conjecture 2.6.1 for *realizations*, as claimed by Steinitz. Indeed, we know from examples such as the one in Figure 2.6.1 that some representable configurations are not realizable, hence Conjecture 2.6.1 cannot be generally valid for realizations.

Exercises.

1. Find a geometric construction analogous to the one given above, for the combinatorial configuration of Table 2.5.1, but with the choice of point q and line D as the exceptional elements.

2. Find the analogous construction for the combinatorial configuration which has as its table the first three rows of the orderly table obtained in the worked example in Section 2.5, and with point a and line A as exceptional elements. Using suitable software, see whether this configuration has a proper realization.

3. Apply the methods of construction we used here to the configurations $(10_3)_3$ and $(10_3)_4$ of Table 2.2.7.

4. Find a connected combinatorial configuration for which every representation is a #3-subfiguration, that is, contains at least three unwanted incidences.

5. Show that there are connected combinatorial configurations (n_3) for which in every representation the number of unwanted incidences is at least $c \cdot n$, for some constant $c > 0$. Open problem: What is the best possible c?

2.7 ASTRAL 3-CONFIGURATIONS WITH CYCLIC SYMMETRY GROUP

We have seen in Section 1.5 that a 2-astral 3-configuration must have two orbits of points and two orbits of lines. By the convention introduced there we simplify the expressions and call such configurations **astral**, for short.

Lemma 2.7.1. If an astral 3-configuration has one orbit of points at infinity, it must have reflective symmetries.

Proof. If such a configuration has no reflective symmetries, then the orbit of points in the finite plane has to coincide with the vertices of a regular polygon; the only alternative would be that they are the vertices of an isogonal polygon – but their equivalence requires reflection. Each of the points at infinity is on three lines, two of which are in the same orbit. Even if these two are related by a rotational (halfturn) symmetry, they must be parallel and of the same length, and by the rotational symmetry the third line parallel to them must pass through the center of the polygon. Thus all lines come in triplets of parallel lines, the middle one serving as mirror for the other two; these mirror lines are spaced at equal angles, hence they are mirrors of the configuration. Hence we again are led to reflective symmetries. □

As a consequence of Lemma 2.7.1 we see that astral configurations (n_3) that have a cyclic group of symmetries are necessarily configurations in the Euclidean plane. Astral 3-configurations with a cyclic group of symmetries and no mirrors will be called **chiral**. (Note that this does not mean that all astral configurations contained in the Euclidean plane have a cyclic group of symmetries. We shall consider those with dihedral symmetry in Section 2.8.) The points of a chiral astral configuration are at the vertices of two concentric regular polygons with m = n/2 vertices each; the polygons clearly have different sizes. As we shall show next, such 3-configurations depend (up to similarity) on three additional integer parameters. The notation we shall use for these configurations is m#(b,c;d); a detailed explanation follows, and an illustration is given in Figure 2.7.1.

The lines of one geometric transitivity class are the diagonals of one of the polygons, those of the other class are diagonals of the other polygon; each line of the configuration contains two points of one polygon and one of the other. The numbers of edges of the polygons bridged (spanned) by the diagonals are the integers b and c of the symbol; usually we shall follow the convention that $m/2 > b \geq c > 0$, but the relative size of b and c is not of intrinsic importance and it is sometimes convenient to disregard the convention. The corresponding points (vertices) are accordingly called the b-points resp. c-points, and the lines are b-lines and c-lines. Starting from an arbitrary b-point denoted B_0, and proceeding in an arbitrary orientation we label the other b-points consecutively $B_1, \ldots, B_{m-1}$. Each b-line is then of the form $L_i = \mathrm{aff}(B_i, B_{i+b})$, and it contains a c-point which we label C_i. The c-line that passes through C_0 determines the labeling of the c-lines. In the orientation of the c-points which is induced by the orientation chosen for the b-points, the earlier point of that c-line is C_0, and the later accordingly is C_c. The remaining c-points are then labeled in the obvious way; the c-lines are labeled by $M_i = \mathrm{aff}(C_i, C_{i+c})$, . Here and throughout, all subscripts are to be understood mod m. From a given (n_3) configuration of the kind considered, the values of m, b and c can be read off instantly. Now we can find a tentative determinations of the symbol d in the notation m#(b,c;d) for the configuration. We consider the b-point that is incident with the c-line $M_0 = \mathrm{aff}(C_0, C_c)$; like all b-points, it already carries a label. This label we take as the value of d in the *preliminary* symbol of the configuration.

The value of d in the final symbol requires a comparison of two possibilities. One is what we have just described, and the other is obtained in the same way but going in the opposite orientation around the b-polygon. As the *final* symbol m#(b,c;d) for the configuration we shall generally choose that one of the alternatives which has the smaller value of d. As is easily verified, the two values of d add up to b+c; hence we may assume that $d \leq (a+b)/2$, which means that in fact only one of the determinations has to be carried out. If it yields such a value of d we take it, otherwise we subtract it from b+c to get the correct value of d. This is illustrated by the examples in Figure 2.7.2.

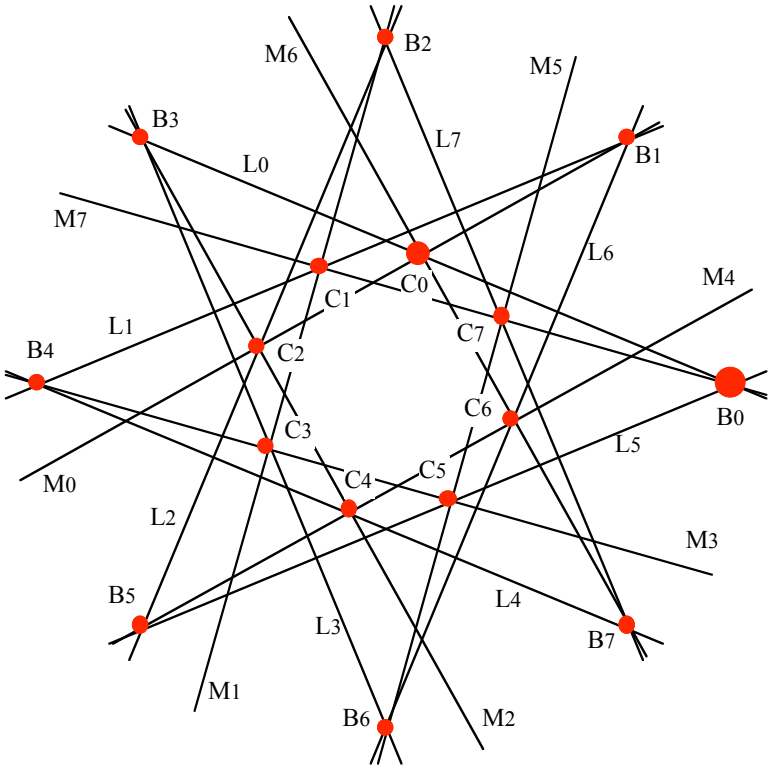

Figure 2.7.1. An example of the labeling and designation of a chiral astral configuration. Following the explanations in the text, this is configuration 8#(3,2;1).

While our conventions assign a unique symbol to each astral (n_3) configuration, the converse is not valid. In general, **two** configurations are represented by the same symbol m#(b c; d). They differ by the ratio of the radius of the circle of c-points to that of the b-points; the one with smaller ratio is denoted by a single tag ', the other one by double tags ". This is illustrated in Figure 2.7.3. Another way of distinguishing the two configurations is by specifying the ratio in which the point C_0 divides the segment B_0B_b; this information is very useful for drawing the configuration, as well as for determining which symbols are possible.

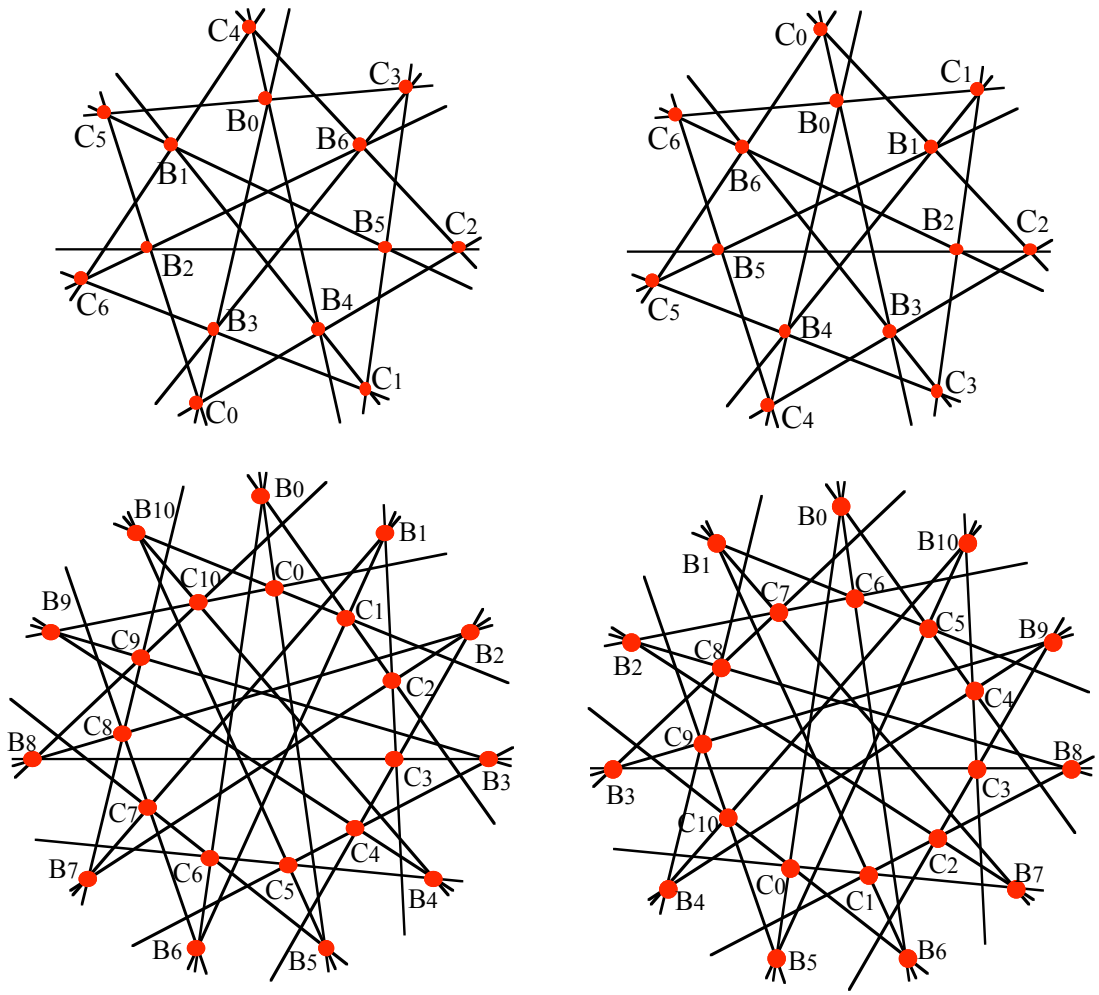

Figure 2.7.2. Additional examples of labeling astral (n_3) configurations. The one in the upper row has symbols 7#(3, 2; 4) and 7#(3, 2; 1), so the latter is the one conventionally accepted. The configuration in the bottom row has symbols 11#(5, 1; 10) = 11#(5, 1; –1) since all subscripts can be taken (mod n) and 11#(5, 1; 7). Hence the conventional symbol is 11#(5, 1; –1).

However, in cases in which either $b = c$ or $2d = b + c$ the symbol m#(b, c; d) represents only a single configuration. Examples of these situations are shown in Figure 2.7.4, for the symbols 6#(2, 2; 1) and 11#(5, 1; 3).

If the highest common factor of m, b, c, d is $f > 1$, then the configuration m#(b,c;d) is not connected, but consists of f copies of the configuration m/f#(b/f, c/f; d/f) . However, exceptions to all the above happen when there are additional "accidental"

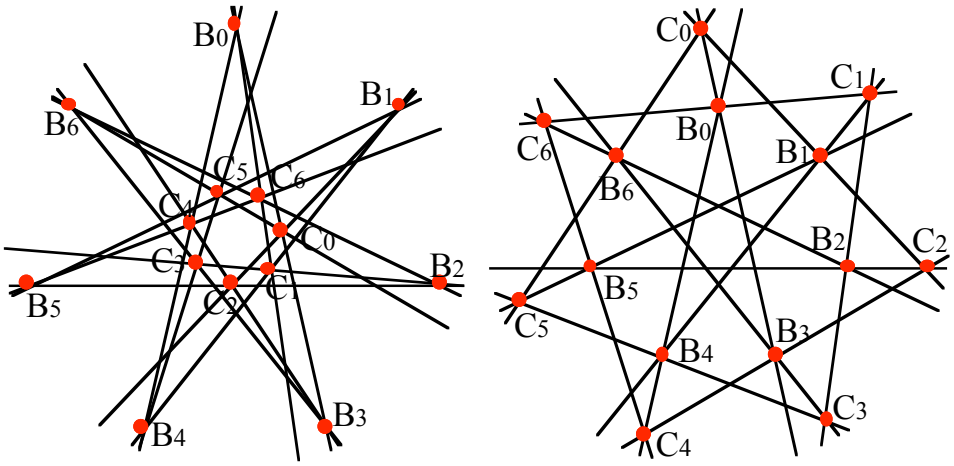

Figure 2.7.3. The two astral configurations with common symbol 7#(3, 2; 1). The one on the left is specified by 7#(3, 2; 1)', the other one by 7#(3, 2; 1)".

incidences. For example, an attempt to draw the configuration 12#(5, 1; 3) leads to the superfiguration shown in Figure 2.7.5a; it has additional incidences and is, in fact, a configuration (24_4). In Figure 2.7.5b we show how sensitive the situation is with respect to correctly drawing the configurations – a seemingly legitimate configuration does not really exist. On the other hand, Figure 2.7.5a can be interpreted as a *representation* of the configuration 12#(5,1;3), as well as a representation of configurations 12#(5,1,-1), 12#(4,4;1) and 12#(4,4;2). Figure 2.7.5b serves to illustrate a *topological* realization of the configuration 12#(5,1;-1).

A different type of unintended incidences is illustrated by the example in Figure 2.7.6. Here the result is a collection of points and lines which is not a configuration under the definitions we adopted at the beginning, since some lines (but not all) are incident with four points, and some points with four lines.

Disregarding the possible presence of unintended incidences, how does one get from the symbol to a drawing, and how does one decide whether a symbol corresponds to any configuration? For the answer to both parts of the question, we can proceed either algebraically or geometrically.

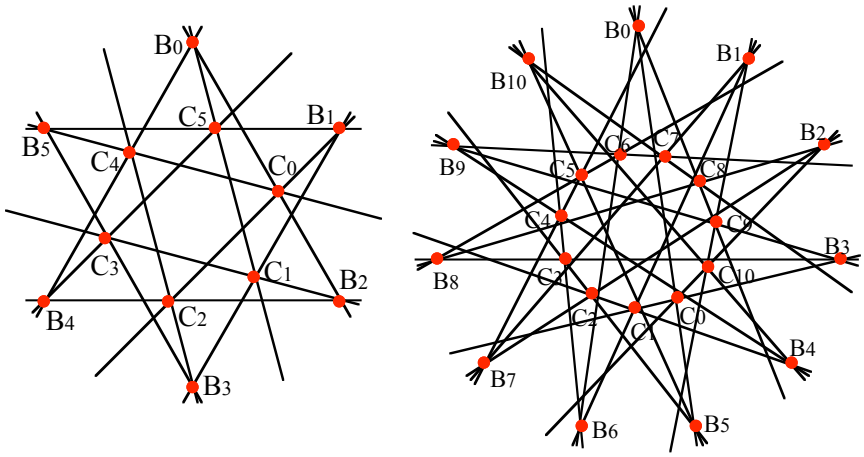

Figure 2.7.4. Astral configurations which are examples of the case in which only a single configuration corresponds to its symbol, here 6#(2, 2; 1) and 11#(5, 1; 3).

In the algebraic approach, given a symbol m#(b, c; d) we start with the vertices of a regular m-gon, and draw all diagonals of span b (or their extensions, if needed). Points of the other orbit will be the vertices of another regular m-gon, situated on the diagonals of the first one. Their location is determined by the ratio which, in the notation of Figure 2.7.1, is given by the still undetermined ratio of lengths $\lambda = B_0C_0/B_0B_b$. The position of C_c is determined by the same ratio, since $\lambda = B_cC_c/B_cB_{b+c}$. Now, the line C_0C_c contains the point B_d of the first orbit. Hence, writing the collinearity condition in terms of a determinant, involving the variable λ and the known coordinates of the B points, yields a quadratic equation for λ. Depending on whether there are two, one, or no solution in real numbers we obtain the pair of isomorphic configurations, a single configuration, or no configuration at all. Thus the complete characterization of possible symbols is, in principle, determinable by the non-negativity of the discriminant of that quadratic equation. In any particular case, the software used (various versions of Mathematica® on different Macintosh computers) had no problem finding the value(s) of λ, and then drawing the configuration(s). However, no amount of effort, on the computer or manually, was successful in explicitly describing the necessary and sufficient conditions on the integer parameters m, b, c, d for the existence of the configurations. The

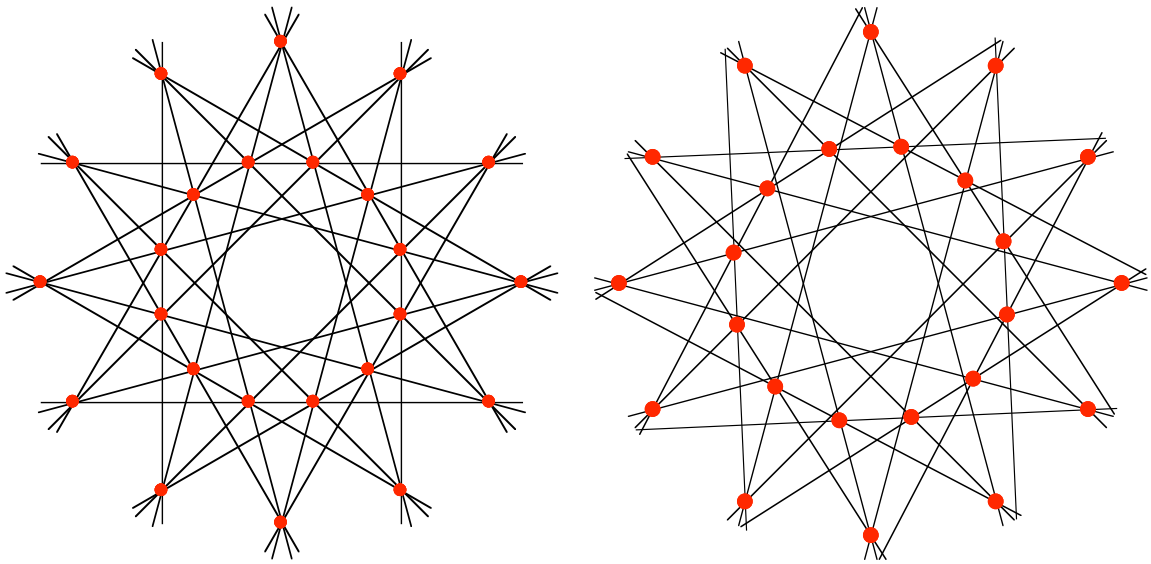

(a) (b)

Figure 2.7.5. The diagram in (a) is supposed to show the configuration 12#(5,1;3); however, additional incidences turn it into an astral (24_4) configuration which, by the conventions we shall specify in Section 3.5, has the symbol 12#(5,4;1,4). Note that the same (24_4) configuration results when drawing any of 12#(5,1,-1), 12#(4,4;1) and 12#(4,4;2). The first of these is illustrated by the pseudoline configuration in (b). Note that these are actually straight lines, but that their incidences are faked (ever so slightly). For a different presentation of these cases see Figure 5.8.1 and the explanations given there.

best I could do is to deduce several necessary conditions from many specific cases, and from an argument to be described below. In any case, the known conditions for a symbol m#(b, c; d) are as follows (this includes the notational conventions introduced earlier):

$$0 < c \le b < m/2$$

$$2[(b + c - m)/2] \le c - b + 1 \le 2d \le b + c$$

$$0 \ne d \ne c$$

$$2 \cos(b\pi/m) \cos(c\pi/m) \le 1 + \cos((b + c - 2d)\pi/m)$$

While the use of calculational and graphic capabilities of appropriate software (Mathematica, Mathlab, Maple, and others) enables one to find out whether a symbol leads to a configuration, it is of same interest to note that geometric means can yield the same result. In fact, if the vertices of a regular m-gon are given, the configurations m#(b, c; d) can be drawn with just the classical Euclidean tools. (Naturally, the construction of the regular m-gon may or may not be possible with Euclidean tools, depending on the value of m.) Here is how the construction proceeds, illustrated for m#(b,c;d) = 11#(5,1;2) by the steps in Figure 2.7.7.

- (a) Draw the lines determined by the diagonals of span b = 5; this yields a regular polygon P of type {m/b}.
- (b) Construct the isosceles triangle T determined by two vertices V_1 and V_2 of P, that are separated by span c = 1, and the center O of P.
- (c) Construct the circumcircle C of the triangle T described in (b).
- (d) Label the sides of the polygon P. We label "0" the two lines of P that touch T at V_1 and V_2, but do not go through the interior of T. The other lines of

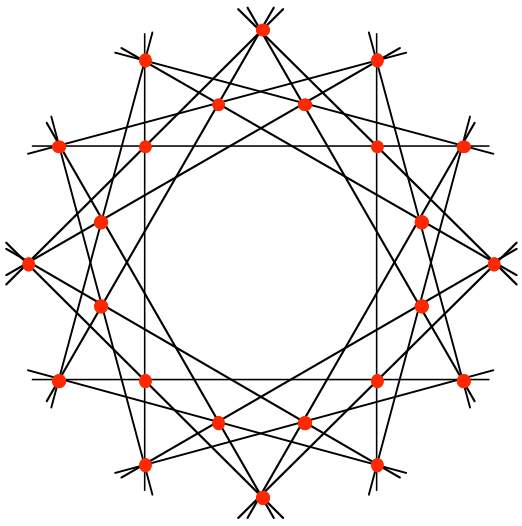

Figure 2.7.6. A drawing of the astral configuration 12#(3, 3; 1) shows unintended incidences. The resulting family of points and lines is not a *configuration* according to our definitions; it is a *superfiguration*. In fact, by ignoring some incidences, it could be interpreted as a *representation* of the astral configuration 12#(3, 3; 1).

P are numbered by their sequence at the central convex m-gon determined by these lines. The sides closer to the center of C are labeled "1", "2", ... in order, the ones farther from the center of C are labeled "-1", "-2", ...

- (e) Find the intersection points of the lines of P with the circle C.

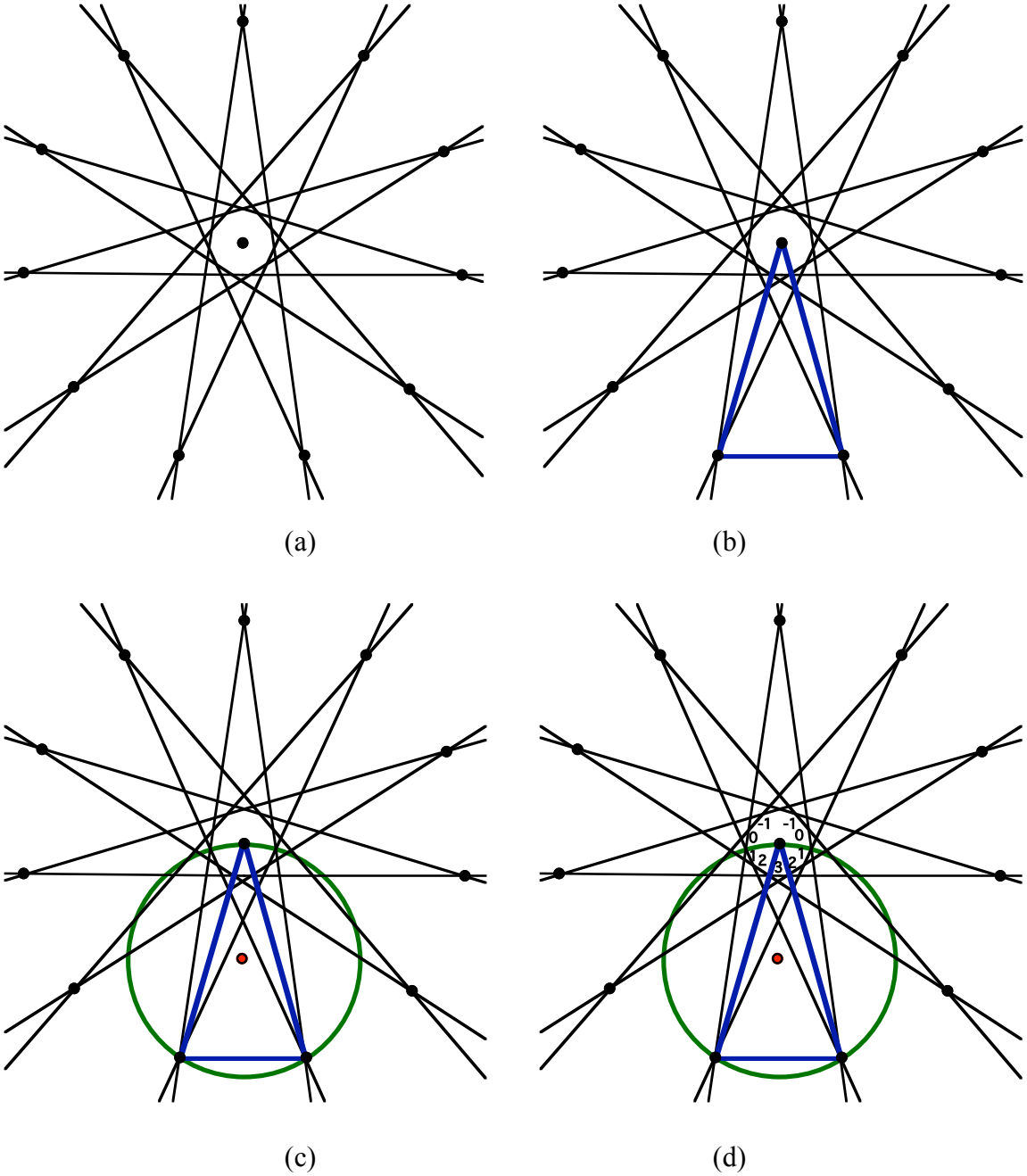

Figure 2.7.7 (first part). The geometric construction of the configuration 11#(5,1;2).

- (f) Label these intersection points by the labels of the lines.
- (g) Select one of the points labeled d = 2, and draw the line connecting it with one of the points V_1, V_2.
- (h) Rotate through all the multiples of $2\pi/m = 2\pi/11$ the point chosen in (g) and the line constructed there. A configuration m#(b,c;d) = 11#(5,1;2) is obtained.

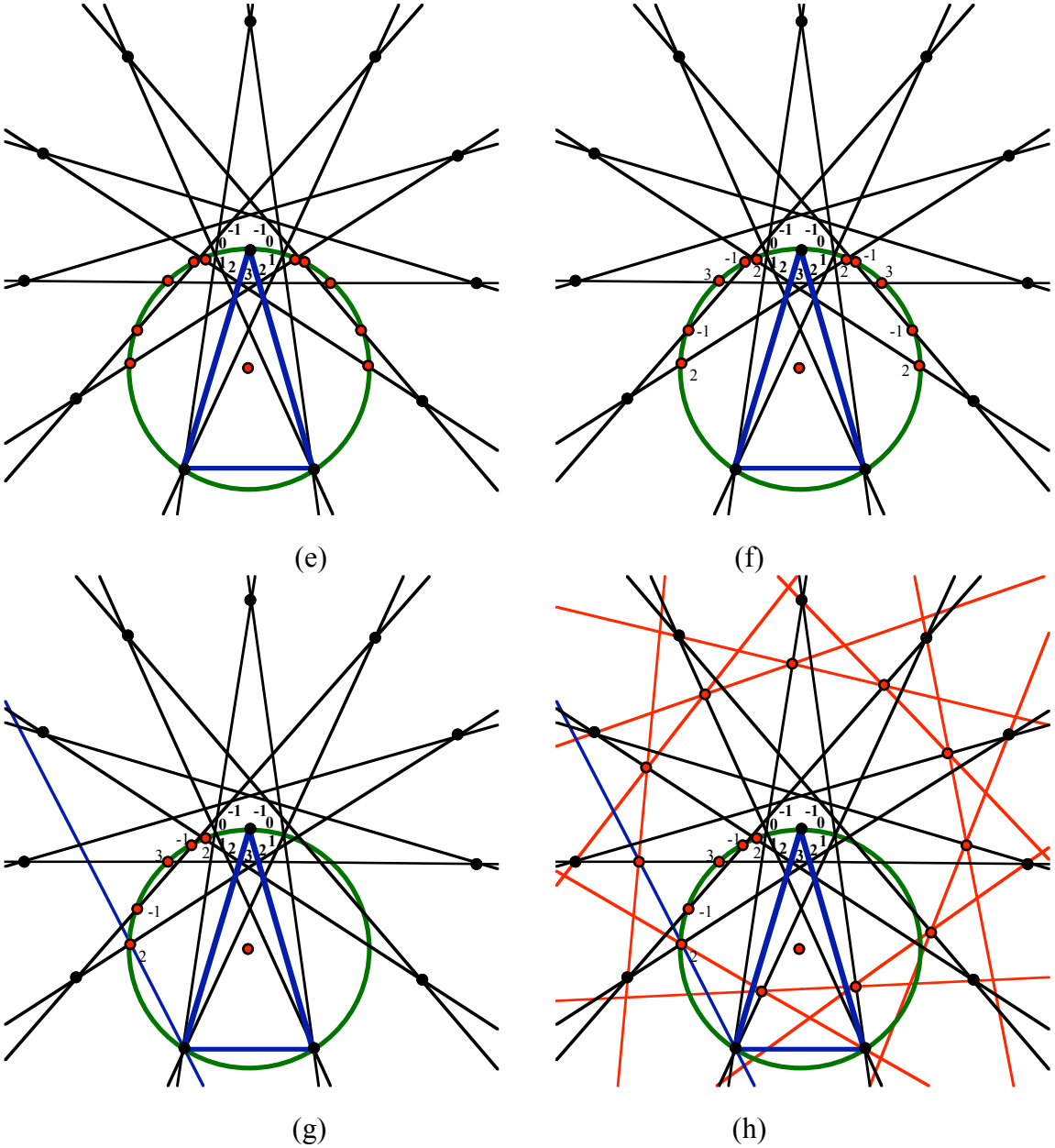

(e) (f)

(g) (h)

Figure 2.7.7. (second part)

- (i) The same construction as in (g) and (h), but with the other point labeled d = 2, yields the other configuration 11#(5,1;2). The remaining possibilities of pairing a point labeled "2" with the other V_j yield configurations congruent to the ones in (h) and (i).
- (j) An analogous construction but with a point labeled "3" yields the configuration 11#(5,1;3). As we shall see in Section XY this configuration is selfpolar.

Naturally, these constructions need justification, which we shall provide below. However, it is appropriate to recall that establishing results by using graphical means can be rigorously justified; see, for example, [M19].

The reasoning follows the above method of construction, and is illustrated in Figure 2.7.8 by the example of the configuration 11#(4,3;2).

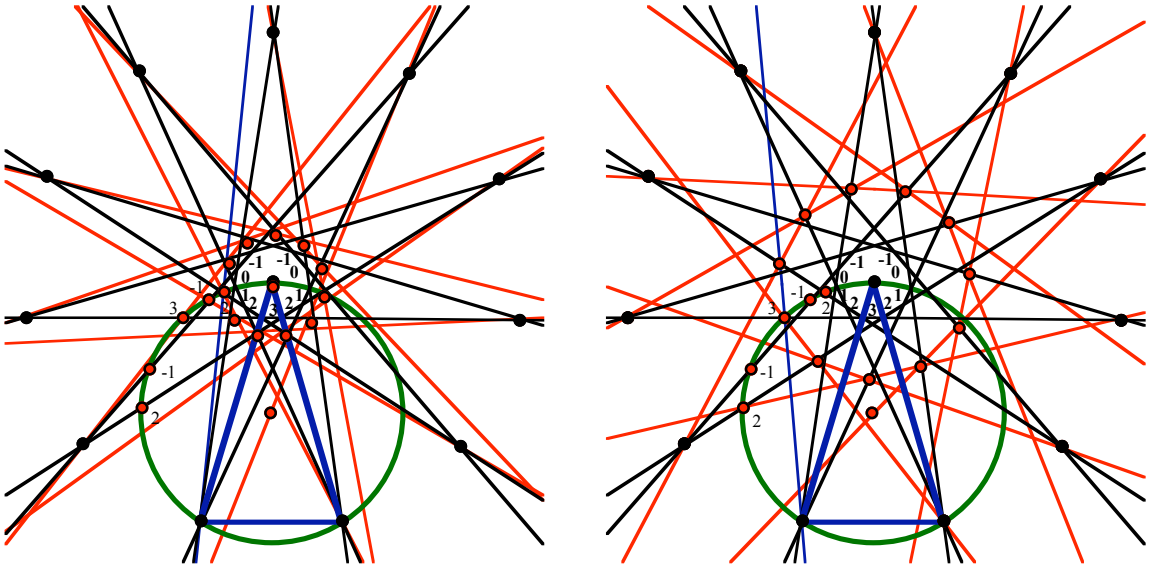

(i) (j)

Figure 2.7.7. (third part).

The triangle O V2 V1 is isosceles. The angle O V(2) V1 equals the angle O V2 V1 since both are peripheral angles over the same arc O V1. Let X be the point on the ray V(2) V1 such that the angle V(2) O X equals the angle V2 O V1. Then the triangle O X V(2) has correspondingly equal angles with the triangle O V1 V2, hence is similar to it.

Therefore it is also isosceles, so OX has the same length as OV(2) and is thus on the circle centered at O and with radius OV(2). As the angle V(2) O X is the same as the angle V2 O V1, which spans a diagonal of span c = 3 of the m-gon (m = 11), it follows that follows that V(2) X spans the same diagonal on the m-gon determined by the rotates of V(2). The existence of the configuration m#(b,c;d) = 11#(4,3;2) is established. □

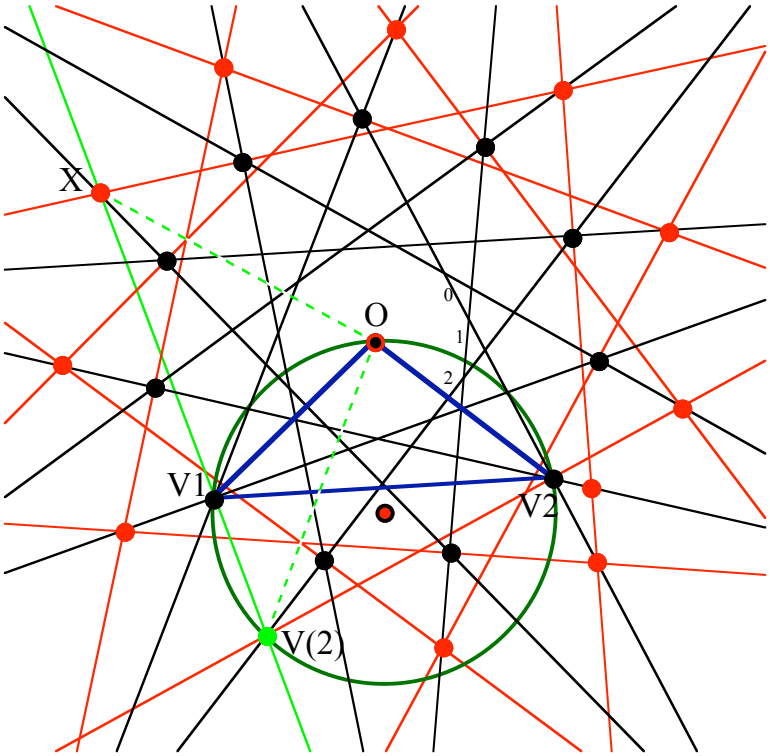

Figure 2.7.8. Starting with the {11/4} polygon (black points and lines), the configurations 11#(4,3;2) is constructed by the method described above.

Using the description of the determination of the symbol m#(b,c;d) of an astral configuration (n_3) it is immediate that the reduced Levi graph is as shown in Figure 2.7.9. The simplicity of the reduced Levi graph of such a configuration can be interpreted as the source of the usefulness of such graphs, but it also serves to indicate that the encoding of such an astral configuration by our symbol is natural and not arbitrary.

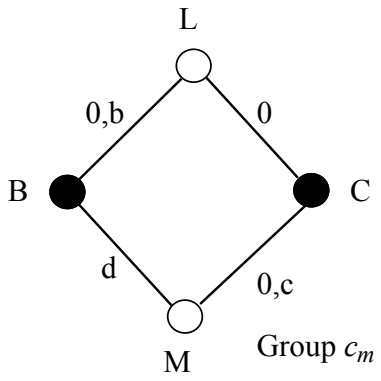

Figure 2.7.9. The reduced Levi graph of an astral configuration m#(b,c;d); the notation is analogous to the one used in Figure 2.7.1.

Astral 3-configurations of were first defined in [G39], but isolated examples occur in earlier publications. The first seem to be by Zacharias [Z4]; he shows examples of astral (10_3), (12_3) and (14_3) configurations and comments on their star-like appearance, but reaches no general conclusions or constructions. Similarly, van de Craats [V1] shows the astral (10_3) and notes various interesting properties associated with it; he also shows an astral (14_3), and mentions that analogous astral (n_3) can be found for all $n = 2m+2$, where $m \geq 2$. Several other examples can be found in [B19], as well as in [G46].

Exercises and problems 2.7.

1. Derive explicitly the quadratic equation for λ mentioned in the text in the case of 9#(4,2;3), and use this to draw this configuration using suitable software.

2. Derive explicitly the quadratic equation for λ in the general case m#(b,c;d), and try to find criteria on these parameters that will imply that the solutions of the equation are real.

3. Use the geometric construction to draw the configuration 9#(4,2;3).

4. Show that the configurations 12#(5,1;2) and 12#(5,1;4) are congruent. Explain this, and generalize.

5. The configuration 5#(2,2;1) has a cyclic automorphism group that acts transitively on its points and lines. Describe this group, and determine whether it acts transitively on the flags of the configuration.

6. The automorphisms group of the astral chiral configurations 5#(2,2;1) is transitive on its points. Find other astral chiral configurations with this property. Can you characterize all such configurations?

2.8 ASTRAL 3-CONFIGURATIONS WITH DIHEDRAL SYMMETRY GROUP

In contrast to the chiral astral configurations that — in a certain sense — are all formed alike, the dihedral ones come in several very different varieties.

The first variety consists of configurations that are astral in the **e**xtended **E**uclidean plane but are not contained in the Euclidean plane itself; we shall refer to them as EE configurations. It is clear that such configurations must have one orbit of points at infinity, hence the other orbit of points needs to consist of the vertices of an isogonal polygon. In fact, the polygon must be regular. Indeed, consider any point at infinity and the three lines incident with it, hence mutually parallel. Since there are only two transitivity classes of lines, two of these lines must be in the same orbit; this implies that the third line is situated between these two, and is in fact a mirror interchanging the two lines. Therefore the sides of the polygon contained in these lines are congruent, that is, the pairs of points are at equal distance apart. But since each vertex must be on a third line (besides the two determined by the sides of the isogonal polygon), that line must be a mirror as well and therefore the adjacent sides of the polygon are of equal length. Hence the polygon is regular, and the configuration can be described as follows:

Theorem 2.8.1. If C is an (n_3) configuration of type EE, hence with dihedral symmetry group, that is astral in the extended Euclidean plane but is not contained in the Euclidean plane itself, then $n = 3m$ for some $m \geq 3$. The points of C are of the vertices of a regular $(2m)$-gon M and the m points at infinity in the directions of the m longest diagonals of M. The lines of C are the ones determined by the m longest diagonals of M, together with the $2m$ lines determined by pairs of points of M at span $m - j$ for some $0 < j < m/2$ with $j \equiv m \pmod 2$. The symmetry group of C is d_{2m}.

The EE configurations can therefore be characterized by a pair of integers m and j, and denoted by $EE(3m;m,j)$, with $0 < 2j < m \geq 3$ and with $j \equiv m \pmod 2$. Several examples of EE configurations are shown in Figure 2.8.1.

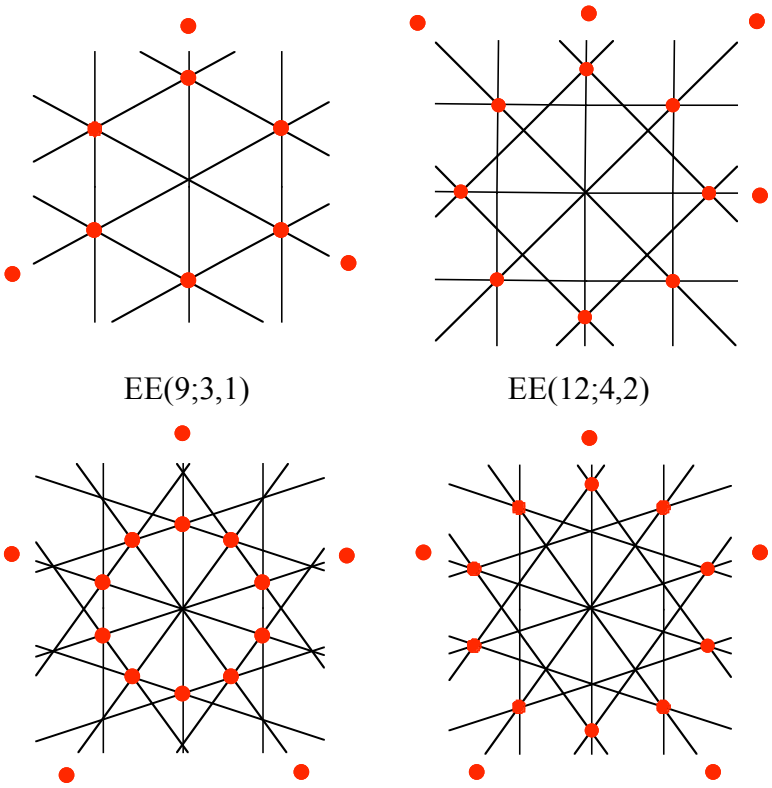

Figure 2.8.1. Examples of configurations of type EE. In each case, points at infinity in the directions of the longest diagonals are indicated by the detached dots.

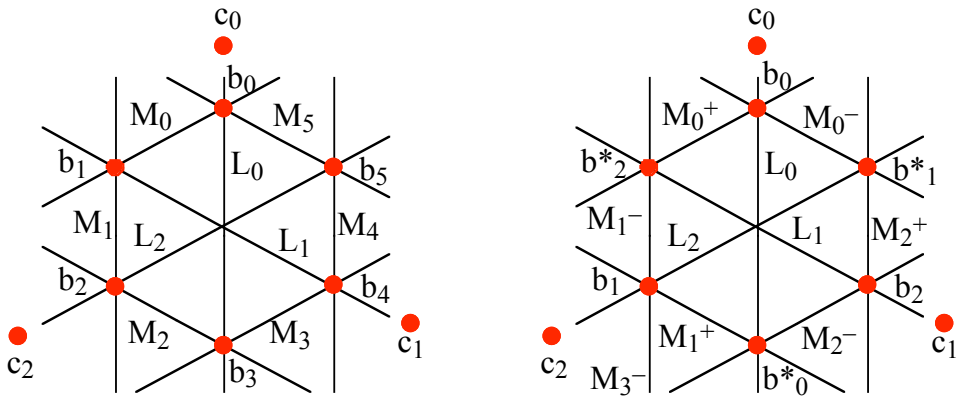

Figure 2.8.2. The configuration EE(9;3,1) labeled with the symmetry group c_6 (at left) and d_6 (at right). In both cases, the c points and the L lines are mapped onto themselves by halfturns.

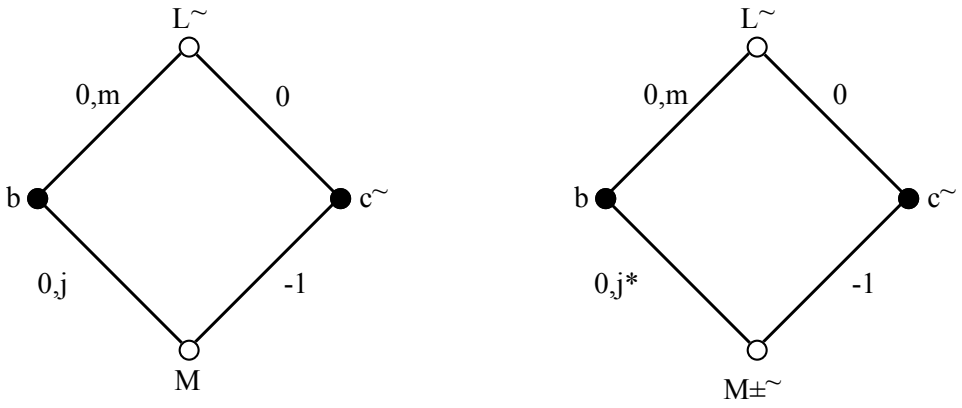

Symmetry group c_{2m} Symmetry group d_{2m}

Figure 2.8.3. The reduced Levi graphs of configurations EE(3m;m,j). All labels are understood mod 2m.

The second variety of dihedral astral 3-configurations may be thought of as **d**ihedrally **d**oubled-up chiral astral configurations, and we shall call them DD configurations. The typical notation is m#(b,c;d;μ); it will be explained soon. The DD configurations resemble chiral astral configurations in many respects, but there is one large difference.

First, the difference. The construction of chiral astral configurations starts with a set of points at the vertices of a **regular** polygon. In the dihedral case, the 2m vertices of any **isogonal** polygon can serve as starting points of a DD configuration ($(4m)_3$). Such vertices fall into two subsets of equal size, the m points in each subset being related by rotational symmetries of the whole set. The two subsets of points are images of each other under reflective symmetries of the whole set. The last entry μ in the symbol m#(b, c; d; μ) of a dihedral astral (n_3) configuration of type DD refers to the ratio (not exceeding 1) of the angles subtended by the sides of the isogonal (2m)-gon used in the construction.

Next, the similarities. There are again — naturally, in view of the definition of astrality — two orbits of points and two orbits of lines. Due to the presence of reflections, each orbit of elements has two suborbits, each suborbit consisting of m elements that are equivalent under rotations, without the need for reflections. In the example shown in Figure 2.8.4, and in general, the points in the two suborbits of the first class are

denoted by B_j^+ and B_j^-, those in the second class by C_j^+ and C_j^-. If $b \neq c$, we shall usually assume $b > c$. The points B_j^+ and B_j^- are on endpoints of diagonals of span b of each of the two m-gons determined by points of the suborbit, while C_j^+ and C_j^- are on diagonals of span c of the other two m-gons. One of the mirrors is the bisector of $B_0^+B_0^-$; it is indicated in Figure 2.8.4 by the dashed vertical line. The B_j^+ and B_j^- points are obtained by rotation in counterclockwise orientation. The construction of the configuration m#(b, c; d; μ) proceeds as follows; it is illustrated in Figure 2.8.4, where $m = 5$, $b = 2$, $c = 1$, $d = 1$, and $\mu = 0.6$.

B_0^+ and B_b^+ determine the line L_0^+ and the point C_0^+, which divides the segment $B_0^+B_b^+$ in a ratio λ; this ratio is fixed throughout the construction, but still undetermined. More generally, B_j^+ and B_{j+b}^+ determine C_j, clearly with the same ratio λ. Then the line M_0^+ in determined by C_0^+ and C_c^+; it passes through B_d^-, and more generally, C_j^+ and C_{j+c}^+ determine the line M_j^+ that is incident with B_{j+d}^-. This requirement determines the value of λ through a quadratic equation. In turn, the line L_d^- through B_d^- and B_{d-b}^- passes through C_d, and finally C_d^- and C_{d-c}^- are collinear with B_0 on the line M_d^-. As always, the subscripts are understood to be modulo m. These requirements can all be met simultaneously, due to the symmetry of the sets of points involved.

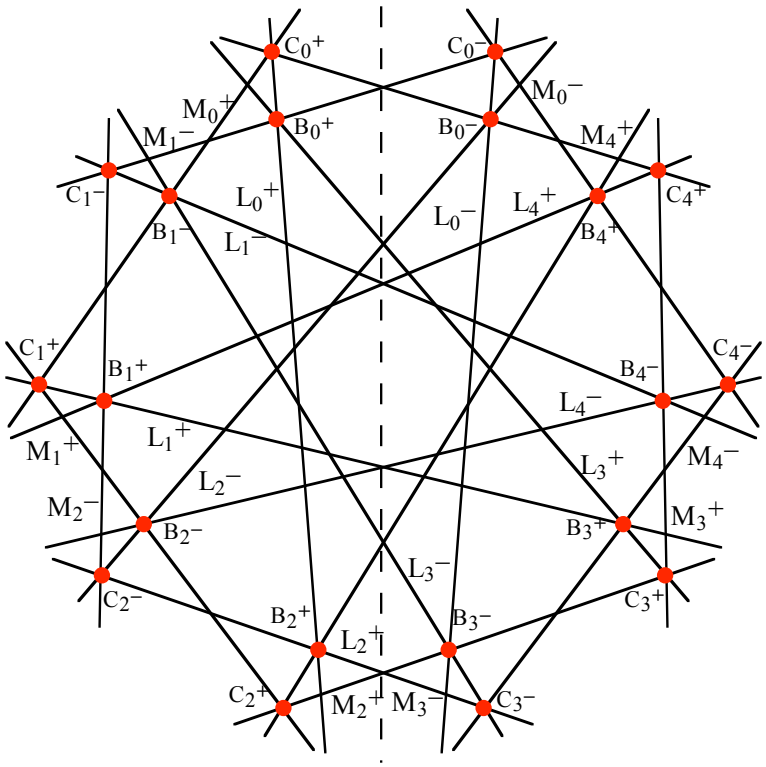

Figure 2.8.4. A dihedral astral configuration (20_3), with symmetry group d_5. The labeling illustrates the description given in the text. The configuration has symbol 5#(2,1; 1; 0.6).

As in the case of chiral astral configurations, the construction leads to a quadratic equation for λ. Again, the various possibilities and properties encountered with the chiral astral configurations (n_3) are largely present. In particular, depending on the values of the parameters m, b, c, d, μ of the configuration m#(b, c; d; μ), there can be two, one, or no real solutions. Moreover, for suitable values of these parameters the resulting construction leads to superfigurations. However, there has been very little done on a systematic investigation of the DD configurations. Several additional examples of such configurations and a case of superfiguration are shown in Figures 2.8.5 and 2.8.6.

There is no information available concerning the range of values of d for given m, b, c and μ, or concerning the possible values of λ for given m, b, c, d, μ. Equally missing is any knowledge concerning duality, polarity, selfduality and selfpolarity of DD configurations.

As with chiral astral configurations, the reduced Levi diagrams for dihedral astral 3-configurations are very simple and straightforward. This is illustrated in Figure 2.8.7, which demonstrates the mutual reinforcing of the notation introduced above, and the graphs.

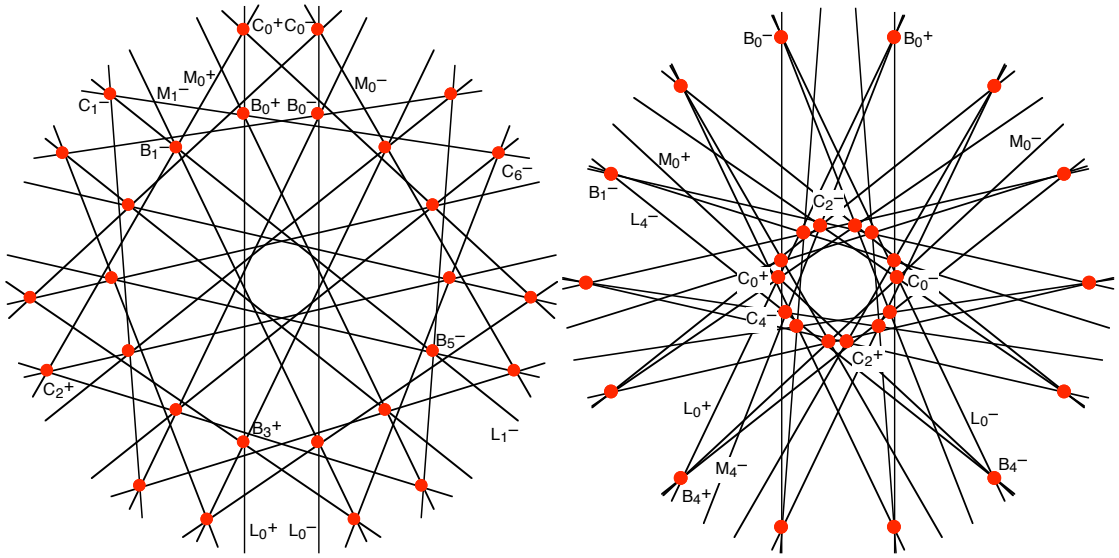

(a) (b)

Figure 2.8.5. Two dihedral astral configurations (28_3). To reduce clutter, only the labels needed for the determination of the symbol are shown. (a) 7#(3,2;1;1.0) (b) 7#(3,2;4;1.0).

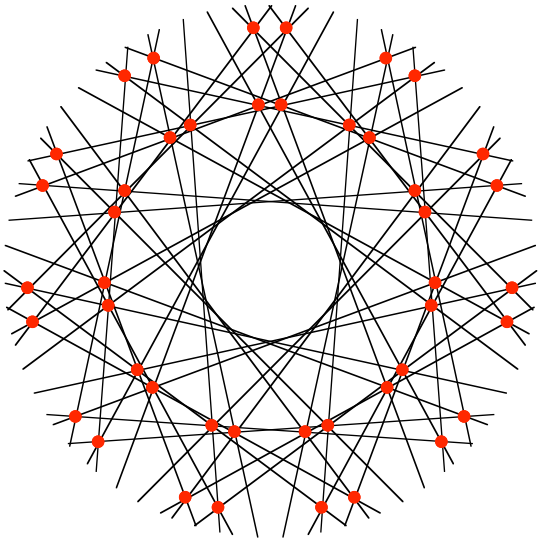

Figure 2.8.6. For a value of μ close to 0.5, the construction of the configuration 7#(4,3;1;μ) leads to a superfiguration: there are unintended incidences, yielding points on four lines and lines through four points.

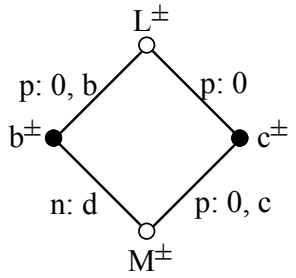

Symmetry group d_{2m}

Figure 2.8.7. The reduced Levi graph of the dihedral astral configuration m#(b,c;d;μ). The construction of the graph follows the method given in Section 1.6, based on the labeling of these configurations described above and illustrated in Figures 2.8.4 and 2.8.5. If the inclusion of the parameter in the graph is desirable, it can be attached to the 0 on the edge going from $L^{\pm}$ to $c^{\pm}$.

First examples of the third variety of dihedral astral 3-configurations were discovered only last year, and appear in the paper [B11] by L. W. **B**erman and J. **B**okowski.[1] We shall designate all configurations of this variety by BB with appropriate parameters attached. Any BB configuration (n_3) has $n = 3m$ for an integer $m \geq 5$. The configuration depends on two other parameters which we call s and t. The meaning of these parameters will be explained as we describe the construction of the configuration BB(m; s, t). We shall illustrate the construction in the case of BB(5; 2, 2), see Figure 2.8.8, but use general terms in the explanation of the steps.

The first step (Figure 2.8.8a) is the construction of a regular m-gon P, and selecting the midpoints of its sides; these midpoints are m of the points of the configuration, and the lines L_j determined by the sides of the m-gon are m of the lines. (The vertices of the m-gon play no added role in the construction, and are not marked in Figure 2.8.8.)

The second step (Figure 2.8.8b) is the selection of a chord of P of span s, and constructing the circumcircle C of the triangle determined by the endpoints of the chord and the center of P. The parameter s needs to be in the range $2 \leq s < m/2$.

---

[1] I had the privilege of receiving a preprint of this paper from the authors.

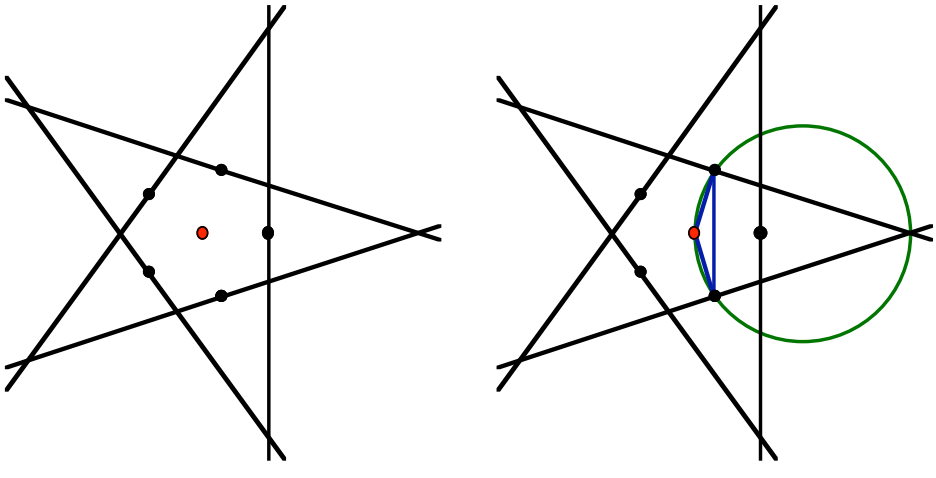

(a)

(b)

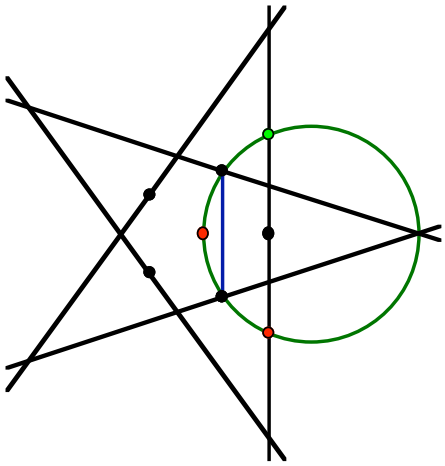

(c)

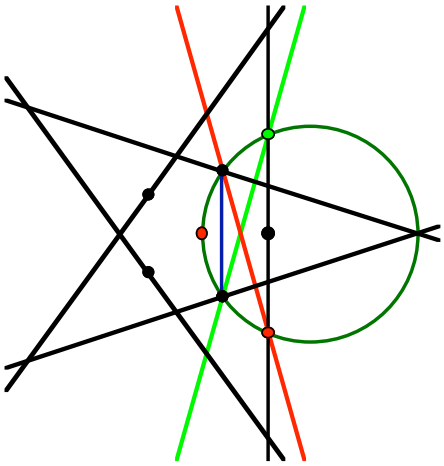

(d)

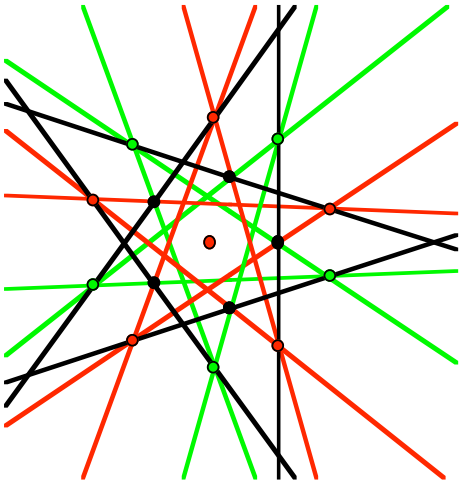

(e)

Figure 2.8.8. The steps in the construction of the configuration BB(5;2,2).

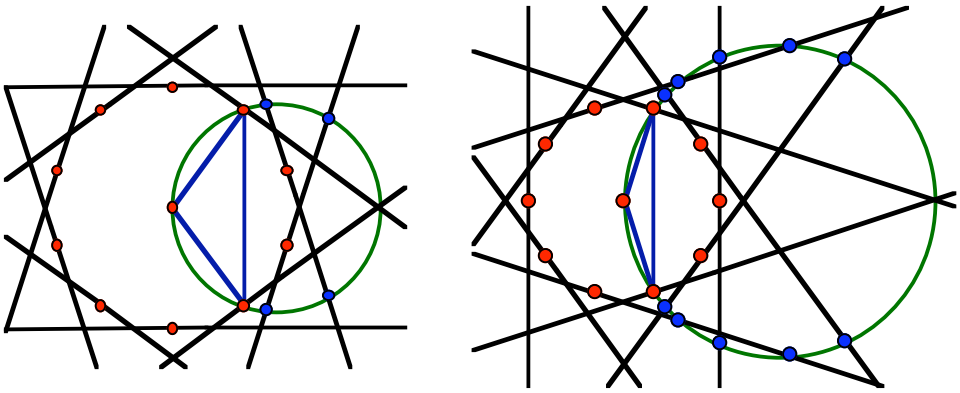

(a) (b)

Figure 2.8.9. Illustration of the possibilities in the third step of constructing configurations BB(10; s, t). In part (a) $s = 3$ and t is either 2 or 3. In part (b) $s = 4$ and $2 \le t \le 6$.

The third step (Figure 2.8.8c) consists in determining the intersections of the circle C with the lines L_j constructed in the first step. These intersection points always came in symmetric pairs. In case $m = 5$ (hence $s = 2$) there is only one such pair; the examples in Figure 2.8.9 show other possibilities. There are always at least $s–1$ pairs, and no more than $2s – 3$. The precise number depends on m and s in a manner that has not been explicitly determined.

In the fourth step (Figure 2.8.8d) a selected pair of these intersection points is connected by lines with the endpoints of the chord of span s with which we started in the second step. (To avoid clutter, in Figure 2.8.8d each point of the pair is connected with only one endpoint of the chord.) The parameter t is the label that can be given to the pairs, counting from the endpoints of the chord.

The fifth and final step (Figure 2.8.8e) consists in creating the images of the chosen pair of points and the lines generated in the previous step, by rotations about the center of the polygon P through all the multiples of $2\pi/m$.

Some remarks about the BB configurations. First, just as in the case of the DD configurations (and the chiral astral ones), in some instances the construction does not yield the expected configuration; instead a superfiguration is obtained. This is illustrated

in Figure 2.8.10. Also, the precise relations between the parameters of a BB configuration have not been determined so far. This is illustrated in Table 2.8.1, which shows the (experimentally determined) maximal value of t for given m and s.

m \ s	2	3	4	5	6	7	8	9	10	11	12	13	14	15	16	17	18
5	2																
6	2																
7	2	3															
8	2	3															
9	2	3	6														
10	2	3	6														
11	2	3	6	7													
12	2	3	4*	7													
13	2	3	4	7	10												
14	2	3	4	7	8												
15	2	3	4	7	8	11											
16	2	3	4	7	8	11											
17	2	3	4	7	8	11	12										
18	2	3	4	7	8	9	12										
19	2	3	4	7	8	9	12	15									
20	2	3	4	7	8	9	12	13									
21	2	3	4	7	8	9	12	13	16								
22	2	3	4	7	8	9	12	13	16								
23	2	3	4	7	8	9	12	13	16	19							
24	2	3	4	7	8	9	10*	13	14	17							
25	2	3	4	7	8	9	10	13	14	17	20						
26	2	3	4	7	8	9	10	13	14	17	20						
27	2	3	4	7	8	9	10	13	14	17	18	21					
28	2	3	4	7	8	9	10	13	14	17	18	21					
29	2	3	4	7	8	9	10	13	14	15	18	21	22				
30	2	3	4	7	8	9	10	13	14	15	18	19	22				
31	2	3	4	7	8	9	10	13	14	15	18	19	22	25			
32	2	3	4	7	8	9	10	13	14	15	18	19	22	25			
33	2	3	4	7	8	9	10	13	14	15	18	19	22	23	28		
34	2	3	4	7	8	9	10	13	14	15	18	19	22	23	26		
35	2	3	4	7	8	9	10	13	14	15	18	19	22	23	26	29	
36	2	3	4	7	8	9	10	13	14	15	16*	19	20	23	26	29	
37	2	3	4	7	8	9	10	13	14	15	16	19	20	23	24	27	32

(*) One of the lines is tangent to the circle at its intersection with another line.

Table 2.8.1. The maximal values of t for given m and s in configurations BB(m; s,t).

The BB configurations considered in [B11] are presented in a way tyat is somewhat different from the one followed here. The Berman-Bokowski construction corresponds to the cases of even s only, and uses only that pair of intersection points which arises by the intersection of the circumcircle with the line parallel to the chord used to construct the circle. This pair is in general the "middle" pair in the third step of our construction.

Another phenomenon — again shared by other classes of configurations — is the possibility of the configuration being disconnected. This happens, for example with the configuration BB(16; 6,6) shown in Figure 2.8.11.

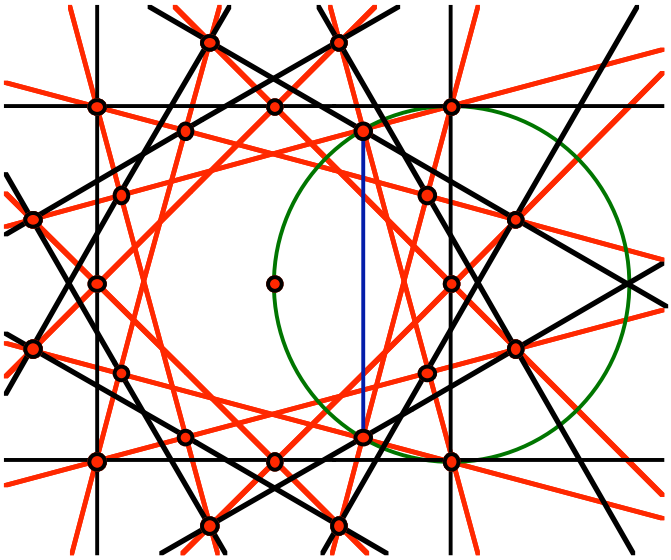

Figure 2.8.10. An example of a superfiguration arising in the construction of a BB type configuration with m = 12 and s = 4.

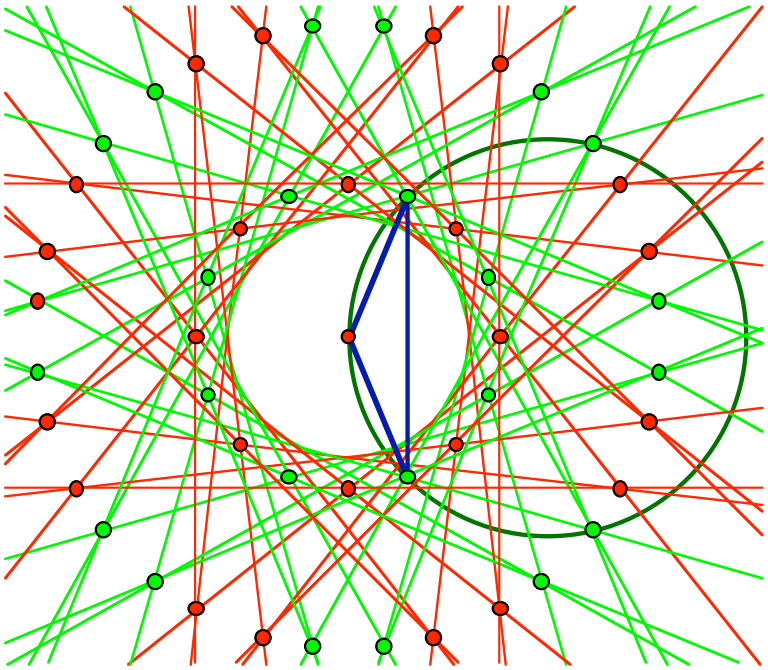

Figure 2.8.11. In the case of BB(16; 6, 6) the construction leads to a disconnected configuration. The two connected components are shown in different colors; each is BB(8; 3, 3).

While the construction procedure seems to be working in the examples given above, there is an obvious need for justification in the general case. It is, in fact, quite simple; we explain it for the configuration BB(m; s, t) by using the notation in the illustrative example shown in Figure 2.8.12, where $m = 9$, $s = 3$, and $t = 3$.

The chord of span s (used to generate the circumcircle K) spans an angle of $2\pi s/m$ at the center O of K. The line CB*, the legs of the isosceles triangle generated by the chord and O, and the segment OC are all well determined. Rotating this complex and the circle K about O through an angle of $2\pi s/m$ brings K to K*, CB* to C*B, and OC to OC*. The five angles denoted γ are all equal to each other because they are either basis angles of isosceles triangle, or spanned by congruent arcs of K. Hence the basis CC* of the isosceles triangle COC* encloses with the segment OC* the same angle γ as the line through C*B; hence that line passes through C, which justifies the construction.

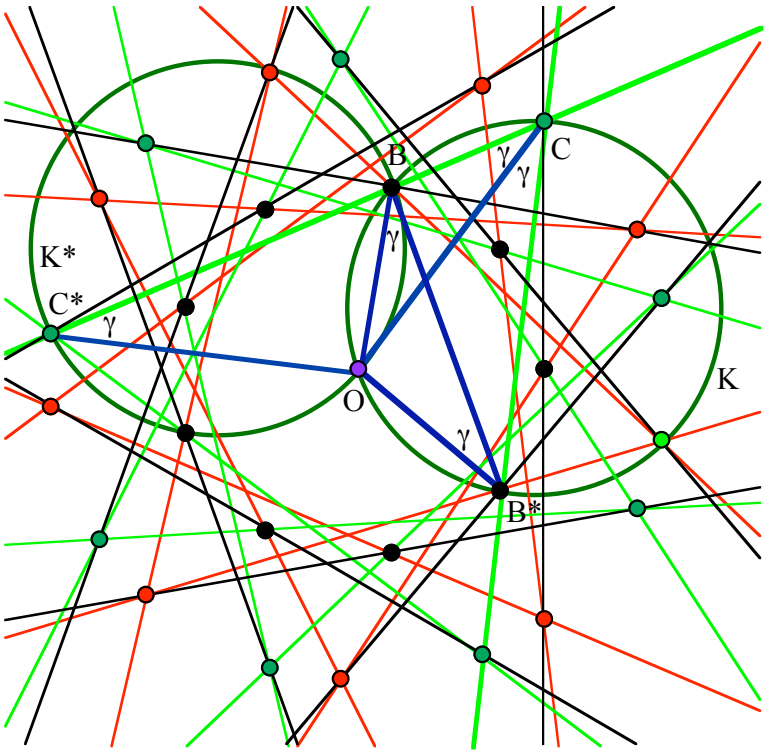

Figure 2.8.12. The validation of the construction of the BB configurations.

It should be noted that the procedure used to justify the construction dealt exclusively with the green lines. This leaves open the possibility to use a different value of t for the red lines. Naturally, the resulting configuration will not be astral.

Another point that needs to be made is the following. For each s, the set of values of t possible is a (non-strictly) decreasing function of m. The experimental results in Table 2.8.1 are a consequence of reasonably complicated trigonometric relations. The main problem in this context is to determine the maximal value of t possible in a BB(m; s,t) configuration. From numerical evidence (see Table 2.8.2) it seems that this t_{max} grows approximately as 7s/5 for sufficiently large m, although this appears a strange dependence.

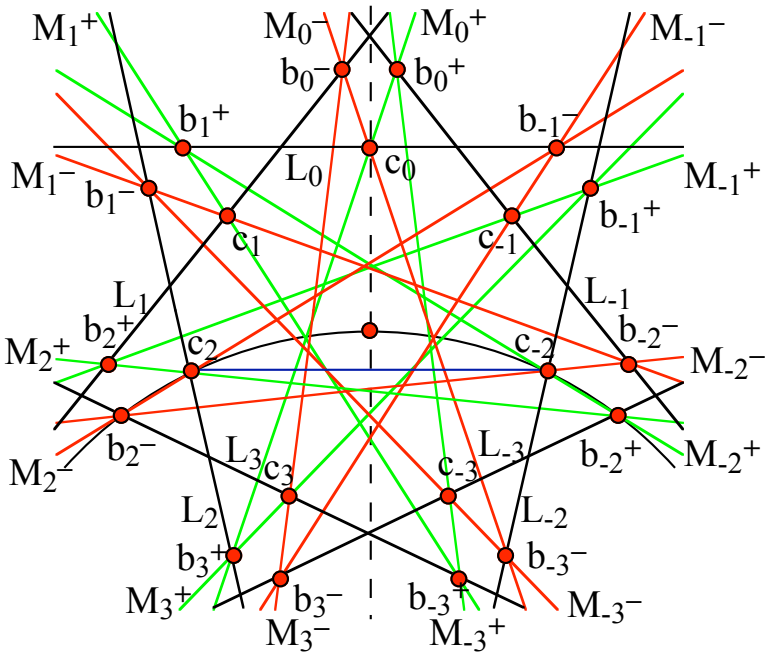

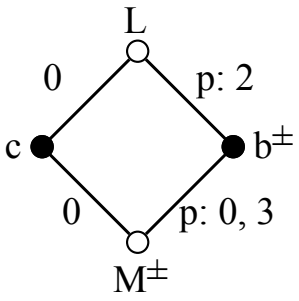

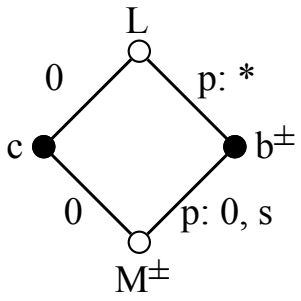

Figure 2.8.13. The labeling of BB configurations, and the resulting reduced Levi graphs. The graph at right corresponds to the general configuration BB(m; s, t); the asterisk indicates that no definite relation to the parameters has been found so far.

s	t_{max}	For m ≥
2	2	5
3	3	7
4	4	12
5	7	11
6	8	14
7	9	18
8	10	24
9	11	42
10	14	24
11	15	29
12	16	36
13	17	50
14	18	92
15	21	41
16	22	48
17	23	61
18	24	84
19	25	78
20	28	60

s	t_{max}	For m ≥
21	29	72
22	30	90
23	31	127
24	32	372
25	35	84
26	36	99
27	37	125
28	38	183
29	41	95
30	42	110
31	43	131
32	44	167
33	45	256
34	48	121
35	49	139
36	50	167
37	51	217
38	52	335
39	55	149
40	56	172

Table 2.8.2. The largest value t_{max} of t possible in configurations BB(m; s, t) for a given s and for all sufficiently large m.

Exercises and problems 2.8.

1. Determine what symbol could result for the configuration in Figure 2.8.4 if the role of B_0^+ and B_0^- were reversed, while still assuming conterclockwise orientation.

2. Determine what symbol could result for the configuration in Figure 2.8.4 if the role of the B-points and the C-points were reversed, while still assuming conterclockwise orientation.

3. Verify the assignment of symbols to the configurations in Figure 2.8.5.

4. Formulate a general criterion for the configuration BB(m; s,t) to be disconnected.

5. Draw all the different configurations BB(11; 5,t).

6. How many different configurations 4#(b, c; d; 0.3) are there?

7. Find some restrictions on the parameters of the DD and BB kinds of astral configurations.

8. Find disconnected configurations m#(b, c; d; μ).

9. Find a geometric construction for configurations m#(b, c; d; μ).

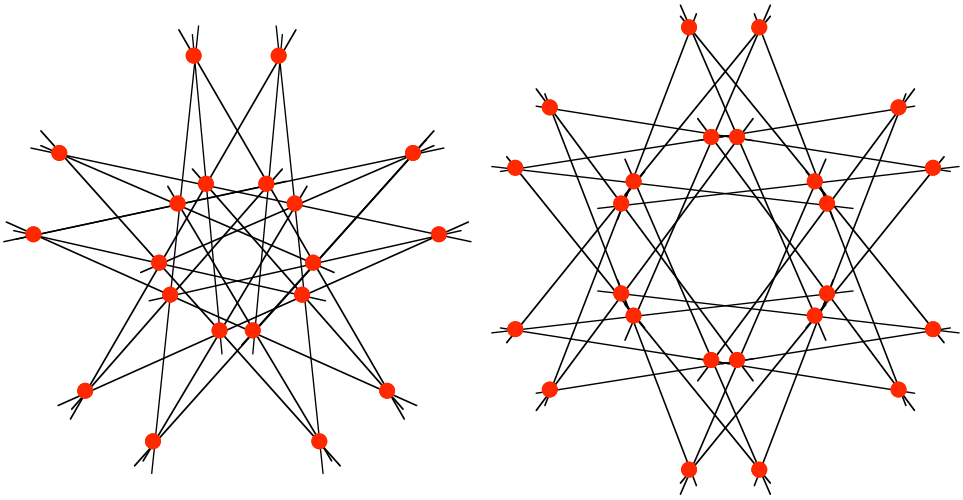

Figure 2.8.14. Two dihedral astral 3-configurations.

10. Find the symbols for the configurations in Figure 2.8.14.

2.9 MULTIASTRAL 3-CONFIGURATIONS

A geometric configuration is said to be of **symmetry type** $[h_1, h_2]$ provided its points form h_1 orbits, and its lines h_2 orbits under the group of its isometric symmetries. We shall also say that such a configuration is $[h_1, h_2]$**-astral**, or, if the precise values of h_1 and h_2 are not important in the discussion, that it is **multiastral**. Clearly, if a configuration of type [q, k] is $[h_1, h_2]$-astral then $h_1 \geq (k+1)/2$ and $h_2 \geq (q+1)/2$. If h_1 and h_2 have these minimal values we shall simplify the language and say that the configuration is **astral**. In cases where $h_1 = h_2 = h$, we shall say that the configuration is h**-astral.**

The study of these configurations is much less advanced, and promises to be more challenging than the investigation of the 2-astral 3-configurations. There are two sources of the variety possible for h-astral 3-configurations. On the one hand, similarly to the situation with dihedral astral configurations, in many cases there is at least one parameter that can assume a continuum of different real values. On the other hand, if $h \geq 3$, a line of the configuration can contain points from either two or three different orbits. The case $h = 2$ is radically different from those with $h \geq 3$.

The h-astral 3-configurations come in three varieties:

- **projectively h-astral**, that is, configurations that are h-astral in the *extended Euclidean* (that is, *projective*) plane E^{2+}, but not in the Euclidean plane E^2 itself.
- **h-chiral** that is, configurations in the Euclidean plane E^2, with a cyclic symmetry group.
- **h-dihedral,** that is configurations in the Euclidean plane E^2, with a dihedral symmetry group.

Throughout, the use of a numerical prefix h- means that there are *at most* h orbits of points and *at most* h orbits of lines, with *equality in at least one case*.

Examples of **projectively astral** configurations are shown in Figure 2.9.1 and 2.9.2. The configuration in Figure 2.9.1 is a realization of the Pappus configuration. Two 3-astral realization of the Desargues configuration (10_3) in E^{2+} are shown in Figure

2.9.2; they are among the illustrations given by Coxeter [C8]. Two examples of projectively 3-astral configurations (15_3) are shown in Figure 2.9.3. It is clear that similar examples of projectively h-astral configurations could be found for all $h \geq 4$. At least for small h, the complete characterization of projectively astral configurations may be feasible but has not been worked out.

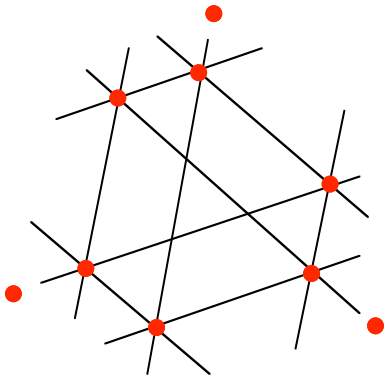

Figure 1. A 3-astral version of the Pappus configuration ($_{93}$) in the extended Euclidean plane.

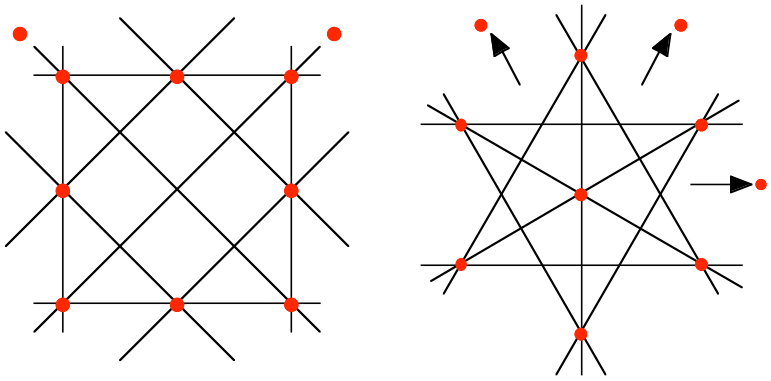

(a) (b)

Figure 2.9.2. Two projectively 3-astral realizations of the Desargues configuration (10_3) (after [C8]). In (b) the line at infinity is included.

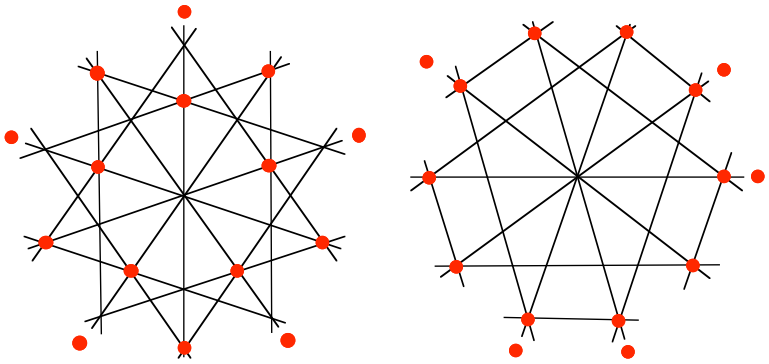

Figure 2.9.3. Two examples of projectively 3-astral configurations (15_3). Notice that the one at left is [3, 2]-astral, and the one at right is [2, 3]-astral.

h-chiral astral configurations (n_3) are much more interesting. We have discussed the 2-astral chiral configurations in Section 2.7. For $h \geq 3$ there is more than one possibility. We begin by explaining the notation for h-chiral configurations in which each line is incident with points of two orbits only; the remaining case — some lines incident with three orbits of points — will be described later. The notation used in Section 2.7 will be expanded here; the general form for h-chiral configurations (n_3) of this kind is $m\#(b_1, b_2, \dots, b_h; b_0; \lambda_1, \lambda_2, \dots, \lambda_{h-2})$ — or in a shorter symbol $m\#(b_1, b_2, \dots, b_h; b_0)$. Here $n = hm$ and we have $h-2$ real parameters λ_j besides $h+1$ discrete ones b_j. Together these parameters lead to a quadratic equation for an additional parameter λ. This equation can have 2, 1 or 0 real solutions — in the last case there are no corresponding real configurations. Our explanation is illustrated in Figure 2.9.4, using a 3-chiral configuration (27_3) as an example.

The detailed study of h-chiral configurations was initiated by Boben and Pisanski [B20] under the name "polycyclic configurations", and with slightly different notation. As pointed out in [B20], the dual of a configuration $m\#(b_1, b_2, \dots, b_h; b_0)$ is the configuration $m\#(b_h, b_{h-1}, \dots, b_1; b_1+b_2+ \dots +b_h-b_0)$. For $h = 2$ this reduces to the facts we shall discuss at length in Section 2.10.

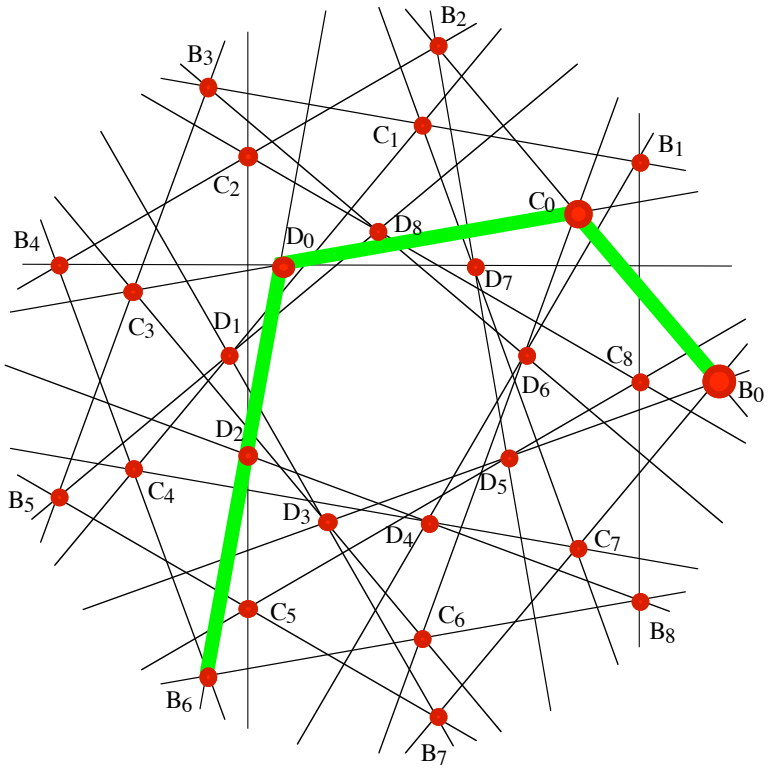

Figure 2.9.4. The characteristic path in a 3-chiral configuration (27_3).

As mentioned earlier, the symbol for an h-chiral configuration (n_3), where $n = hm$, is of the form $m\#(b_1, b_2, \dots, b_h; b_0; \lambda_1, \lambda_2, \dots, \lambda_{h-2})$; the parameters are again determined along a **characteristic path**. The entries $b_1, \dots, b_h$ are the spans of the diagonals in the different regular m-gons that are determined by the path; all the diagonals are oriented in the same way — all clockwise or all counterclockwise — and the real numbers $\lambda_1, \lambda_2, \dots, \lambda_{h-2}$ denote the ratios in which each diagonal determined by a segment of the path is divided by the endpoint of the segment. The path returns to the starting polygon, but not necessarily to the starting point of the path. The parameter b_0 indicates the vertex of the starting polygon at which the characteristic path ends. These data lead to a quadratic equation for the ratio λ on the next-to-last segment; the ratio applicable to the last segment is then completely determined. Thus there are either two, or one,

or no real geometric configurations corresponding to a given symbol. There are also possibilities of unintended incidences similar to the ones we encountered earlier, hence we are in general talking about **representations** of the symbols, rather than **realizations**. In case the parameters $\lambda_1, \lambda_2, \dots, \lambda_{h-2}$ in a symbol $m\#(b_1, b_2, \dots, b_h; b_0; \lambda_1, \lambda_2, \dots, \lambda_{h-2})$ are not relevant or not known, we abbreviate the symbol to $m\#(b_1, b_2, \dots, b_h; b_0)$.

The example in Figure 2.9.4 presents a 3-chiral configuration with symbol 9#(2,3,2;6;0.5). The points of the three orbits are denoted by B_j, C_j, D_j. The determination of the symbol is highlighted by the three-step characteristic path. Note that the ratio λ_1 can be chosen freely, and in the illustration it was taken as $\lambda_1 = 0.5 = C_0B_0/B_2B_0$. Once the first h-2 ratios λ_j are chosen, the last ratio λ_{h-1} (determining the position of the point of last orbit on the penultimate diagonal) is determined by a quadratic equation. (For details see [B20].) In the illustration we have $h = 3$, hence $\lambda_{h-1} = \lambda_2$ (which is about 2/3). Naturally, the symbol is not unique since it depends, besides the λ_j's for $h \geq 3$, on the orbit of the starting point, and on the orientation chosen. The influence of the parameter λ_{h-2} is illustrated in Figure 2.9.5.

Using symbols like u, v, w, ... for elements of the different orbits of points, we can say that the h-chiral configurations considered so far have lines of type {u,u,v}, {v,v,w}, ... But other possibilities exist in which the incidences of lines with orbits of the points are different. For example, in case h = 3, it is possible to have three orbits of lines, all three of the type {u,v,w}, or else, one of the type {u,v,w} and the other two of types {u,v,v} and {u,w,w}. Three example of the former variety are shown in Figure 2.9.6, while examples of the second kind are illustrated in Figure 2.9.7; the diagrams in Figure 2.2.1 show the $(9_3)_2$ and $(9_3)_3$ configurations, which is of these two kinds. A notation for the configurations in Figure 2.9.6 is explained in the caption. An apparently convenient notation is proposed for the kind of configurations shown in Figure 2.9.7. It assigns the first symbol to the line and the point that are incident with three orbits of the other kind, and the other symbols in the obvious manner. For the notation one conven-

iently chooses the one that involves the smallest maximal parameter. No additional details about either of these kinds of configurations are available as of this writing.

Naturally, for $h \geq 4$ it is possible to imagine an increasingly large number of types of h-chiral configurations. However, so far nothing has been done in this direction.

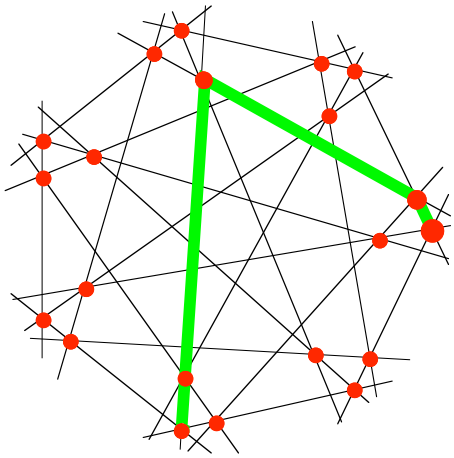

7#(1, 2, 3; 5; 0.2)

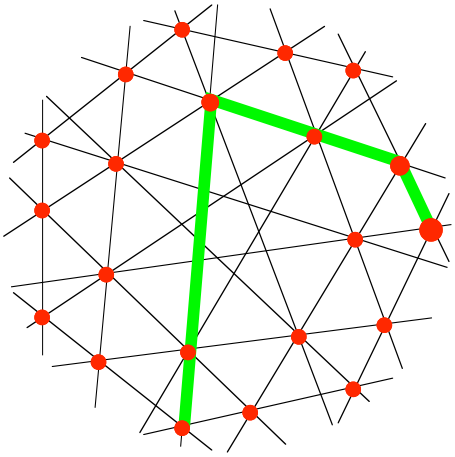

7#(1, 2, 3; 5; 0.4)

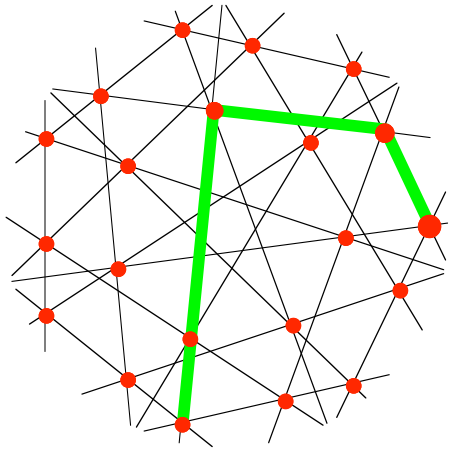

7#(1, 2, 3; 5; 0.6)

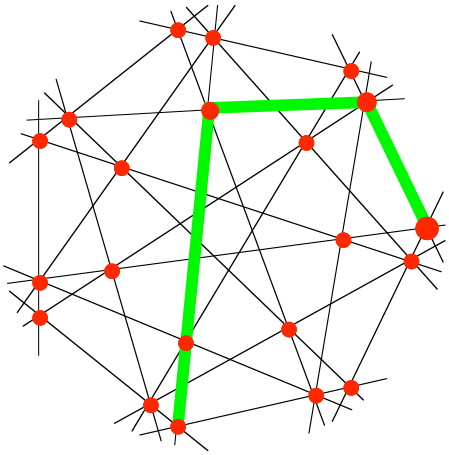

7#(1, 2, 3; 5; 0.8)

Figure 2.9.5. An illustration of the dependence of a 3-chiral configuration (21_3) on the parameter λ_1.

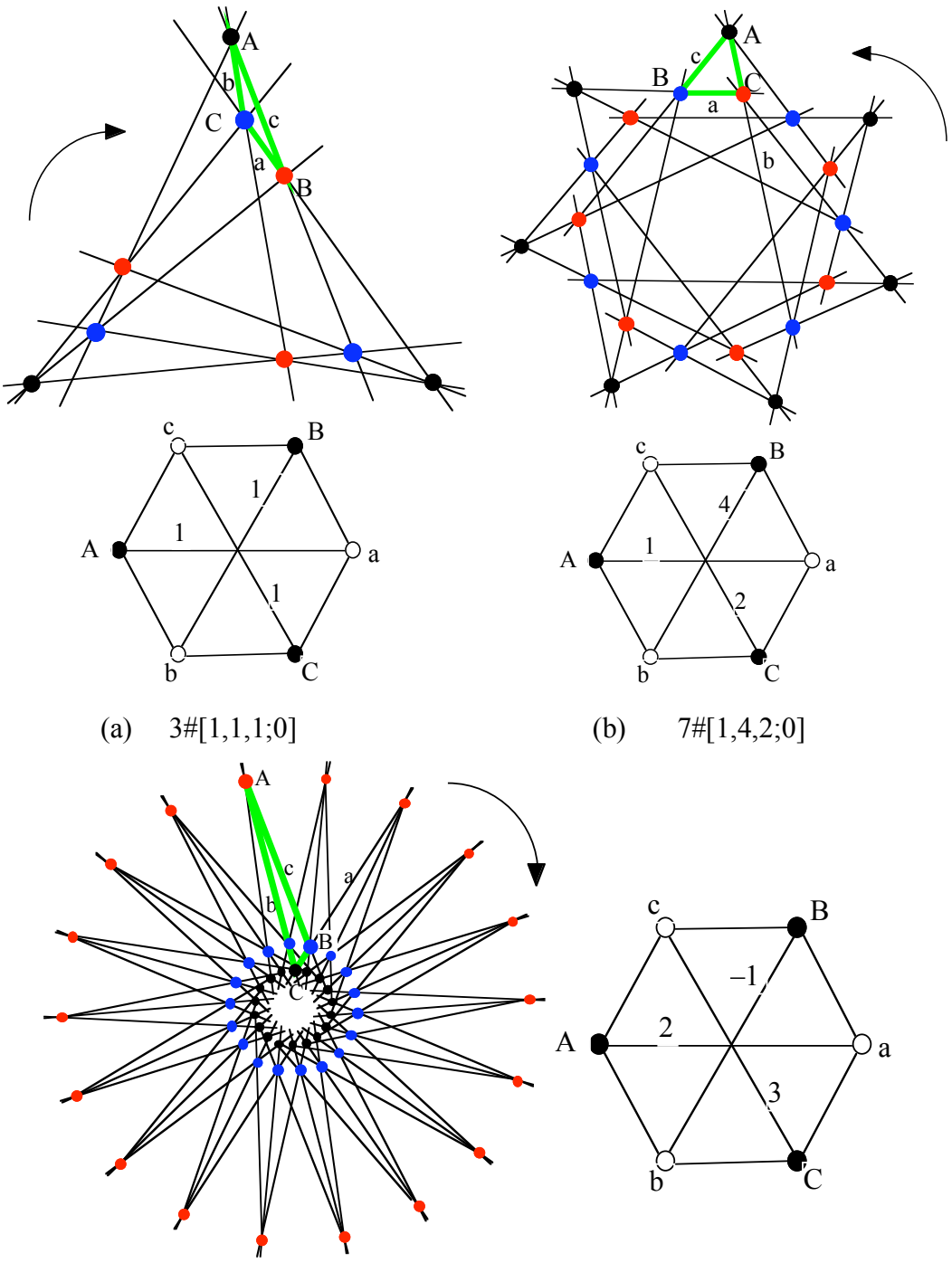

Figure 2.9.6. Two examples of 3-chiral configurations in which every line meets all three orbits of points, and every point meets lines of the three orbits. The characteristic path (which does not have to be closed) leads to a symbol for the configuration. The configuration in (a) is another realization of the Pappus configuration. With each we show a reduced Levi diagram.

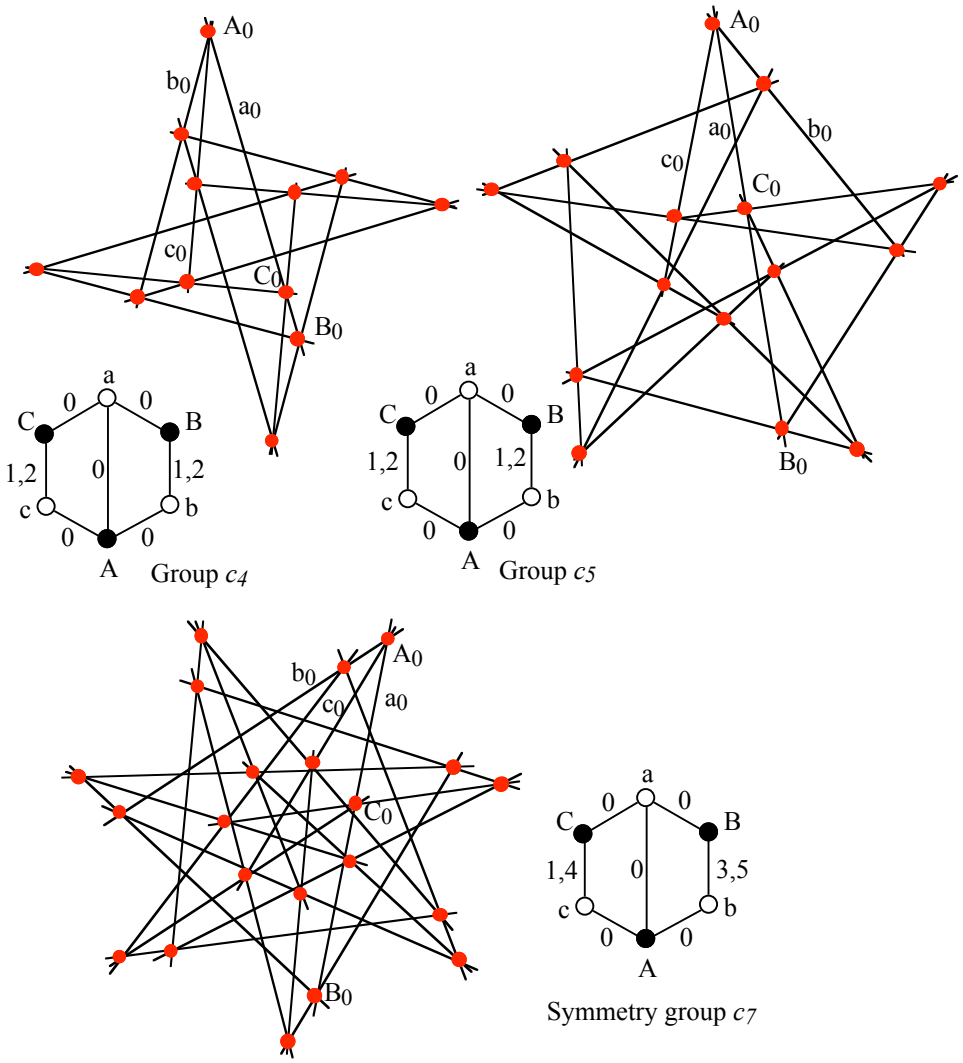

Figure 2.9.7. Examples of 3-chiral configurations in which each line of one orbit is incident with points of each of three orbits, while the other lines are incident with two points from one orbit and one point from another orbit. Each is accompanied by a reduced Levi diagram. As symbols for these configurations we can use 4#[1,2;1,2], 5#[1,2;1,2] and 7#[1,4;3,5]. The configuration 5#[1,2;1,2] appears in van de Craats [V1].

h-dihedral configurations are unexplored as well. In Figures 2.9.8, 2.9.9 and 2.9.10 are shown a few examples. The examples in Figure 2.9.8 are obviously typical of an infinite class of analogous constructions. In Figure 2.9.9 only two orbits of points are shown, the points of the third orbit can be chosen at several distinct locations. This kind

of configurations can obviously be generalized in a variety of ways. Figure 2.9.10 illustrates the degree of complication possible with h-astral configurations for larger h.

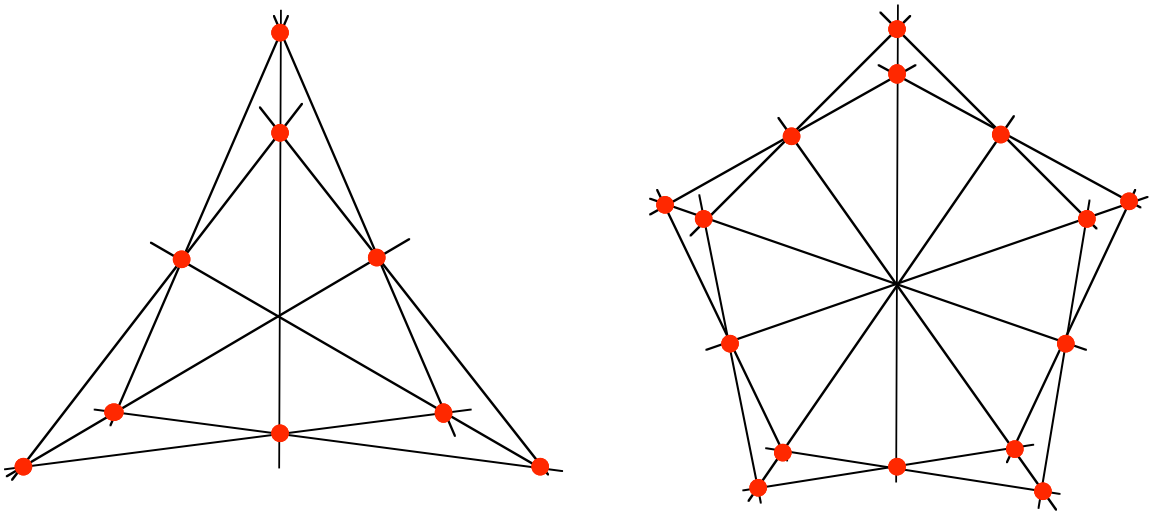

Figure 2.9.8. Two examples of 3-dihedral 3-configurations. The one at left is another realization of the Pappus configuration.

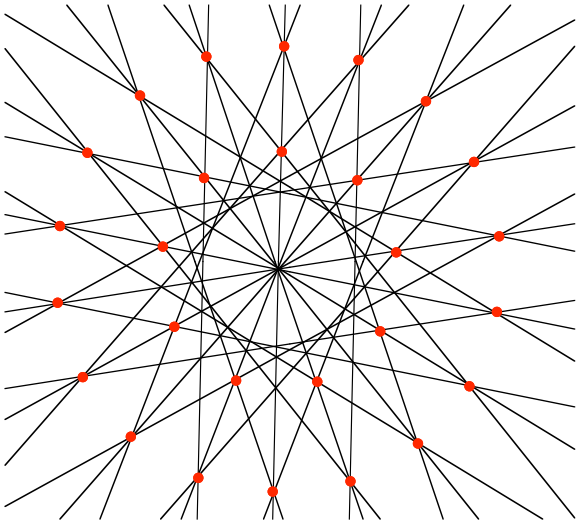

Figure 2.9.9. Adding an orbit of points at suitable intersections leads to several different 3–dihedral configurations. Notice that such configurations are, in fact, [3, 2]-dihedral.

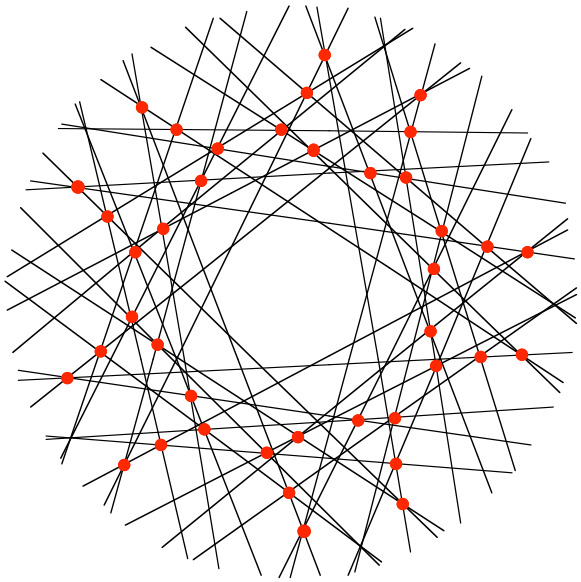

Figure 2.9.10. A [4,5]-dihedral configuration (40_3) found by L. Berman.

Exercises and problems 2.9

1. Decide whether the two configurations in Figure 2.9.3 are dual — or even polar – – to each other. Is either of them isomorphic to the (15_3) configuration in Figure 1.1.1?

2. Determine the number of distinct ways in which it is possible to replace the points in Figure 2.9.9 in such a way that the result is a [3, 2]-dihedral configuration.

3. By moving the outer vertices in Figure 2.9.8 along the mirror, a continuum of (projectively) distinct configurations can be obtained; all these are isomorphic. Are there any analogous configurations (15_3) that are not isomorphic to the one in Figure 2.9.8 ?

4. For $h_1 = 2$ and $h_1 = 3$, determine the possible values of h_2 for which there exist $[h_1, h_2]$-astral configurations of the various kinds. Provide examples for all existing types.

5. Construct examples of 4-chiral configurations (n_3) with the smallest n. Justify your answer. Generalize.

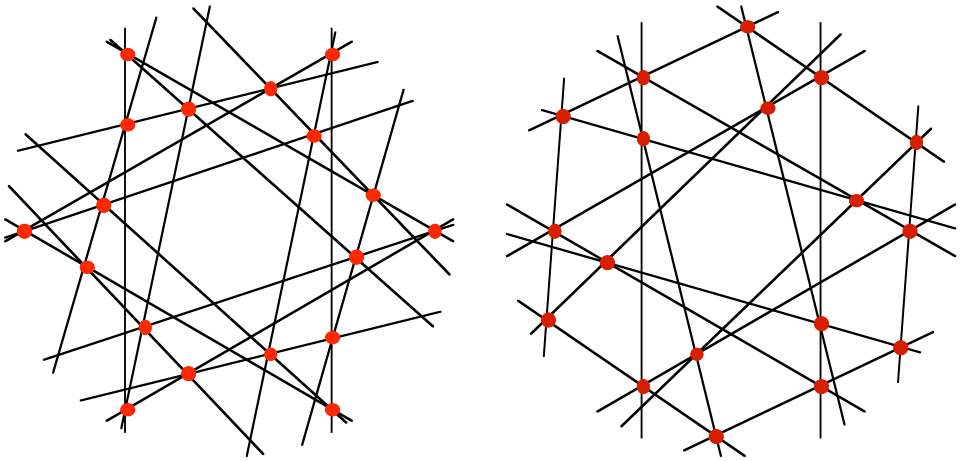

Figure 2.9.11. Two (18_3) 3-chiral configurations.

6. Determine the symbols of the two configurations is Figure 2.9.11.

7. Verify that the Cremona-Richmond configuration (15_3) shown in Figure 1.1.1 is of the type represented by the examples in Figure 2.9.7. Find its symbol.

8. Find the criteria for the property of the first two configurations of Figure 2.9.7 (but not the third) that there are only two orbits of points (and two orbits of lines) under automorphisms.

2.10 DUALITY OF ASTRAL 3-CONFIGURATIONS

In this section we shall investigate the duality and polarity properties of the chiral astral configurations (n_3). It should be kept in mind that the presentation is based on the assumption that we know all such configurations although, in fact, we are certain only to the extent that the topic has been explored by numerical calculations. As we have seen in Section 2.7, to a symbol m#(b,c;d) correspond either two, or one, or no chiral astral configurations (n_3), where n = 2m. In the case of two configurations, by their very construction they are isomorphic. But more is true:

Theorem 2.10.1. Every chiral astral configuration m#(b,c;d) is selfdual.

Proof. From the definition given above of the labels of points and lines of such configurations, illustrated in Figure 2.10.1 (which is a copy of Figure 2.7.1), we see that the line L_j contains the points B_j, C_j, B_{j+b}, and the line M_j contains the points B_{j+d},C_j,C_{j+c}. The resulting incidences can then be described by the following criteria:

$B_j \in L_k \Leftrightarrow j - k \equiv 0 \text{ or } b \pmod m$

$B_j \in M_k \Leftrightarrow j - k \equiv d \pmod m$

$C_j \in L_k \Leftrightarrow j - k \equiv 0 \pmod m$

$C_j \in M_k \Leftrightarrow j - k \equiv 0 \text{ or } c \pmod m$.

From these relations there follows at once that for every configuration m#(b, c; d) the mapping δ determined by $\delta(B_j) = L_{-j}$, $\delta(C_j) = M_{-j-d}$, $\delta(L_j) = B_{-j}$ and $\delta(M_j) = C_{-j-d}$ is a selfduality. □

Another consequence is:

If two distinct configurations have the same symbol m#(b, c; d) then they are dual to each other.

This follows from the fact that they are isomorphic. But even more is true:

Theorem 2.10.2. If two distinct configurations have the same symbol m#(b, c; d) then they are polars of each other.

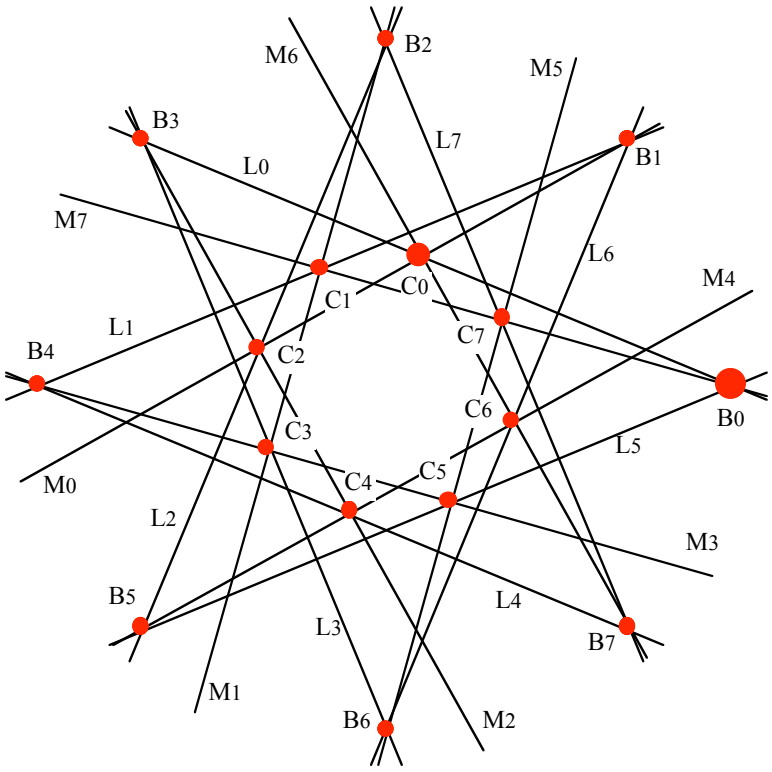

Figure 2.10.1. The labeling of the configuration 8#(3, 2; 1) explained in the text.

Proof. Indeed, polars are combinatorially dual to each other, and the only combinatorially dual astral configuration of an astral configuration m#(b, c; d) is either the configuration itself, or the other one with the same symbol. Since there are two configurations m#(b, c; d), neither is polar to itself, but each is polar to the other. □

This fact is illustrated in Figure 2.10.2.

It is almost selfevident that in general there are other duality maps from a configuration to its dual. For example, Figure 2.10.3 presents the same pair of configuration as Figure 2.10.2(a), with a labeling that shows that the map ε from the red configuration to the black one is a duality different from the duality δ described above.

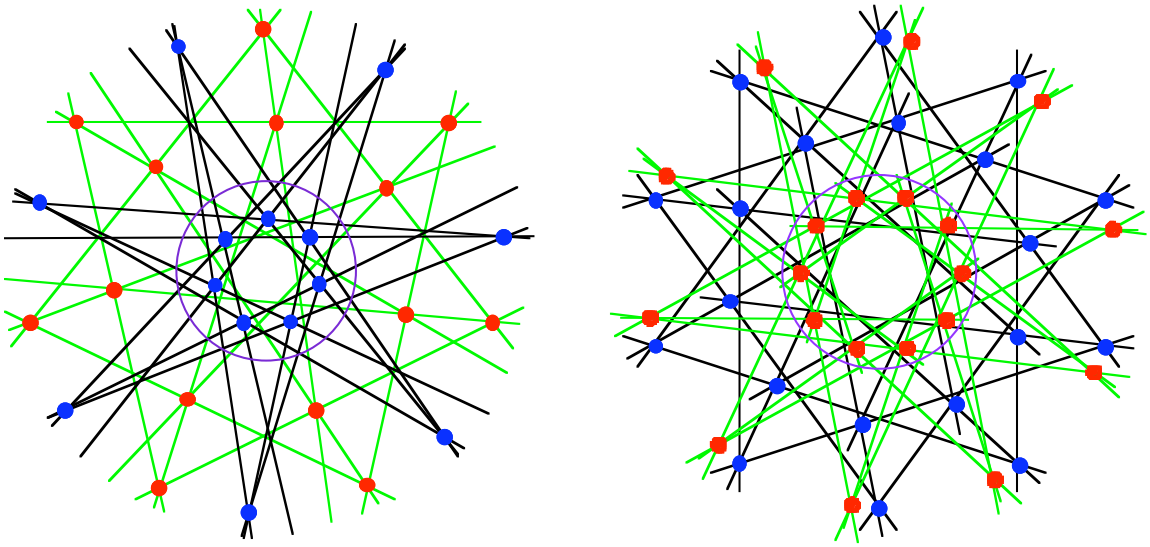

(a) (b)

Figure 2.10.2. (a) The configuration 7#(3,2;1)' (red points and green lines) and its polar 7#(3,2,1)" (blue points and black lines). Polarity is with respect to the purple circle. (b) The same for 10#(4,3;2)' and 10#(4,3;2)".

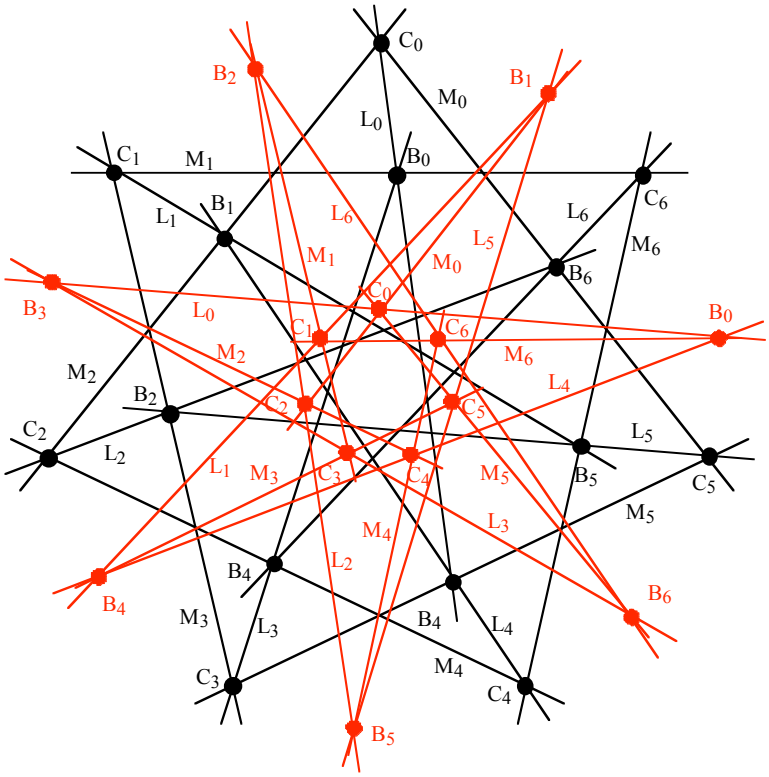

Figure 2.10.3. The dual configurations of Figure 2.10.2(a) illustrate a duality map ε.

In case that only a single configuration m#(b,c;d) exists (that is, if b + c = 2d, or if b = c), the configuration is not only selfdual, but selfpolar. The map δ is applicable to all selfdual configurations, and is concordant with selfpolarity. The polars (in an appropriate circle) are *congruent* to each other, but only after a reflection in a suitable mirror.

For configurations of this type, the map δ and its rotates are the *only* maps compatible with the polarity. We say that these configurations are **oppositely selfpolar**. This happens for the selfpolar configurations with symbol m#(b,b;d). Examples are shown in Figure 2.10.4.

Other configurations, called **directly selfpolar configurations**, have symbols of type m#(b,c;d) with 2d = b+c. Here the polar pairs are congruent without reflection. There are two subtypes: In the first, both b and c are even, in the second they are both odd. In the former case the polars actually coincide with each other, while in the latter they are related by reflection in the common center (that is rotation through 180°). The two subtypes are illustrated in Figures 2.10.5 and 2.10.6.

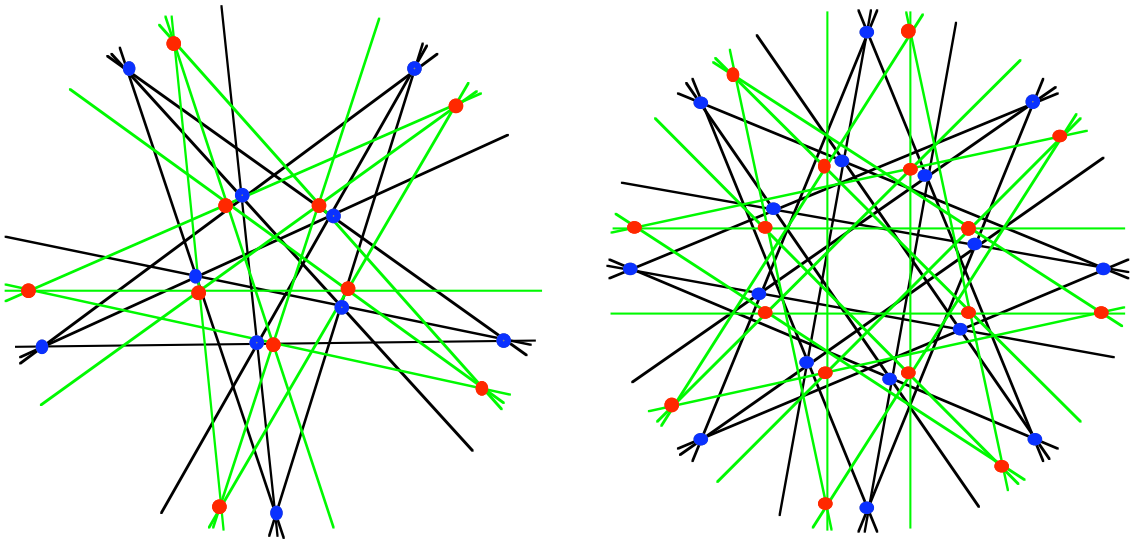

(a) #(2,2;1) (b) 8#(3,3;2)

Figure 2.10.3. Two examples of oppositely selfpolar configurations, characterized by symbols of the type m#(b,b;d).

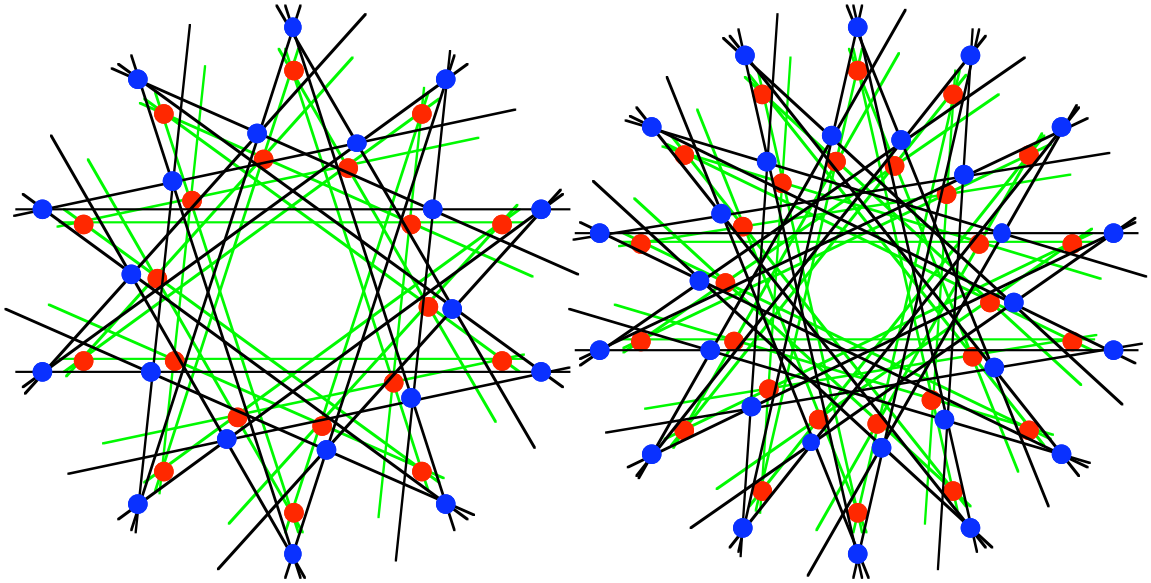

(a) 10#(4,2;3) (b) 13#(6,4;5)

Figure 2.10.4. Two examples of directly selfpolar configurations m#(b,c;d) with b and c even. In this subtype the polars may coincide (for an appropriate circle). In the illustration the circle was chosen to yield different sizes, in order to improve intelligibility.

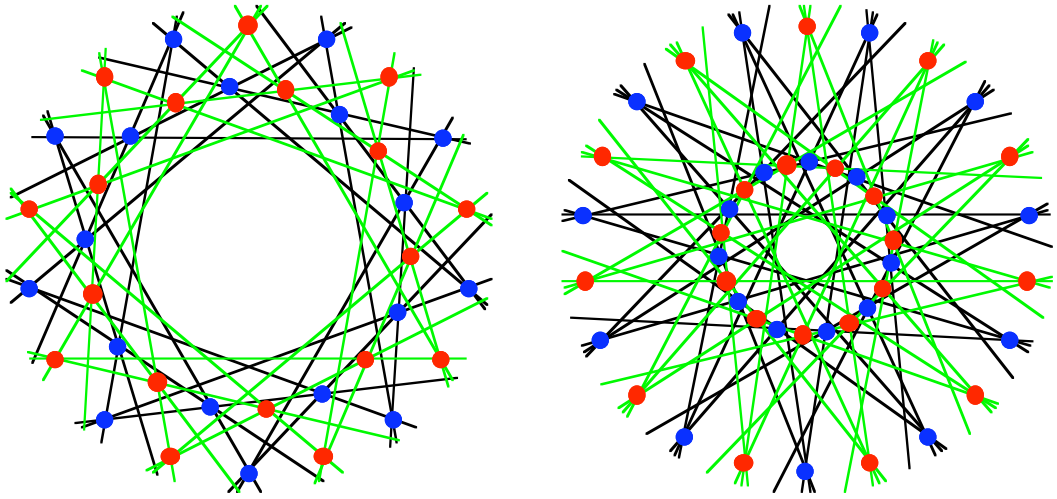

(a) 9#(3,1;2) 11#(5,1;3)

Figure 2.10.5. Two examples of directly selfpolar configurations m#(b,c;d) with b and c odd. In this subtype the polars are congruent but coincide only after reflection in the common center (that is, a rotation of 180°). We also say that these configurations are **selfpolar*.**

Exercises 2.10.

1. Verify that the correspondence δ is a duality. Determine whether this correspondence establishes a selfduality.

2. Describe the duality introduced by the polarity, for the polar configuration in Figure 2.10.2(b); use the labels on the two configurations that are given by their isomorphism.

3. Label the selfpolar configurations in Figures 2.10.4 and 2.10.5 to show that they are selfdual.

4. Verify that the Cremona-Richmond configuration (15_3), shown in Figure 1.1.1 and mentioned in Exercise 2.9.7, is selfdual. Is it selfpolar, and if it is, what is its type?

5. Find criteria for dual pairs of configurations of the various kinds discussed in Sections 2.8 and 2.9.

6. R. Artzy [A1] considers selfdual configurations and for a given selfduality δ describes a RLG ("reduced Levi graph" — this is not the same concept we are using throughout the book!) by identifying each element B with its image $\delta(B)$. This clearly depends on the selfduality chosen, but in each case the original Levi graph can be retrieved in a unique way. As observed by Artzy, the RLG may contain loops, this occurs in case B and $\delta(B)$ are incident. Artzy illustrates the use of RLGs by investigating special cases of the Desargues configuration. (On this topic see also Killgrove *et al.* [K10].) Assign labels to the RLG in Figure 2.10.6b to show that it corresponds to the Pappus configuration in Figure 1.10.6a, with the selfduality δ indicated by the upper and lower case letters.

7. Find a selfduality δ of the Desargues configuration in Figure 2.10.7a that leads to the RLG in Figure 2.10.7b.

8. Is there a meaningful extension to all polar pairs of astral 3-configurations of the distinction between directly and oppositely selfpolar ones?

9. Describe the polars of the configurations BB(m; s, t), and determine whether there are any selfpolar ones among them.

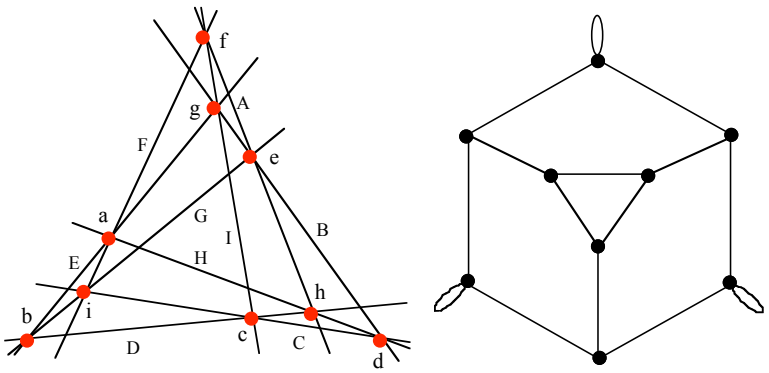

(a) (b)

Figure 2.10.6. (a) A version of the Pappus configuration (9_3), with a selfduality indicated by upper- and lower-case letters. (b) An RLG corresponding to the selfduality in (a).

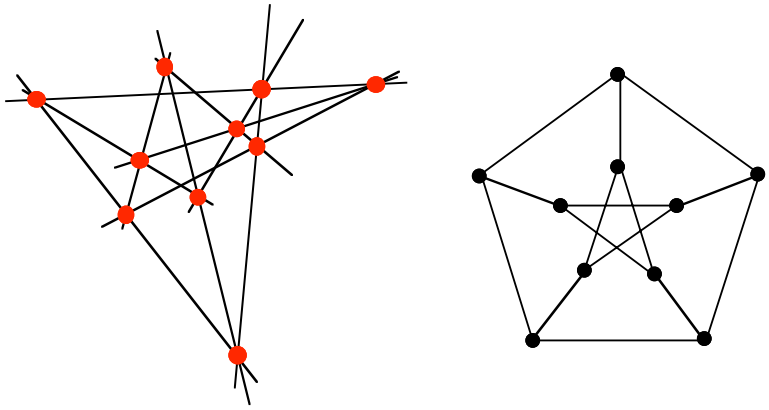

(a) (b)

Figure 2.10.7. (a) A version of the Desargues configuration (10_3). (b) An RLG of (a).

10. (Refresh your memories of elementary geometry.) Given a pair of astral configuration for which it is claimed that they are polar to each other with respect to a circle – how do you find the circle that justifies the assertion? Practice your solution on the selfpolar configurations in Figures 2.10.3, 2.10.4 and 2.10.5.

2.11 OPEN PROBLEMS (AND A FEW EXERCISES)

Many unsolved problems and open question have been mentioned in the preceding sections. While some of these may be challenging and others may hold interest for some people, there are a few problems concerning 3-configurations that seem to be of a fundamental nature; these problems exhibit the paucity of our understanding of what makes geometric configurations work. Some of the problems are related to Steinitz's geometric theorem of Section 2.6.

1. The first problem concerns geometric realizations of connected combinatorial configurations. By Theorem 2.6.1 we know that a (geometric) prefiguration representation is always possible if one incidence is disregarded. As shown by the examples of the (7_3) and (8_3) configurations, even allowing pseudolines it is not possible to achieve the last incidence. However, it is well possible that all connected (n_3) configurations with $n \geq 9$ admit realizations as topological *con*figurations, or even (for $n \geq 11$) realizations as geometric *pre*figurations. On the other hand, it may well be that already for $n = 13$ some counterexamples can be found for either version of the question. A subsidiary question is to determine the maximal number $t(n)$ of "lines" in a topological configuration (n_3) that may need to be non-straight pseudolines in each *realization* of the configuration in question. It seems that $t(n) \geq c\, n$ for some $c > 0$.

2. The second problem deals with obstructions to geometric realization of 2-connected 3-configurations with $n \geq 11$ lines. All known examples that include unwanted incidences (superfigurations) contain either a Pappus or a Desargues subfiguration (one incidence of the configuration is missed), or several such subfigurations. Are there any other obstructions to the geometric realizability, or is the presence of at least one of these two a characterization of 3-configurations with unwanted incidences?

3. The third problem, simply stated, is this: Is the combinatorial configuration $(10_3)_4$ using the notation in Section 2.2, the **only** 3-connected configuration (n_3) with $n \geq 9$ that does not have a geometric realization? A negative answer may appear at any time — if somebody hits upon an appropriate example — possibly even with $n = 13$. On the other

hand, a positive solution would seem to require several breakthroughs in directions for which we are not even dimly aware of how to start. These would have to include the elimination of *super*figurations (unwanted incidences) as well as *sub*figurations (missing incidences, as in Steinitz's theorem). As a possible example of a negative solution consider the abstract configuration (14_3) derived from the geometric configuration in Figure 2.11.1 on replacing the existing incidences of points A and B with the lines a and b, and insisting instead that A be incident with a, and B with b.

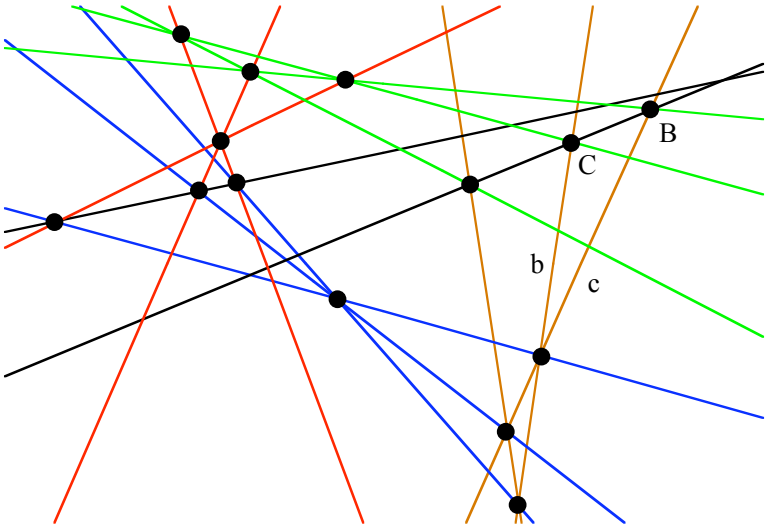

Figure 2.11.1. Is there a geometric realization of the combinatorial configuration (14_3) obtained from the above by keeping all indicated incidences except that C is to be incident with c (and not with b) and B be incident with b?

4. Is it true that if a 3-configuration admits a geometric realization in the Euclidean plane then it admits a realization in the rational plane? Or is it (at least) true that every geometrically realizable 3-configuration can also be realized in a plane over a quadratic extension of the rational field? In contrast, it is easy to verify that the #2-superfiguration shown in Figure 1.3.4 is realizable in the Euclidean plane but not in the rational plane.

5. For the various classes of very symmetric 3-configurations (such as astral, 3-chiral, k-dihedral, BB, ...) determine the precise range of the parameters for such configurations.

6. For connected astral configurations m#(b,c;d), is m = 12 the only case in which various superfigurations occur?

7. Is there any relation between the automorphism group of a configuration and the symmetries of its possible realizations? In particular, if the automorphisms act transitively on the points (or lines, or flags), does there have to exist a realization with non-trivial symmetry?

8. The object in Figure 2.11.2 is not a configuration, but the labeling clearly indicates that it is selfdual; the same can be said for the superfiguration in Figure 1.3.4. These seem to be interesting objects, analogous to configurations in the sense used in this book — but without any systematic framework to support their investigation. A formal proposal to consider such "generalized configurations" was made in [Z9] by K. Zindler as long ago as 1889. An example described by Zindler (as well as in the review [S11] of [Z9] by H. Schubert) is shown in Figure 2.11.3. However, it seems that Zindler's general challenge has never been met.

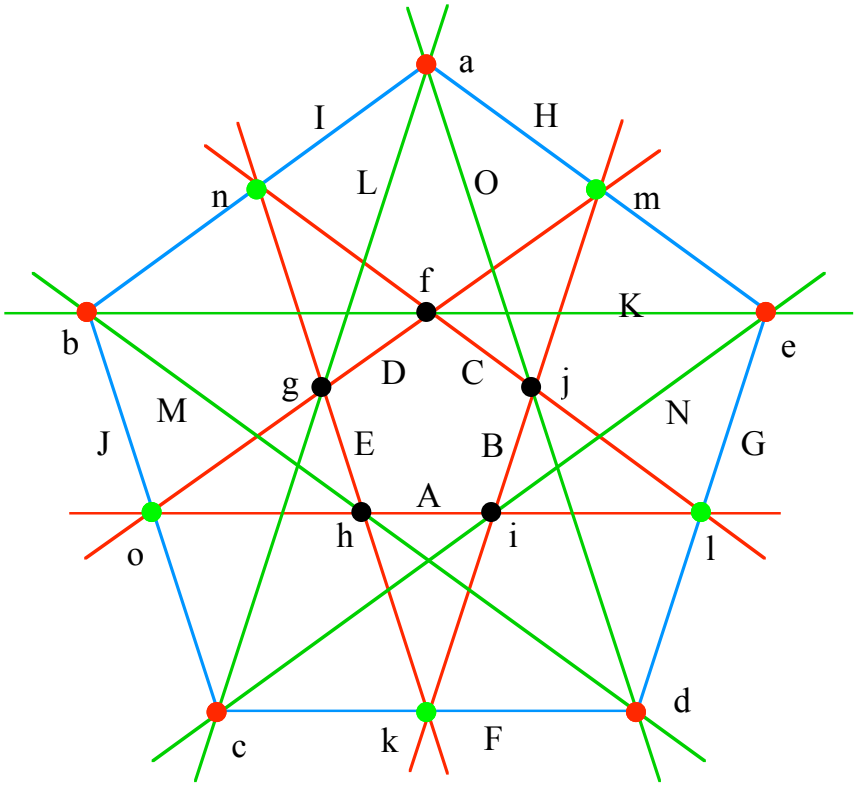

Figure 2.11.2. An intriguing selfdual collection of 15 points and 15 lines.

9. Decide whether the selfduality of the superfiguration in Figure 2.11.2 is a selfpolarity.

10. Prove that the incidences claimed in Figure 2.11.3 are valid.

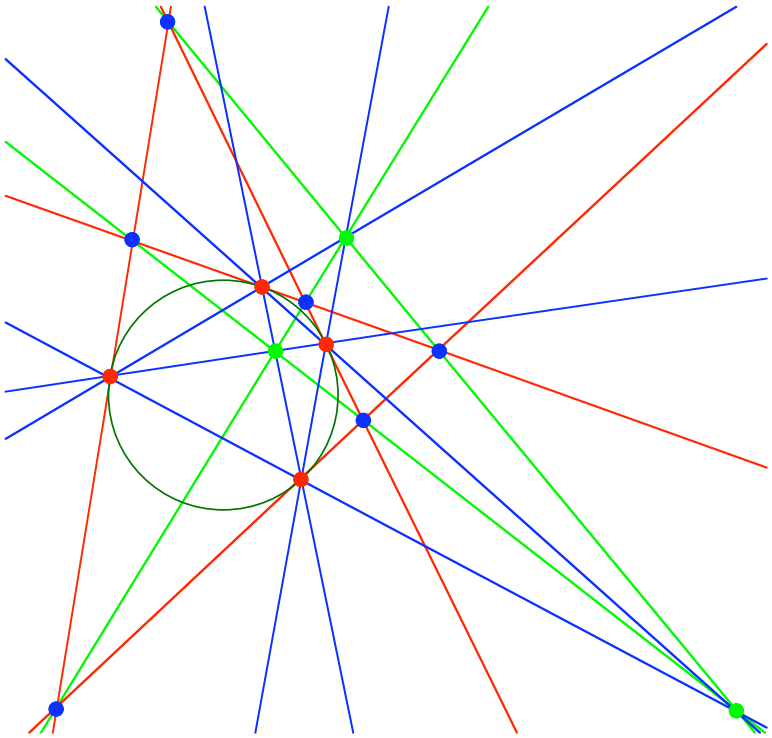

Figure 2.11.3. A "generalized configuration" of 13 points and 13 lines from Zindler [Z9]. It consists of four concyclic points (red) that determine a complete quadrangle (six blue lines) and its three "diagonal points" (green). The four tangents (red) to the circle at the four concyclic points are a complete quadrilateral that determines the six blue points and the three "diagonal lines (green). The selfpolar "configuration" has six points incident with three lines each, and seven points incident with four lines each, and dually for lines.